TITLE PAGE

Report Title: Technical Progress Report 15418R05

Report Type: Final Report

Reporting Period Start Date: October 1, 2003

Reporting Period End Date: September 30, 2005

Principal Authors: M. Karrenbach

Date: November 30, 2005

DOE Award Number: DE-FC26-03NT15418

Subject: An Integrated Multi-component Processing and Interpretation Framework for 3D Borehole Seismic Data

DISCLAIMER

This report was prepared as an account of work sponsored by an agency of the United States Government. Neither the United States Government nor any agency thereof, nor any of their employees, makes any warranty, express or implied, or assumes any legal liability or responsibility for the accuracy, completeness, or usefulness of any information, apparatus, product, or process disclosed, or represents that its use would not infringe privately owned rights. Reference herein to any specific commercial product, process or service by trade name, trademark, manufacturer, or otherwise does not necessarily constitute or imply its endorsement, recommendation, or favoring by the United States Government or any agency thereof. The views and opinions of authors expressed herein do not necessarily state or reflect those of the United States Government or any agency thereof.

ABSTRACT

This is the final report for DOE award number DE-FC26-03NT15418. This report summarizes the work covered during the entire project, from October, 2003 through September, 2005. The project has been successfully completed, and we have achieved our goal of building a rich set of tools that allow geoscientists to perform interactive display, processing and interpretation of multi-component 3D VSP data. Technical reports have been submitted throughout the course of the project and deliverables have been met.

TABLE OF CONTENTS

TITLE PAGE 1
DISCLAIMER 2
ABSTRACT 3
TABLE OF CONTENTS 4
EXECUTIVE SUMMARY 5
REVIEW OF OBJECTIVES, SCOPE, and DELIVERABLES 6
RESULTS AND DISCUSSION 7
Task 1 7
Task 2 19
Task 3 33
Task 4 49
Task 5 50
Task 6 51
Task 7 67
Task 8 95
Task 9 102
Task 10 104
Task 11 105
Task 12 106
Task 13 107
Task 14 110
Task 15 111
Task 16 117
Task 17 118
ACKNOWLEDGEMENTS 120
REFERENCES 121
RELEVANT PUBLICATIONS 124
APPENDICES 125
Appendix A. Deliverables 125

EXECUTIVE SUMMARY

The DOE issued a matching funds grant to develop a framework for processing and interpreting multi-component 3D VSP data. A number of tasks were outlined in our original proposal to accomplish this goal. In general, the efforts covered compiling synthetic and real datasets for testing purposes, and the design, development, and testing of a complex software application, which we refer to as the VSP Work Bench.

Both real and synthetic seismic test data were compiled for this effort. These range from simple geologic models to very complicated subsalt models, and include testing with data from the San Andreas Fault Observatory project. The data sets encompass a variety of source and receiver layouts, ensuring that we have tested the application on a wide range of realistic geologic and acquisition scenarios.

The design criteria for the 3D Work Bench included several basic tenants. Among these were flexibility to add new features and modules, the ability to run in Unix or Windows, a user interface that was easy to learn and use, the ability to run tasks on a Beowulf cluster, and the ability to communicate with other programs, in particular a seismic recording system. The first step in the re-design and new design effort was to choose a powerful set of low-level tools upon which we could build middle ware and higher level objects. Next, and perhaps most important, was the extension of our own low-level infrastructure to be compatible with all higher level design and implementation requirements. This served as a foundation on which we were able to build sophisticated modules that relate specifically to our 3D VSP processing and interpretation needs. Our foundation includes such things as the basic data objects, the drawing functionality, the graphical user interface, and the communications library. We have found that time spent re-designing and developing a sophisticated foundation has helped tremendously to reduce the time and effort needed to build high-level modules specifically designed for VSP analysis. In addition, careful attention to changes in the foundation layer reduces significantly the debugging and software maintenance burden.

Rather than design, develop, and test the Work Bench in separate phases, these three activities typically were going on simultaneously. Continuous testing and use of the Work Bench by real users on real world problems gave us instant feedback not only on the basic functionality, but also the user interface design. Many changes and modifications were made as a result of this pattern of work.

All tasks have been successfully completed, as outlined in the original proposal. Interim technical progress reports have been delivered, and all the necessary data and software have been submitted to the DOE. The developed tools were tested extensively in our in-house environment and results obtained have contributed to a number of publications and presentations in trade journals and professional meetings. We would like to thank the Department of Energy, National Energy Technology Laboratory, for the support of this project.

REVIEW OF OBJECTIVES, SCOPE, and DELIVERABLES

The objective of DOE Grant DE-FC26-03NT15418 was to provide financial support to develop, prototype, and test an efficient framework for processing and interpreting multi-component 3D VSP data. We have developed such a framework, by building upon our existing processing software, as well as leveraging off of industry standard open-source graphics and visualization toolkits that are both portable and widely used. The entire framework consists of an extensible base layer of data display and manipulation components, coupled with a library of complex data processing modules which can be used to process and interpret multi-component 3D VSP data.

DOE Grant DE-FC26-03NT15418 was issued in October, 2003 and completed in October, 2005. The work was sub-divided into six phases, consisting of tasks that cover such things as data collection, software design and prototyping, and software testing, and quality control. The next section of this report will review, task by task, the work that has been completed under this Grant.

The deliverables for this grant consist of progress reports, data files, source code, and this final report. A detailed accounting of the deliverables and data files is contained in Appendix A.

RESULTS AND DISCUSSION

Task 1

Examine existing 3D VSP field datasets for use as test and validation data.

Four real datasets were used for testing the software developed in this project. A general description of the geologic setting and the data acquisition and processing histories are given here.

Real Model 1. Single well 3D VSP
This is a single well three-component (3C) 3D VSP survey in a geologically simple setting. The data exhibit a very high signal-to-noise ratio, where the dominant factors are data resolution and amplitude effects. The source is explosives. High quality down-going, reflected and mode-converted energy is clearly visible. The noise level is very low. A few shear sources were used, which show down-going shear and converted modes clearly. Hodogram analyses clearly show clean polarization patterns and confirm the quality of the data. The velocity model is not structurally complex, but rather this is a geologic setting where the seismic resolution and amplitude effects dominate.

Acquisition Summary:

- Receiver array deployment between 189 m – 1,391 m depth
- Receiver spacing: 15.24 m
- Receiver array: (2) P/GSI 40 level 3 component clamped arrays
- Data acquisition system: I/O SYSTEM TWO® with MRX™ boxes
- Seismic source: 1 kg Dynamite (@12 m depth)
- Maximum offset of data used for imaging: 1,500 m
- Number of shot points used for 3D VSP imaging: 243
- Image size at a depth of 3,000 m is a circle with 1,500 m radius centred on the receiver well

Processing Summary:

- Assign and QC Geometry using a receiver relocation method
- 3 C Hodogram analysis and rotation to true XYZ
- Trace Editing – Remove bad shots and flag bad traces
- First break picking on the 3C data rotated toward the source (min. phase data)
- Near-offset velocity inversion, determine best ZO velocity function, compare to well logs
- Zero-offset corridor, corridor stack and L-Plot
- Model-based shot statics
- Design Deconvolution filters on downgoing direct wave
- Estimate usable bandwidth – FK Plots, Spectral Analysis, Bandpass Filtering

- Apply statics and Deconvolution, 3C Wave field separation for upgoing waves
- Prestack Depth Migration (1st pass with 1D Velocity Model)
- Refine velocity model by combining a variety of constraints and methods
- Prestack Depth Migration (2nd pass with refined velocity model)

Figure 1 shows the principal component of a raw near, mid, and far offset shot record with picked first arrival times overlaid. High quality down-going, reflected and mode-converted energy is clearly visible. The noise level is very low. Besides the explosive sources shown in Figure 1, a few shear sources were used as well (Figure 2), which show down-going shear and converted modes clearly. Figure 3 shows the general vector fidelity of the dataset. Hodogram analyses clearly show clean polarization patterns, and confirm the quality of the data.

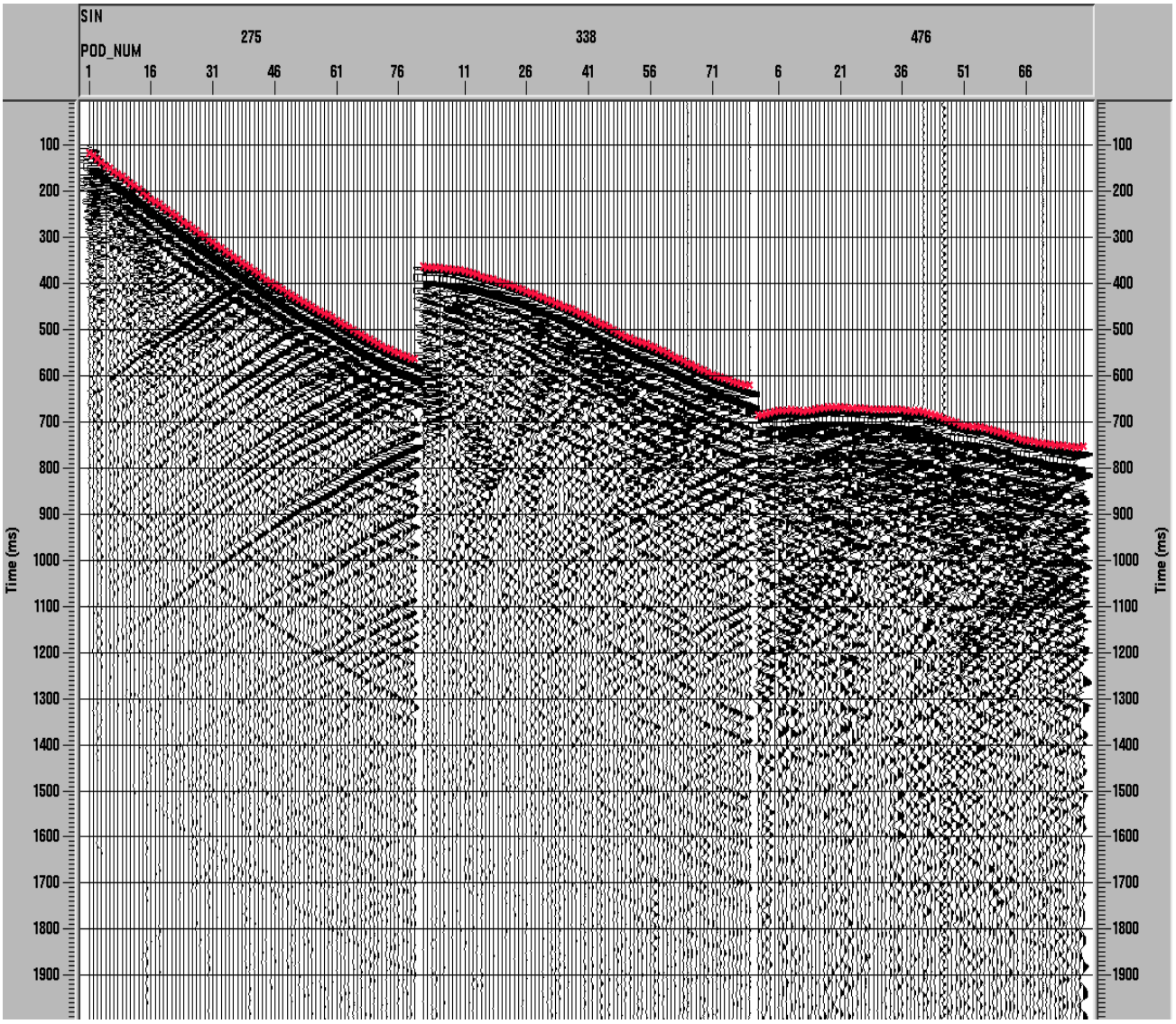

Figure 1 Raw data of principle component at 30m, 700m and 1400m source offset from well.

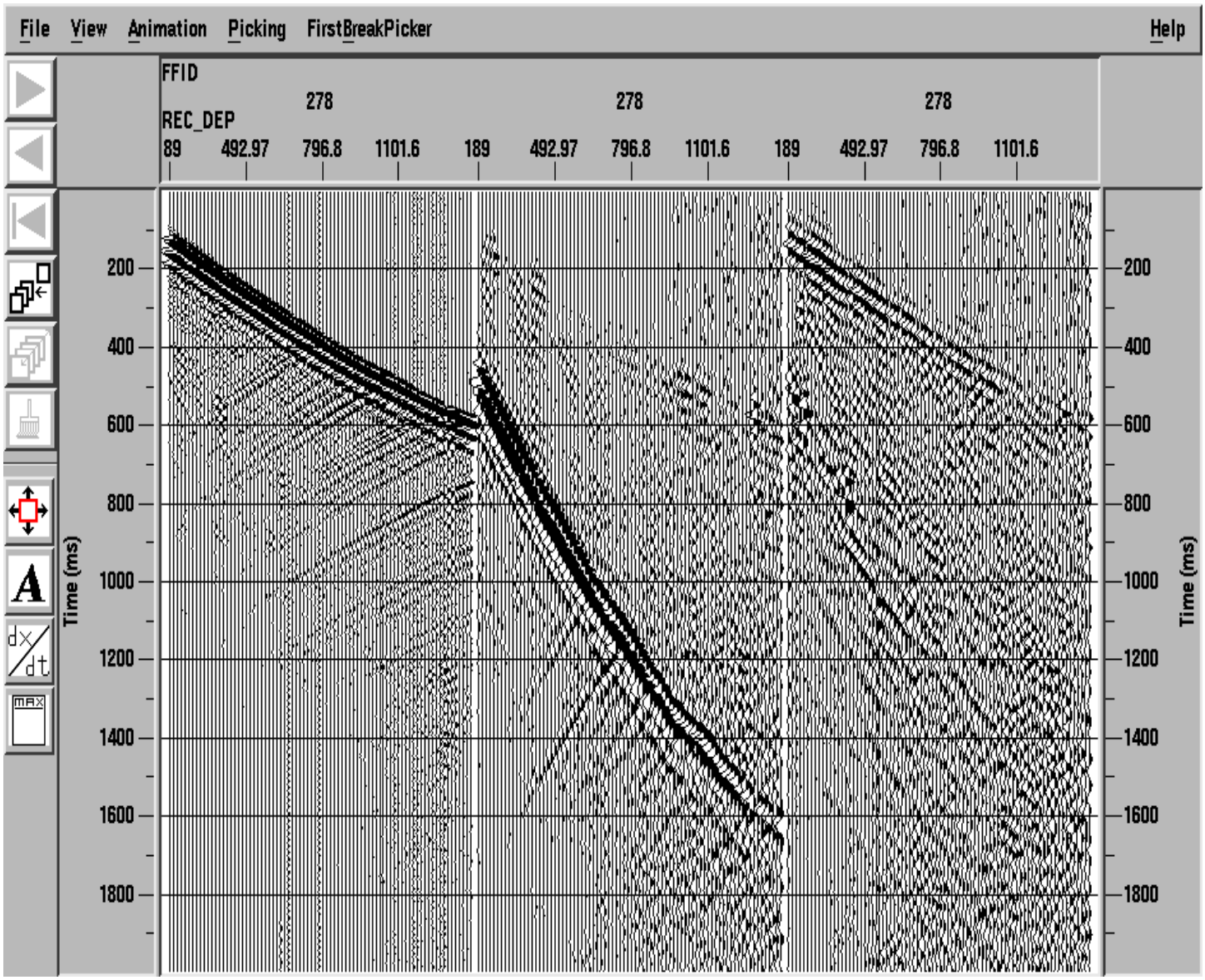

Figure 2 Shear wave source located due North of receiver well. Whereas the direct P arrival is visible only on the vertical component (left panel), the direct S-wave arrival is only visible on the NS component (middle pannel). The EW component shows only minimal energy.

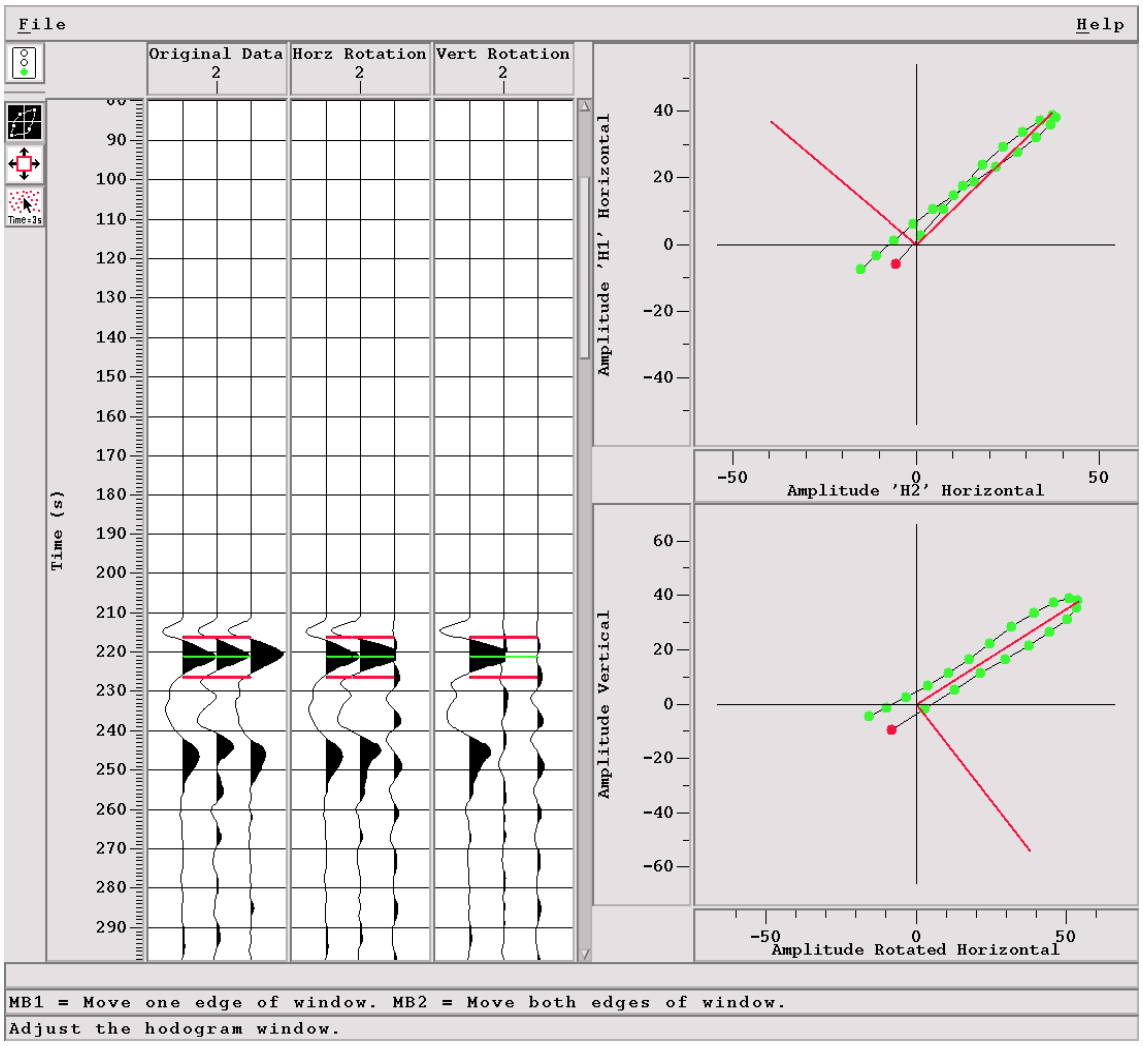

Figure 3 Example of a 3C Hodogram analysis showing linear polarization of particle motion.

Real Model 2. Multi-Well 3D VSP

This is a multi-well three-component 3D VSP survey where the geology is quite complex, and the reservoir is compartmentalized, leading to the desire to use high-resolution 3D VSP imaging to better understand the rock and fluid properties. The data quality is high, yet the data exhibit real world challenges, since the subsurface structure is complex and leads to reflected, refracted and diffracted energy that is recorded in the two arrays. The following processing flow has been determined as a baseline for future testing of the technology being developed in this project.

Acquisition Summary:

- Ground Level (GL) at the 3D VSP receiver wells range from 166 m to 201 m
- KB at the eight 3D VSP receiver wells is 3 m above GL
- Surface seismic source line interval: 76 m; Source point interval: 30.5 m
- Seismic source: A single surface 19,504 kg. I/O AHV II vibrator
- Sweep parameters: sum of four 12 sec. 10-150 Hz sweeps
- Number of shot points: ca 500 into 2 wells
- Shots used for 3DVSP migration within 1,097 m radius of the receiver wells
- Reservoir depth (mKB): 457 - 914
- Receiver well depths: TD (mKB): 610 - 914
- Receiver array depth: 0 - 762 mGL, 2 x 40 levels, dz = 15.2 m

Processing Summary:

- 3C geophone orientation using hodogram analysis
- First break picking on the 3C data rotated toward the source
- Determine zero offset VSP velocities, well log velocities, and the first pass migration velocities
- Estimate useable bandwidth – FK Plots, spectral analysis, bandpass filtering
- Design decon filters
- 3C wave field separation for upgoing waves
- Apply decon filters (calculated from downgoing and applied to upgoing)
- Initial migration with 3D velocity model from near offset VSP and well logs and horizons
- Prestack depth migration of shot gathers
- Stack
- Post stack/migration processing

Figure 4 shows an example of the up-going wave field after deconvolution for a shot gather at mid-offset range. Figure 5 shows a slice of the velocity volume. These data were used to produce a 3D seismic image of the reservoir. Figure 6 shows a slice through this image volume, overlain with well logs and formation tops.

Figure 4 Upgoing deconvolved P wave field and spectrum.

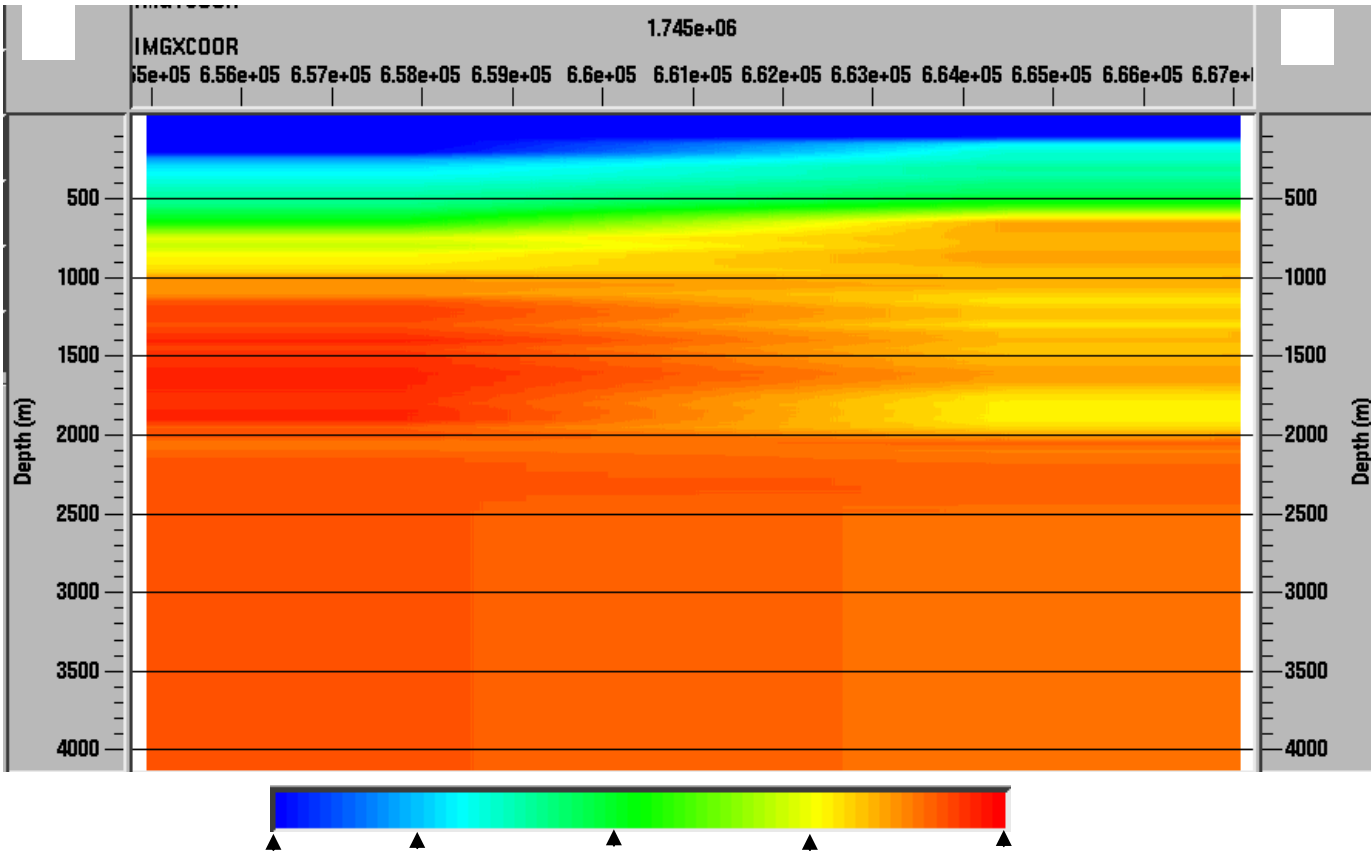

Figure 5 Slice through the P-wave velocity model. Velocities range from 1,500 ft/s at the surface to 9,000 ft/s at depth and exhibit considerable lateral variation.

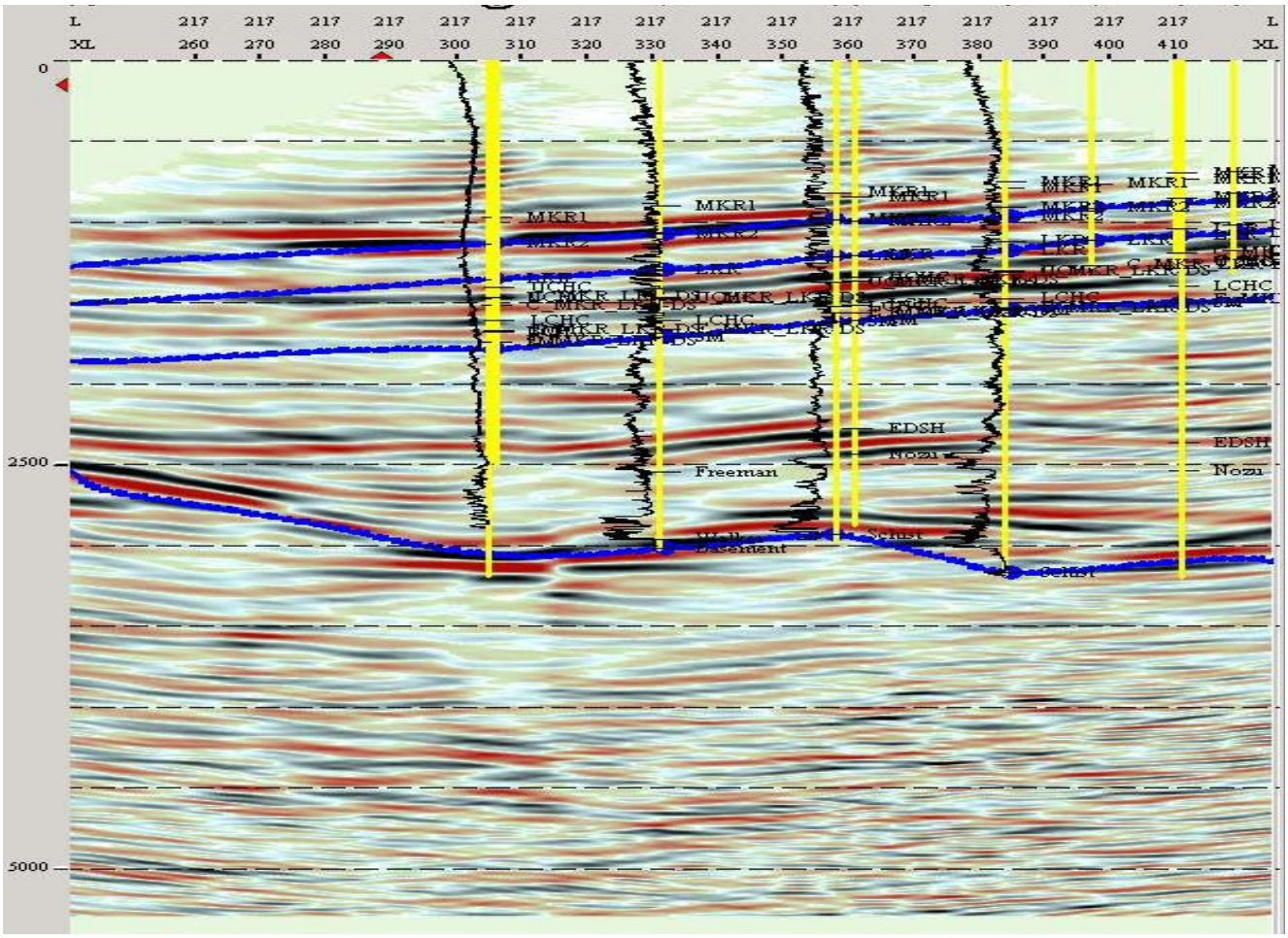

Figure 6 P-wave image slice of a multi-well 3D VSP with tops and well logs as overlay. Two of the wells displayed were equipped with a 40-level receiver array.

Real Model 3. San Andreas Fault Zone

The San Andreas Fault Observatory at Depth (SAFOD) is one of four components of the National Science Foundation's EarthScope initiative (http://www.earthscope.org/), conducted in partnership with the USGS and Stanford University. A 3.2 km-deep deviated drill hole was drilled across the San Andreas Fault near the town of Parkfield, California (http://quake.wr.usgs.gov/research/parkfield/). Phase I drilling of the hole was conducted in the summer of 2004, with the hole reaching a vertical depth of 2.5 km, driving the hole within 0.7 km of the main San Andreas Fault. Phase II drilling, in which the hole penetrated the fault zone, took place this past summer. Scientists from many universities are involved in a myriad of investigations related to the SAFOD site and the San Andreas Fault. Our efforts focused on the capture of VSP, microseismic, and earthquake data from three 80-level receiver strings placed down the SAFOD well, for a total depth of almost 2,743 meters of receivers placed every 15.2 meters. This survey provides the academic community with seismic data that are unprecedented in terms of the lateral resolution and depth of coverage of the San Andreas Fault zone.

Acquisition Summary:

- Surface seismic source for zero offset: 2.25 kg of dynamite at 3.05 m depth
- Surface seismic source for offset shots: 36.3 kg of Pentolite (charge is 18.3 m long) at 30.5 m depth
- Number of shot points recorded: 5 zero offset shots, 13 offset shots
- Horizontal offsets recorded: 50 m – 5,000 m
- Well information: Casing size: 24.5 cm, Casing weight: 69.8 kg/m, drifted diameter 21.6 cm
- Receiver array: (1) P/GSI Cable 80-010, pod spacing: 15.2 m, Phones: 15 Hz OYO Geospace SMC15-1850 Omni, 3C pod
- Receiver depths (Depths below ground level (GL) at well):
    - 1st setting of 80 level array (actual): 46.7 - 1,250.2 m (GL)
    - 2nd setting of 80 level array (actual): 930.3 - 2,133.8 m (GL)

3rd setting of 80 level array (actual): 1,539.7 - 2,743.2 m (GL)

Processing Summary:

- Zero-offset check shot processing:
  With the 80-level array deployed in three different positions down the borehole, we obtained checkshot velocity information over the entire length of the borehole. Checkshot velocities were obtained from first breaks and a corridor was processed from the assembled check shot gather.
- Far-offset shot processing:
    - In a first task, the far-offset shotpoints are used to orientate the horizontal components of the receiver geophones inside the well, which allows to rotate the 3C data to a global true XYZ coordinate system.
    - Although only very sparsely distributed, the 13 far-offset shots can be used to image selected upgoing arrivals that are visible in the prestack data. This was performed using previously existing velocity models.
- Microseismic monitoring.

- Over a 10-day period, about 4 Terabytes of continuous data sampled at 0.25 ms were obtained. About 100 bigger events with magnitudes between 0.0 and 2.7 could be separated out immediately using the listings of the USGS earthquake catalogs. Using typical magnitude scaling relations, we estimate that we recoded over 1000 events of lower magnitude that could not be detected with the currently operating permanent seismological arrays. Directional information obtained from 3-component recordings of some of the bigger events were already used by USGS for last-minute drilling decisions of phase II drilling this summer, where the drill bit was steered in the direction of one of the target events recorded by our array.

Figure 7 shows a 3D velocity model of the rock volume surrounding the deviated drill hole. The velocity model was inverted using seismic tomography of P-wave arrivals recorded in a 32-level receiver array installed in a vertical pilot hole close to the deviated main hole. We used this velocity model for a narrow-aperture prestack depth migration of selected shot points. An example of the migrated images obtained in this fashion is shown in Figure 8.

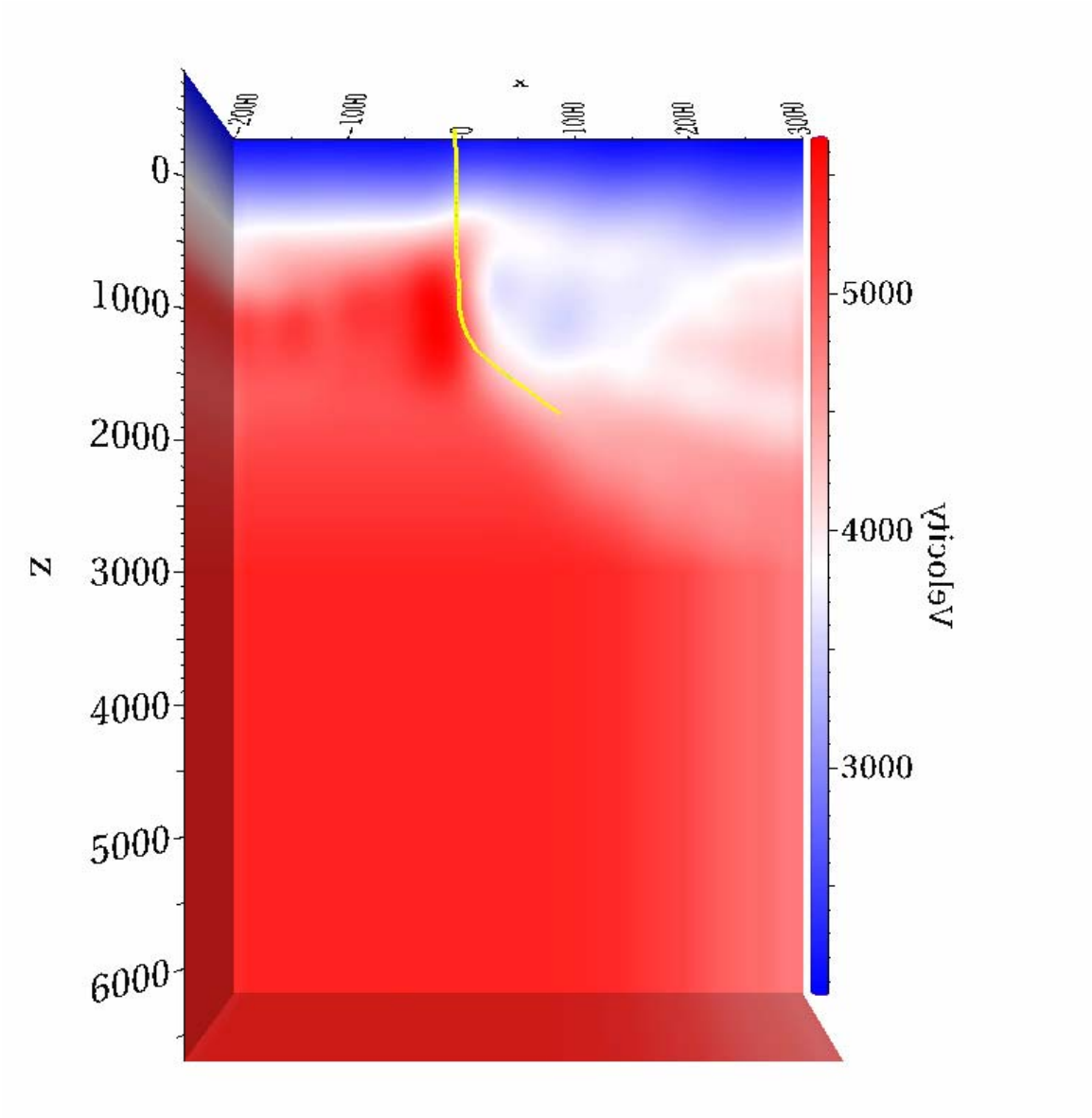

Figure 7 3D velocity model of the volume surrounding the SAFOD drill hole.

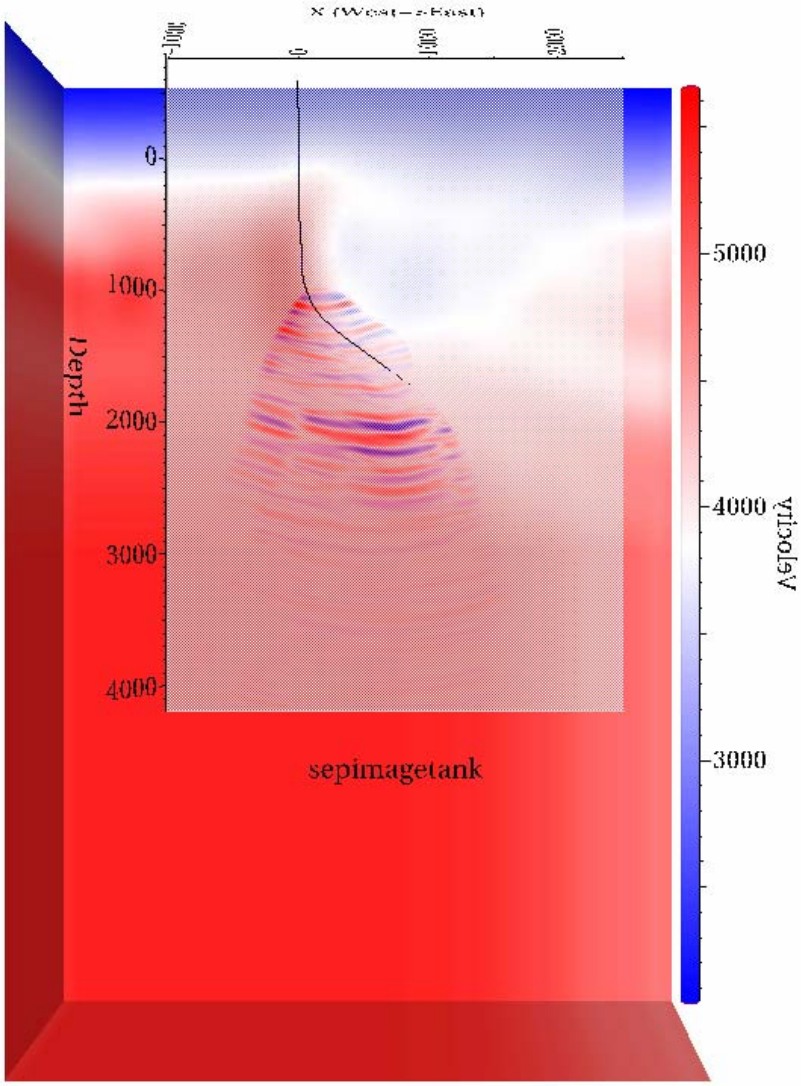

Figure 8 Narrow-aperture prestack depth migrated image of several zero-offset shots into all 3 deployment setting. Reflected energy is mapped to a horizontal interface below the deviated part of the borehole.

Real Model 4. Hot Ice

The Hot Ice reservoir is a sequence thin beds of methane hydrates at shallow depth within the permafrost layer. The resolution provided by surface seismic was not sufficient to image the thin beds. In addition, the permafrost layer presents significant imaging problems for conventional surface seismic. Detailed velocity information obtained from borehole seismic surveys is extremely useful for modeling the near-surface velocity accurately. Some of the data from the Hot Ice reservoir are shown in Figures 39-46 and 80, 87 and 88.

Acquisition Summary:

- Ground Level (GL) at the 3D VSP receiver well is 57.2 m msl.
- RKB at 3D VSP receiver well is 65.2 m over MSL, 7.9 m ft above GL.
- Surface seismic source line interval: 36.5-53.3 m; Source point interval: 36.5-53.3 m using an adaptive circular pattern
- Seismic source: Single AHV4 Vibroseis (28,123 kg), 2 x 8 - 220 Hz 10 sec linear sweeps, 0.2 sec cosine taper
- Number of shot points recorded 1,185
- Maximum Well to Source Offset recorded 838 m
- Reservoir depth (mKB): 701 m
- Receiver well depths: TD (mKB): 701 m
- Well information: Casing: 17.8 cm, 26#, Well nominally vertical, cased to 414 m, open hole to 701 m
- Receiver array depth (m RKB): 89.7 m – 691.6 m
- Receiver arrays: 3rd generation cable 80-006, Phones: 15 Hz OYO SMC1850, 3C pods

Task 2

Build several 3D horizon-based models and generate fully populated rock property grids.

Six geologic models and their corresponding synthetic seismic datasets were constructed. Their characteristics are described below:

Synthetic Model 1. 2D Salt Model
A salt model, with a salt body surrounded by a velocity medium that increases gradually with depth. The model represents a fairly typical Gulf of Mexico sub-salt imaging problem. The velocity model, shown in Figure 9, is essentially two-dimensional with interval velocity changes at key layer boundaries. The velocity within the layers exhibits a linear gradient change. Salt velocity is ca.4,267 m/s. The starting velocity of the background velocity field is 1,524 m/s with a depth gradient of 0.129 m/s- which is typical for the Gulf of Mexico. The shear wave velocity is determined by a constant vp/vs ratio. Gardner's relation determines the density. Note that there is no water layer and the grid spacing of the fully populated velocity grid is 7.6 m.

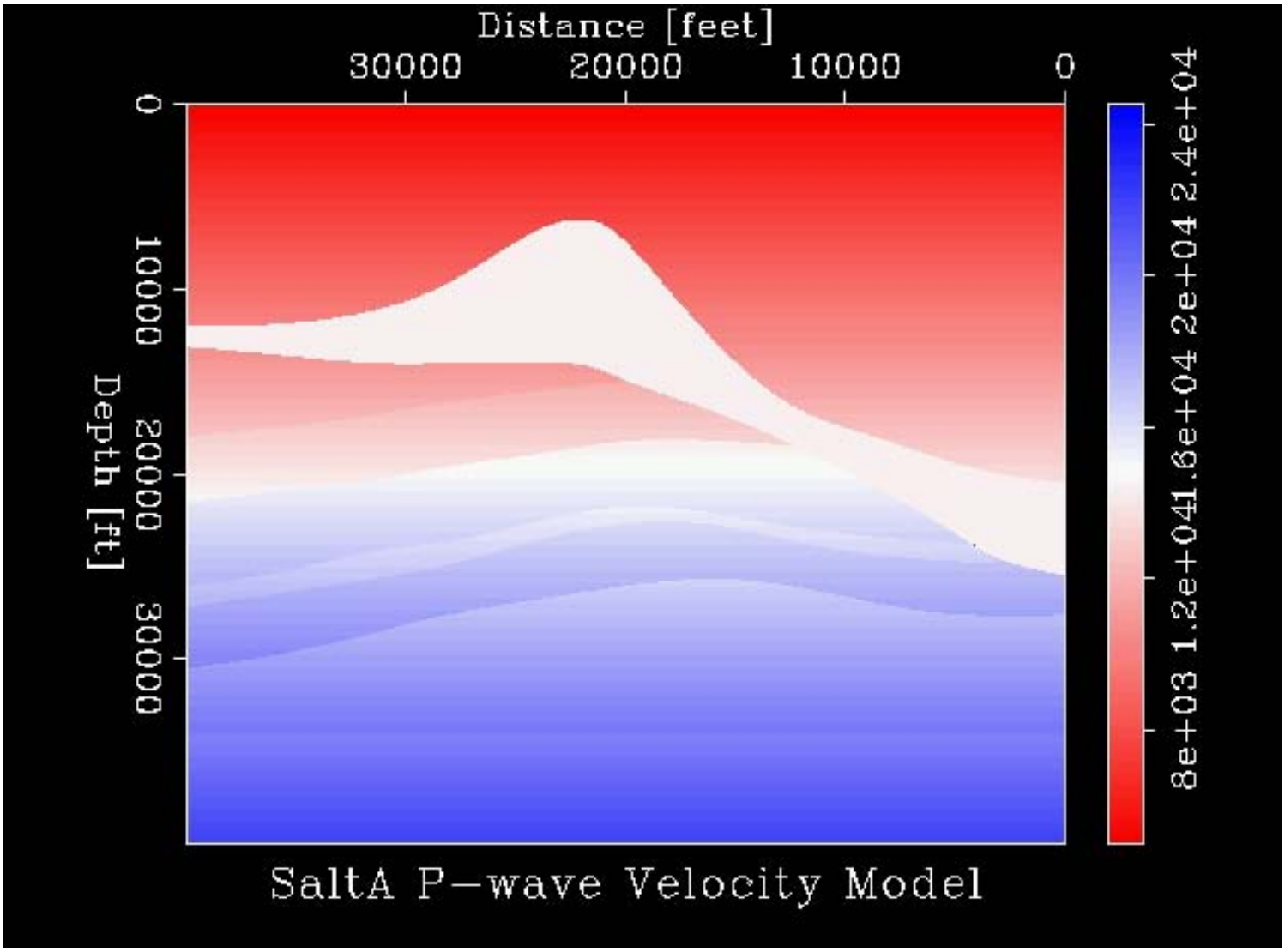

Figure 9 P-wave velocity model that includes a simplified salt body and several first-order discontinuities below the salt.

Synthetic Model 2. 3D Layered Model

This is a geologically simple model, with three dipping layers. The velocity model, shown in Figure 10, is a three-dimensional model with inter velocity changes at key layer boundaries. The velocity within the layers is constant. The background velocity ranges from 1,990 m/s to 3,810 m/s. The shear wave velocity is roughly half the p-wave velocity and density is constant at about 2.0 g/cm^3 throughout the model. Figure 11 shows the source and receiver geometry in the velocity model.

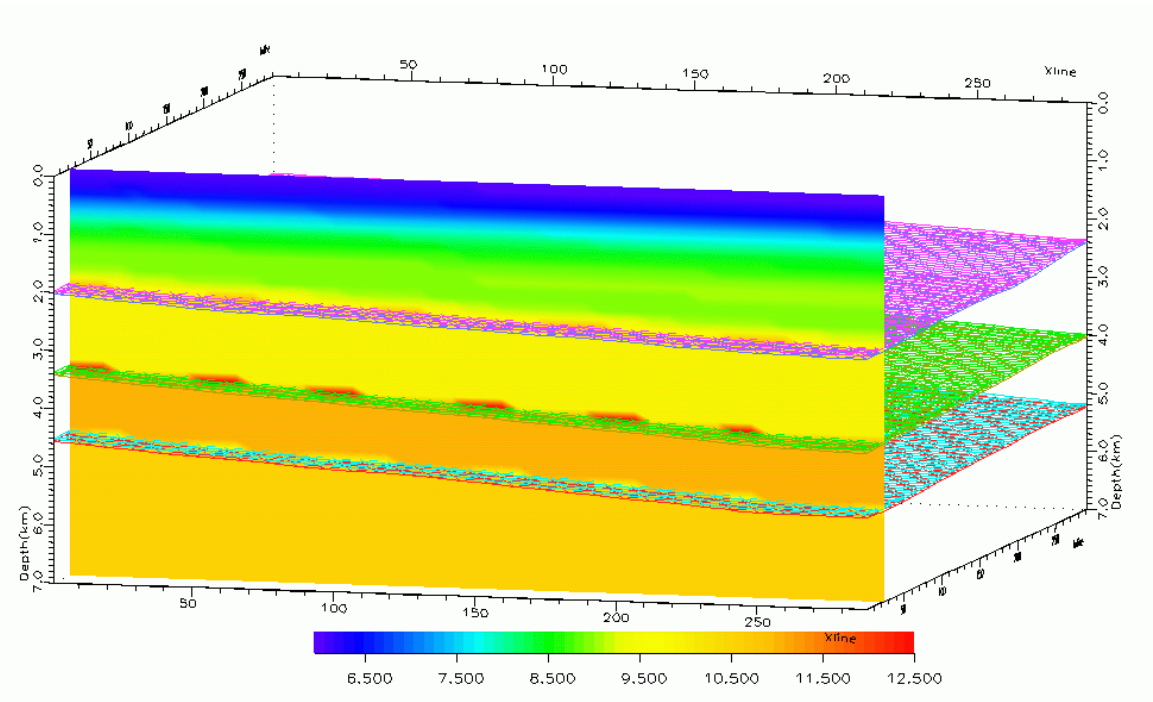

Figure 10 P-wave velocity in a 3-layered dipping model.

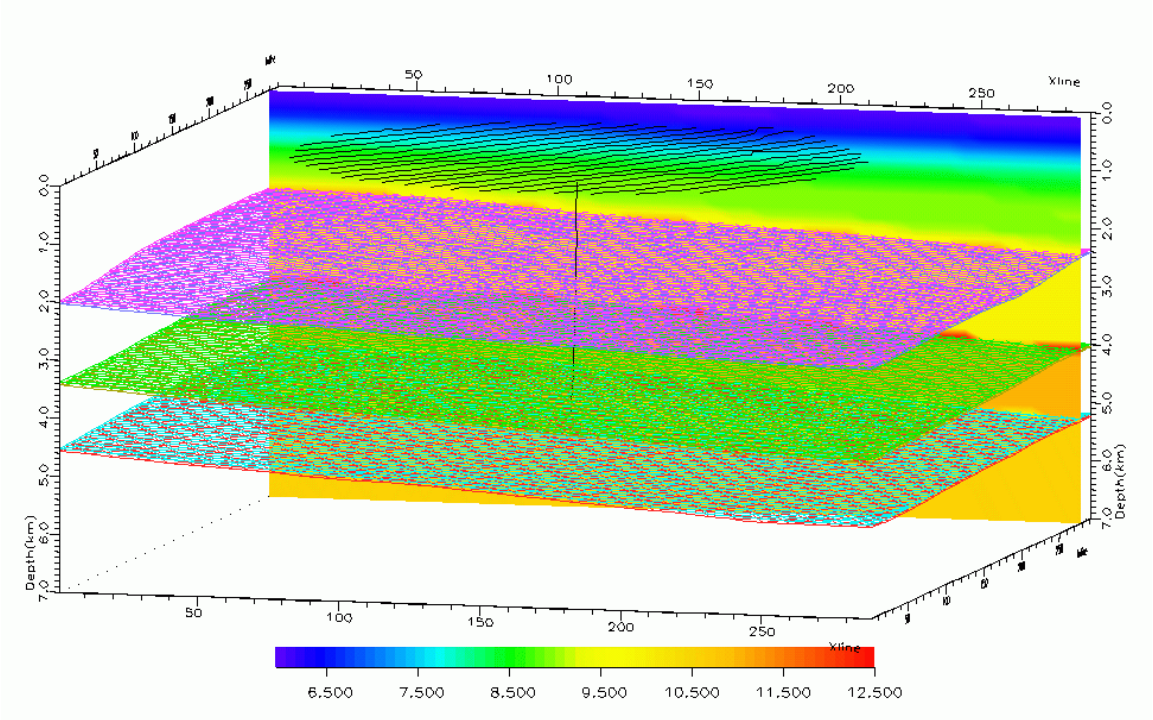

Figure 11 Source and receiver geometry in the P-wave velocity model.

Synthetic Model 3. San Andreas Fault Zone

This model contains strong lateral variations, steeply dipping faults and a very challenging surface imaging problem. A model was constructed that describes the region around the San Andreas Fault Observatory at Depth located in Parkfield, California. The model exhibits strong lateral variations and steeply dipping fault zones. It is a challenge for surface seismic imaging techniques to image this area. A 3D model has been constructed to generate test data in a 3D VSP layout for a receiver array deployed in the deviated main hole. Figure 12 shows the color coded velocity model in which we generated 2D synthetic test data using the Norsar ray tracing package. Two near-vertically dipping strike-slip faults are crossing the receiver array at depth. Sources are distributed on a 2D line across the surface that includes steep topography (black line). The location of the receiver array is indicated and it is crossing two fault zones. Figure 13 shows the envisioned 3D VSP source and receiver geometry along with a slice of the velocity model.

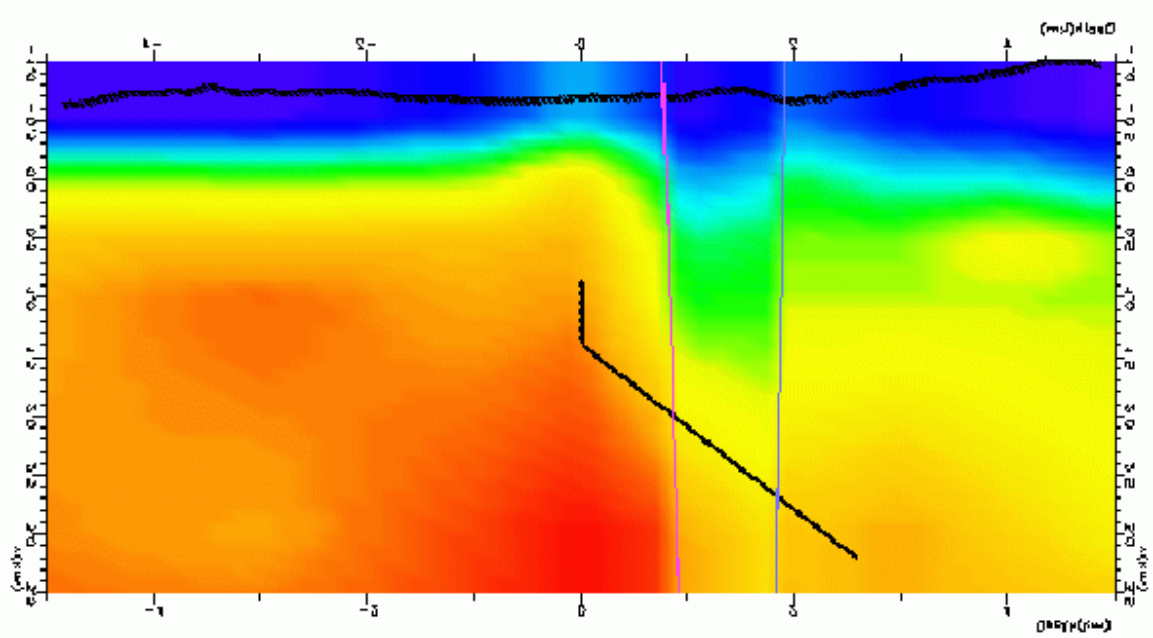

Figure 12 2D fault zone velocity model with deviated well.

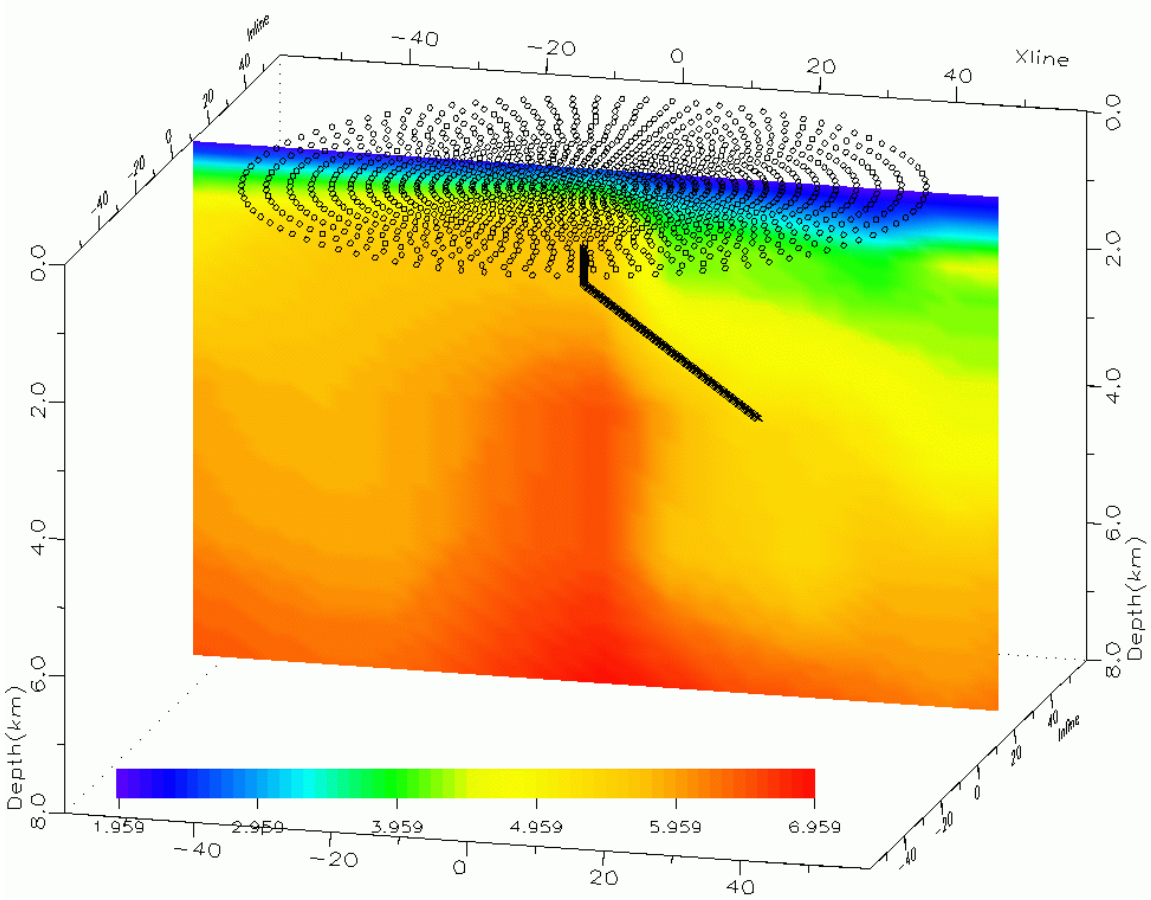

Figure 13 3D view of the velocity model with an envisioned 3D VSP source and receiver geometry.

Synthetic Model 4.

This very simple model was used to model three component hodogram responses and to define and establish standard polarity conventions for the processing of three-component data. It served as a benchmark model to validate existing 3C processing packages as well as newly developed three-component processing algorithms. Although in principle applicable to three-component data, existing polarity standards defined by SEG are geared towards seismic recording at the Earth's surface and may lead to ambiguity for the case of downhole data acquisition. The model consists of a single flat horizon above a homogeneous overburden. Figure 14 shows an isometric view of the velocity model and the distribution of sources and receivers within.

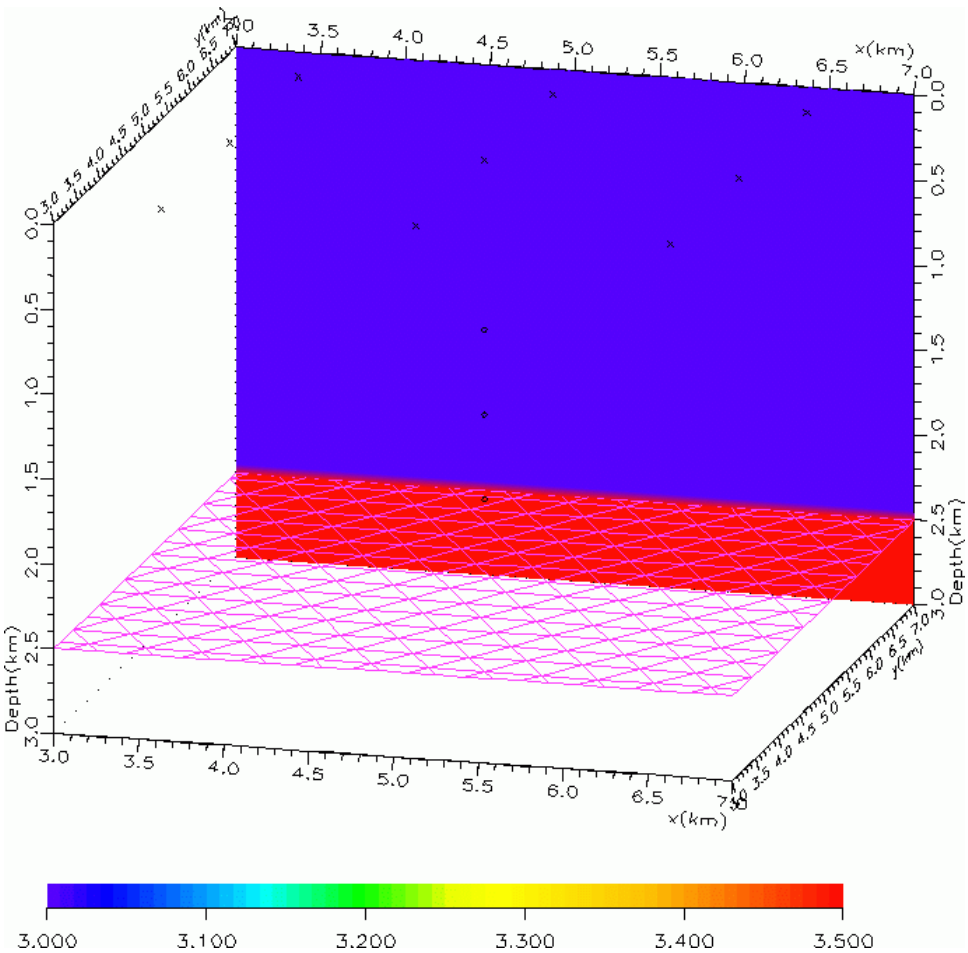

Figure 14 Simple benchmark model with a few sources at the surface and receivers in a vertical borehole used for testing hodogram responses and establish 3-component polarity standards.

Synthetic Model 5.

This model is representative of a more complex structural environment with an anticlinal structure at the target level and a very high velocity contrast in the overburden caused by a salt layer underlying unconsolidated sediments very near the surface. The objectives behind this velocity model are twofold: firstly, test the illumination and imaging of the moderately steep anticline at target level using receivers in several boreholes and shots at the surface, and secondly, investigate the effect of interbed multiples created in the highly reflective overburden on the image. This model is representative of a variety of regions, including some prospects in the intermontane basins of the western United States. A three-dimensional overview of this model is shown in Figure 15. Figure 16 and 17 show an East-West and North-South cross section though that model and indicate the location of the receiver wells with respect to the target anticline.

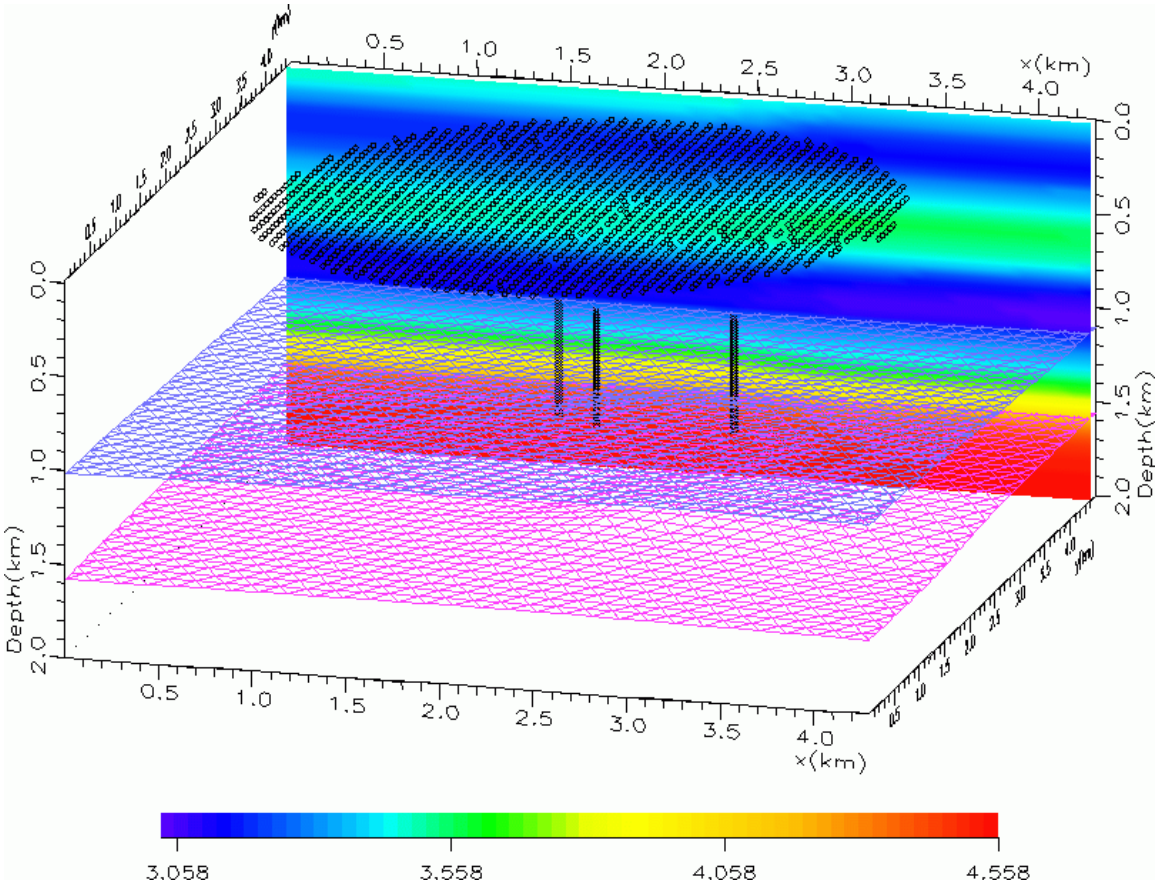

Figure 15 3D view of a raytracing model including 2 target horizons at about 1 km and 1.5 km depth with a moderately steep anticline, and a very high velocity contrast in the overburden. Three wells were assumed to be equipped with receivers for a multi-well 3D VSP geometry.

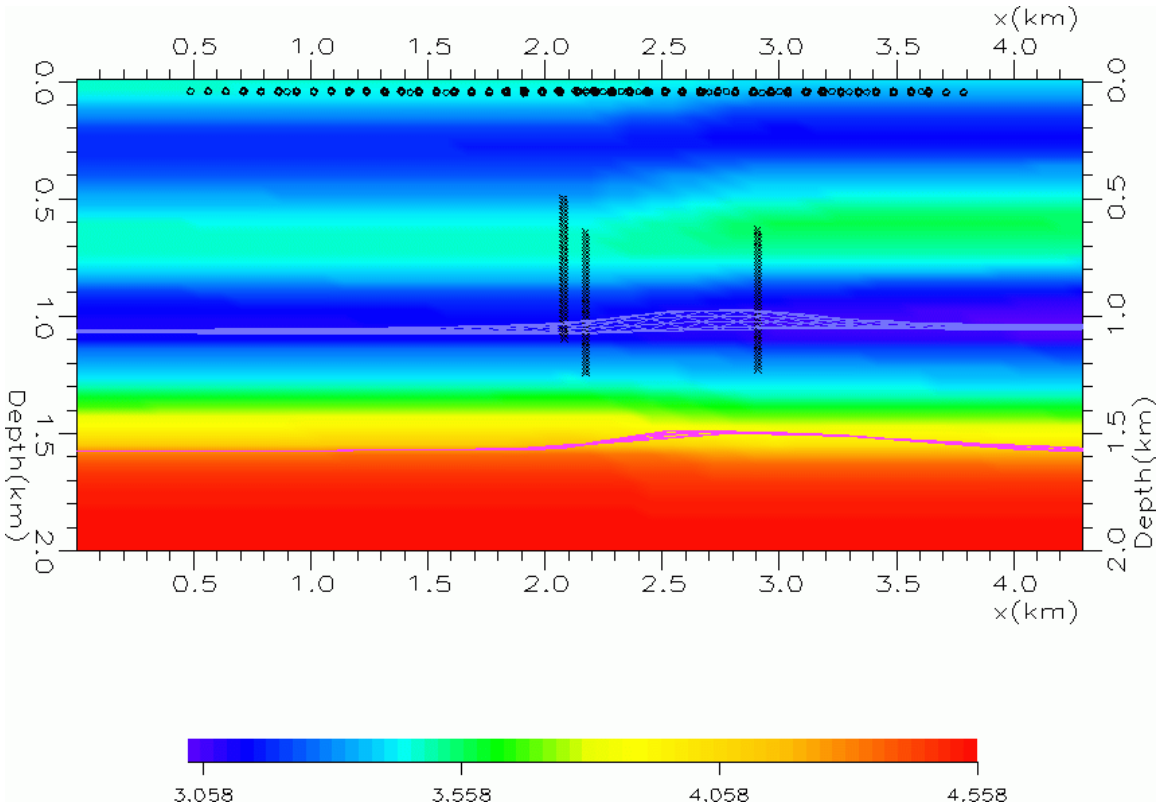

Figure 16 East-West cross section through the center well showing the background velocities, the target horizons and the distribution of sources and receivers.

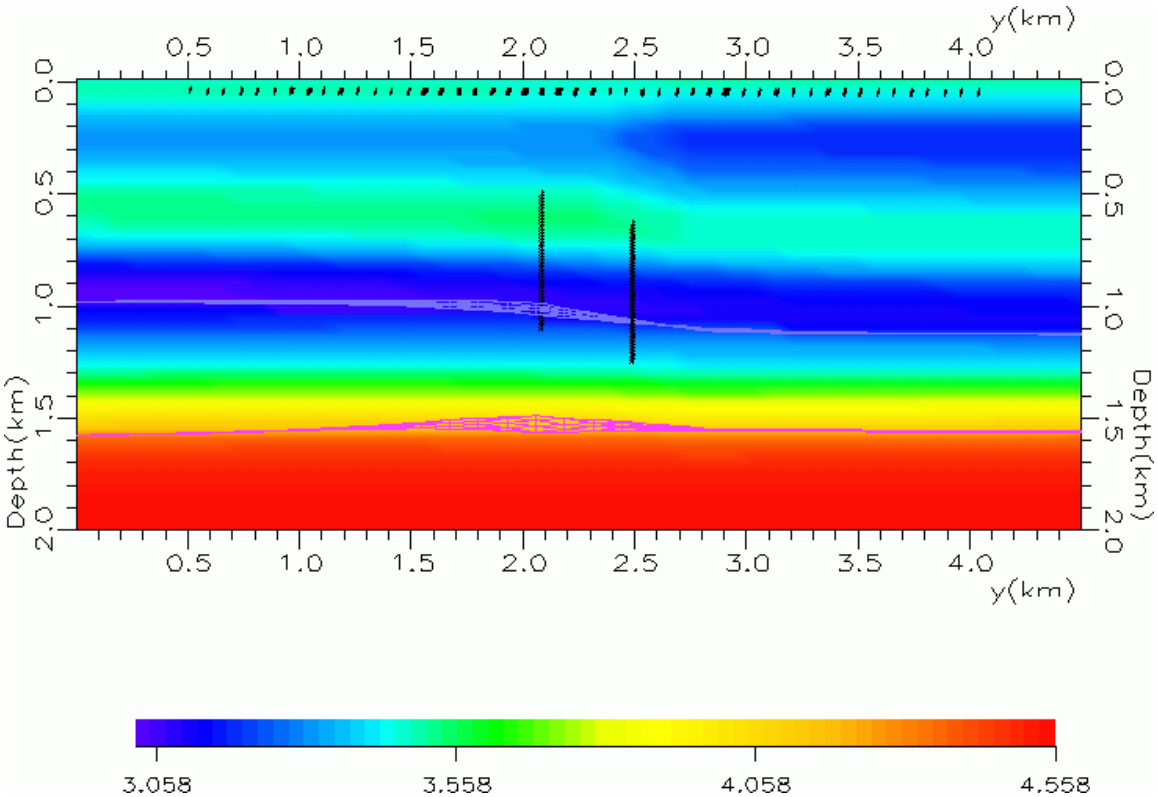

Figure 17 North-South cross section through the same velocity model.

Synthetic Model 6.

This model is mainly used to show the drastic effect of an insufficient and optimal receiver distribution in a 3D borehole seismic survey. The model incorporates horizontally layered strata in the overburden and a target section that includes an escarpment right beneath the single receiver well. In the first scenario, the receiver well is equipped with a standard wireline-based 20-level receiver array and in a second scenario, we assume the well to be equipped with a tubing-deployed 80-level or 160-level receiver array. The drastic effect on the image by using too short of a receiver array can be nicely shown with the target horizon which includes a steep escarpment. The source distribution at the surface is assumed to be dense enough and to extend to very far offsets in order not to have an effect on the illumination.

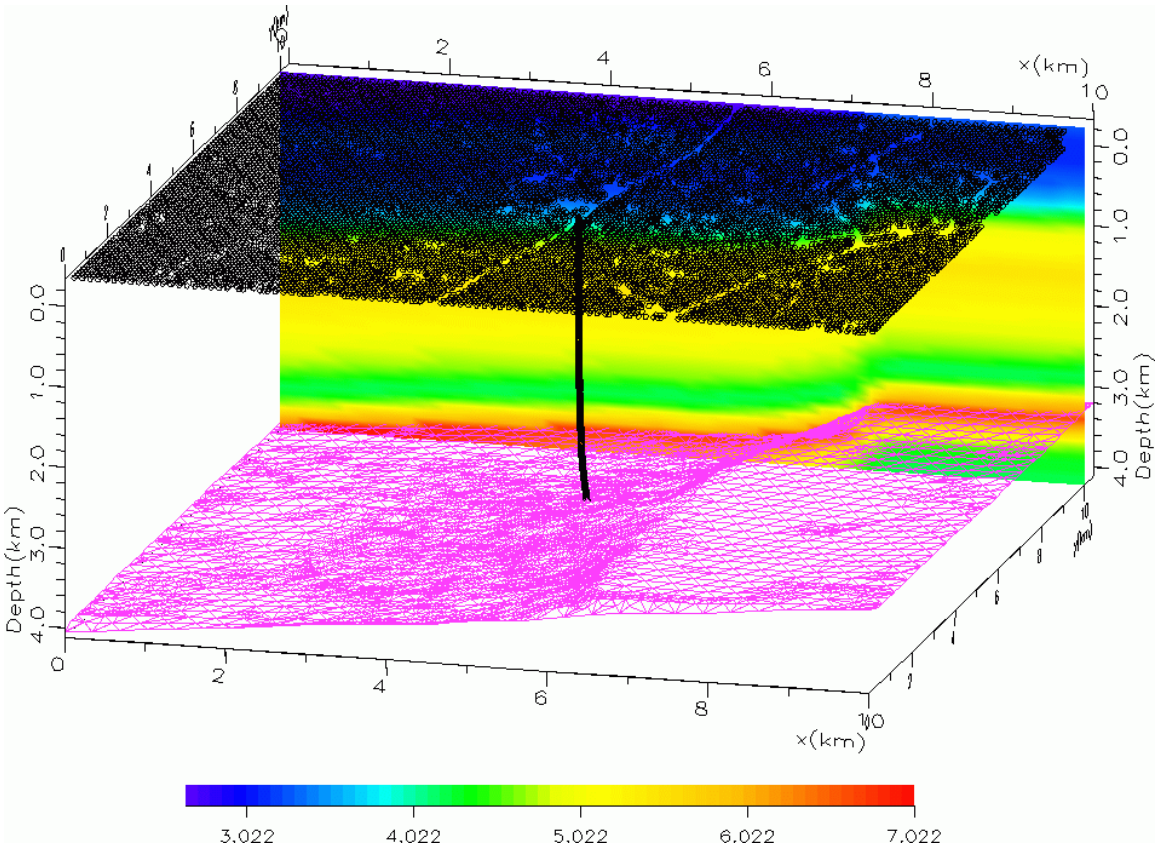

Figure 18 3D model used to investigate the effect of different receiver array settings. The well in the center extends down to the top of the target horizon featuring an escarpment and is slightly deviated. 10,000 surface sources are equally distributed over a 10km by 10km swath.

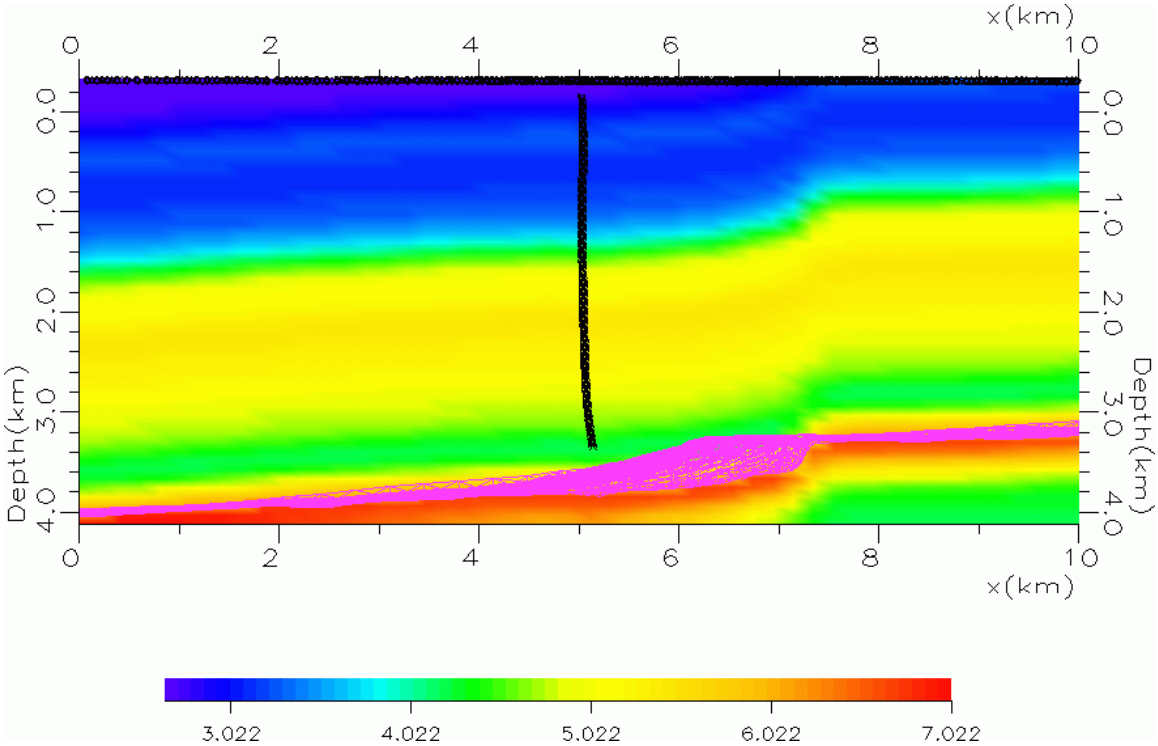

Figure 19 Cross section through the receiver well showing the escarpment on the target horizon and the slight deviation of the well.

Task 3

Generate single wave type and full waveform 3D VSP synthetic data for use as test and validation data using existing finite difference software.

Synthetic Model 1. 2D Salt Model

We used a full waveform modeling technique to generate single-component and multi-component wave field responses for 2D VSP acquisition line through a salt model. We captured the entire wave field in the VSP receiver array to use in test processing. We also captured snapshots of the entire wave field to understand the propagation mechanism in this salt model.

The source wavelet was a pressure pulse located at 7.6 m below free surface. It has a dominant frequency of 25 Hz. The 3D VSP receiver array was located in a vertical well with receiver locations from 0 ft to 9,144 m depth with 7.6 m spacing. Sources were located at 30.5 m spacing from +/- 3,658 m away from a well. The well was located at x = 7,315 m. The number of individual source positions was 241. The receiver array records pressure, z-component displacement and x-component displacement, completing our multi-component data set for later tasks.

Wave field snapshots were generated every 50 msec and both the z-component displacement, and x-component displacement were saved. The data displayed in Figure 20 shows a snapshot of a wave field with a velocity model overlay. Figure 21 shows a comparison between VSP and surface type recordings. Although the array captures the entire wave field, Figure 22 and Figure 23 show the subset array capture for 0-9,144 m receiver depth. These shot records show a clean pressure and multi-component wave field that exhibit many of the complexities that we would expect to see in a real data set.

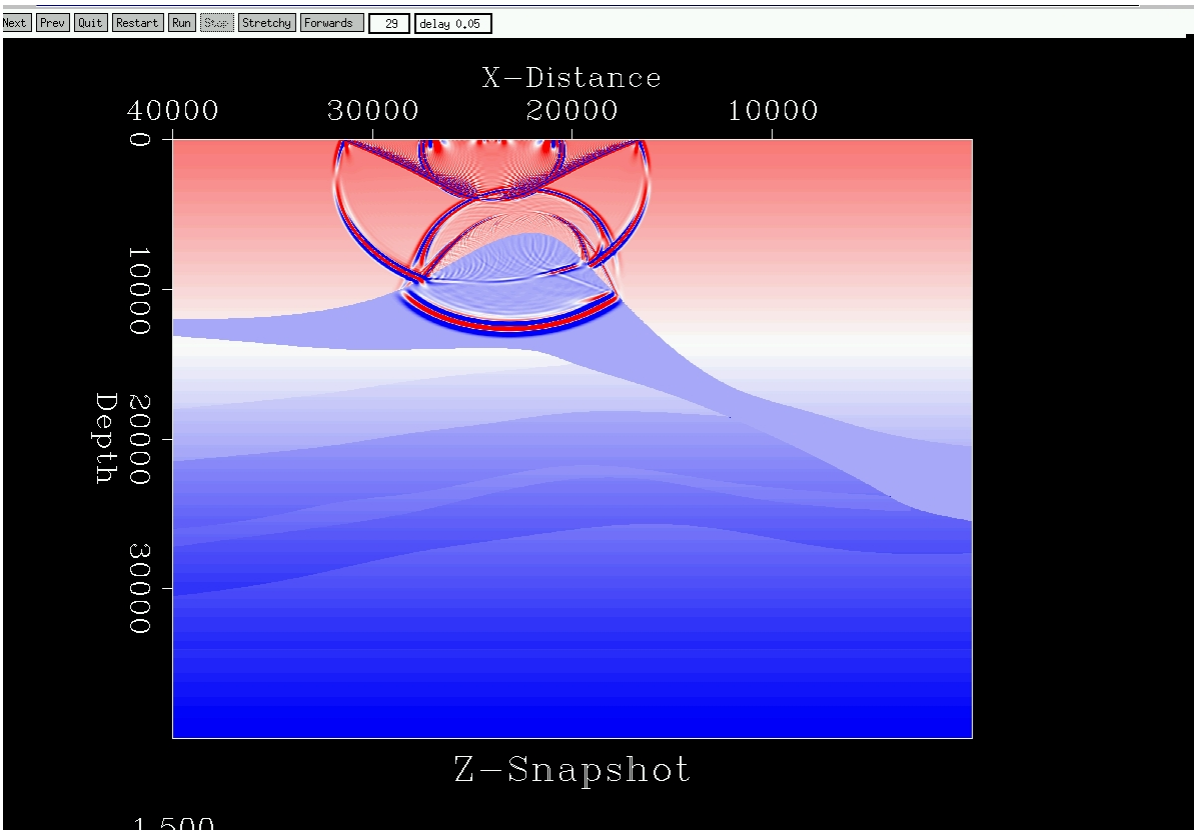

Figure 20 Wave field snapshot at 1.5 sec, z component.

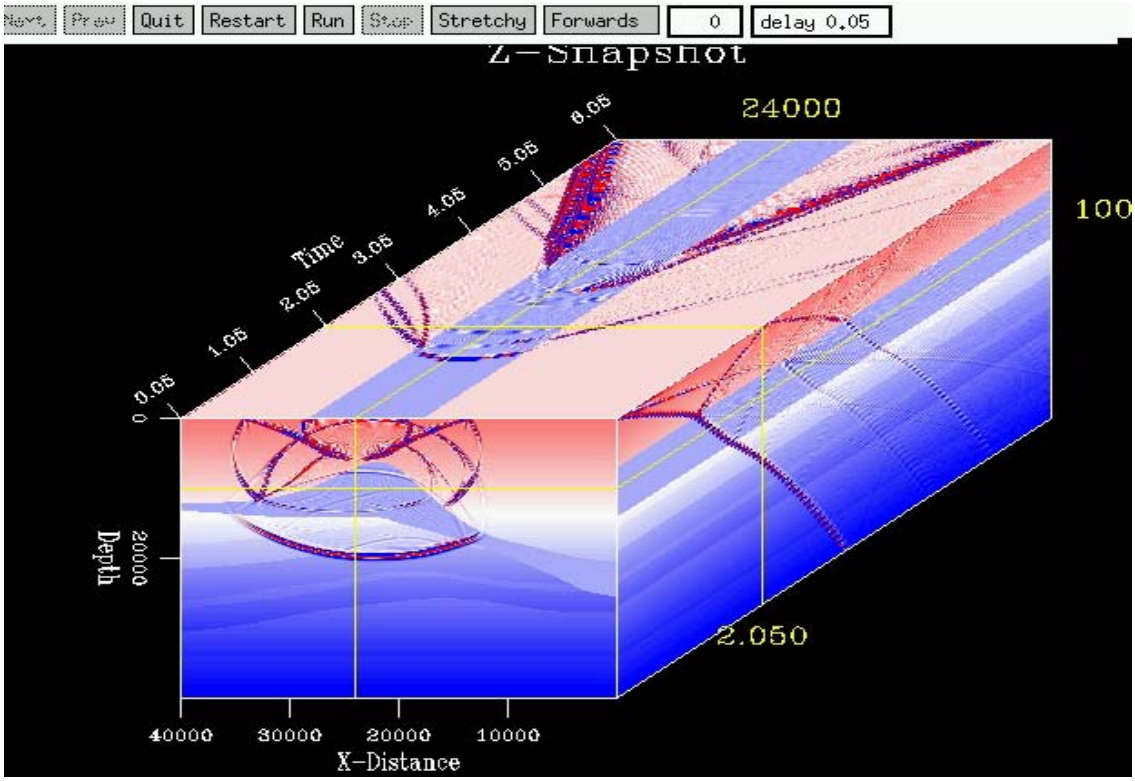

Figure 21 This cube shows the snapshot in the velocity model on the front face. The third dimension is time, thus the side face shows a VSP recording of this shot in the well, whereas the top face of teh cube shows the corresponding surface seismic shot record

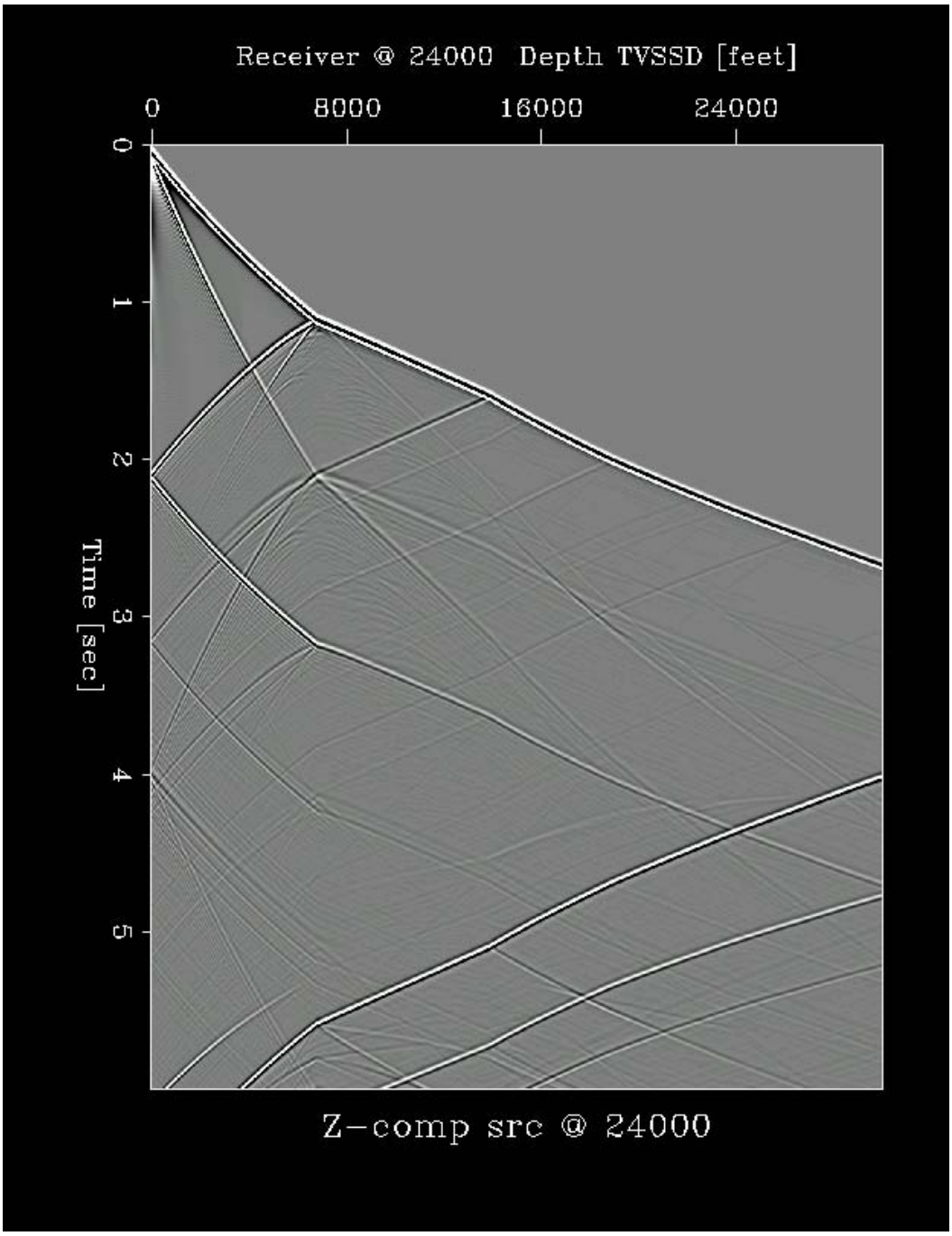

Figure 22 VSP recording of the vertical (Z) component for a hypothetical receiver array deployed between the surface and 9,144 m depth.

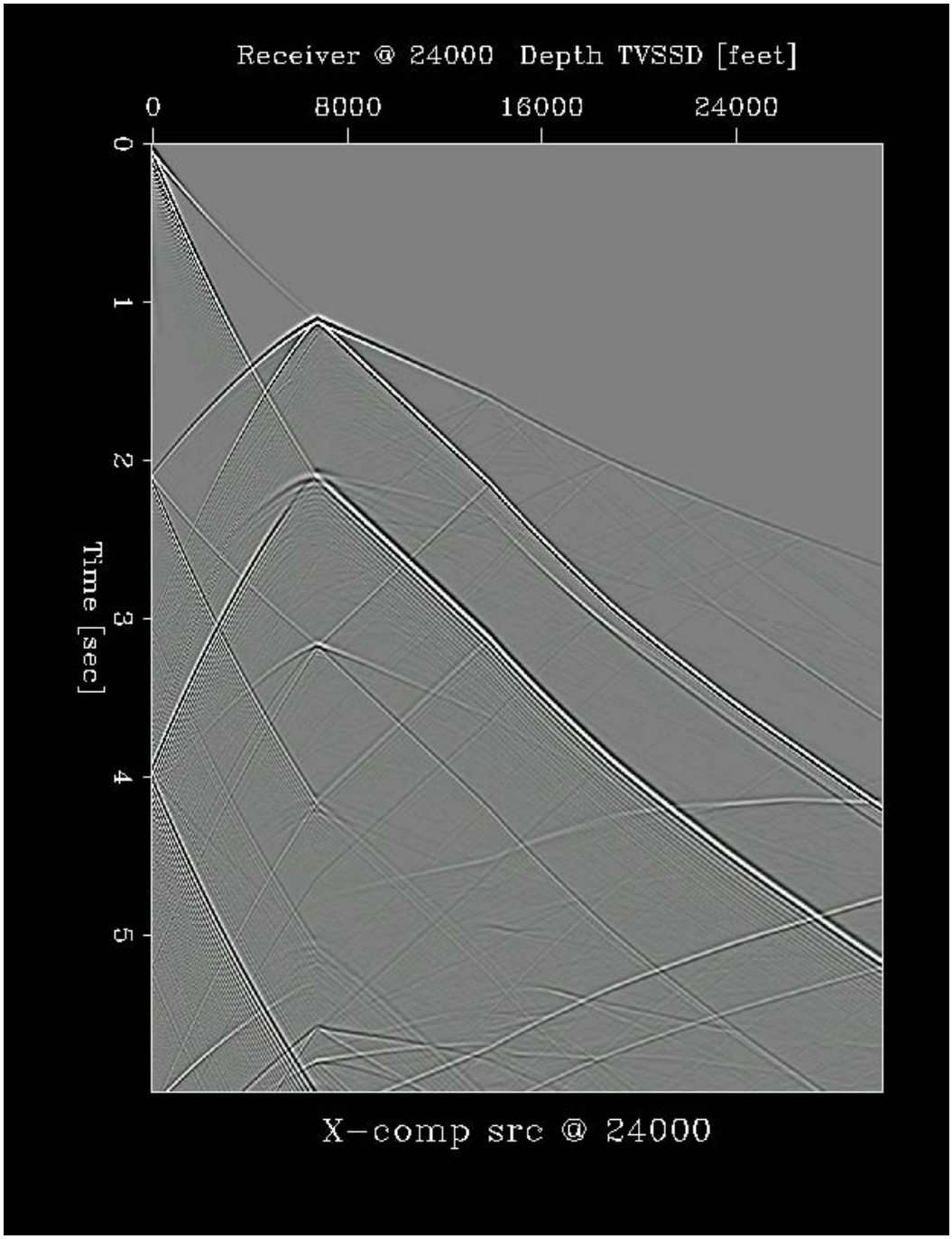

Figure 23 VSP recording of the horizontal (X) component for a hypothetical receiver array deployed between the surface and 9,144 m depth.

Synthetic Model 2. 3D Layered Model

The objective was to use 3D ray tracing modeling techniques to generate true amplitude reflected multi-component seismic data for selective wave field responses for a 3D VSP geometry. For this model, we captured ray codes for PP reflections and PS conversions from target horizons in the VSP receiver array to be used in future test processing. We analyzed wave fronts to understand the propagation mechanism in this model. We generated seismic data with an optimized circular source pattern. The optimization was based on the horizontal width of the Fresnel zone at the target levels. The source wavelet was a zero-phase omni-directional pressure pulse located at the surface.

The 3D VSP receiver array is located in a vertical well with receiver locations from 123.5 m to 1,327 m depth below surface with 15.2 m spacing. Sources are located at the surface at a maximum offset from the well head at 1,524 m. The receiver array records z-component, x-component and y-component displacement. Thus we have a multi-component data set available in later tasks.

During the ray tracing we generated both p-p reflections and converted wave p-s reflections. Figure 24 shows a selected shot record from these data.

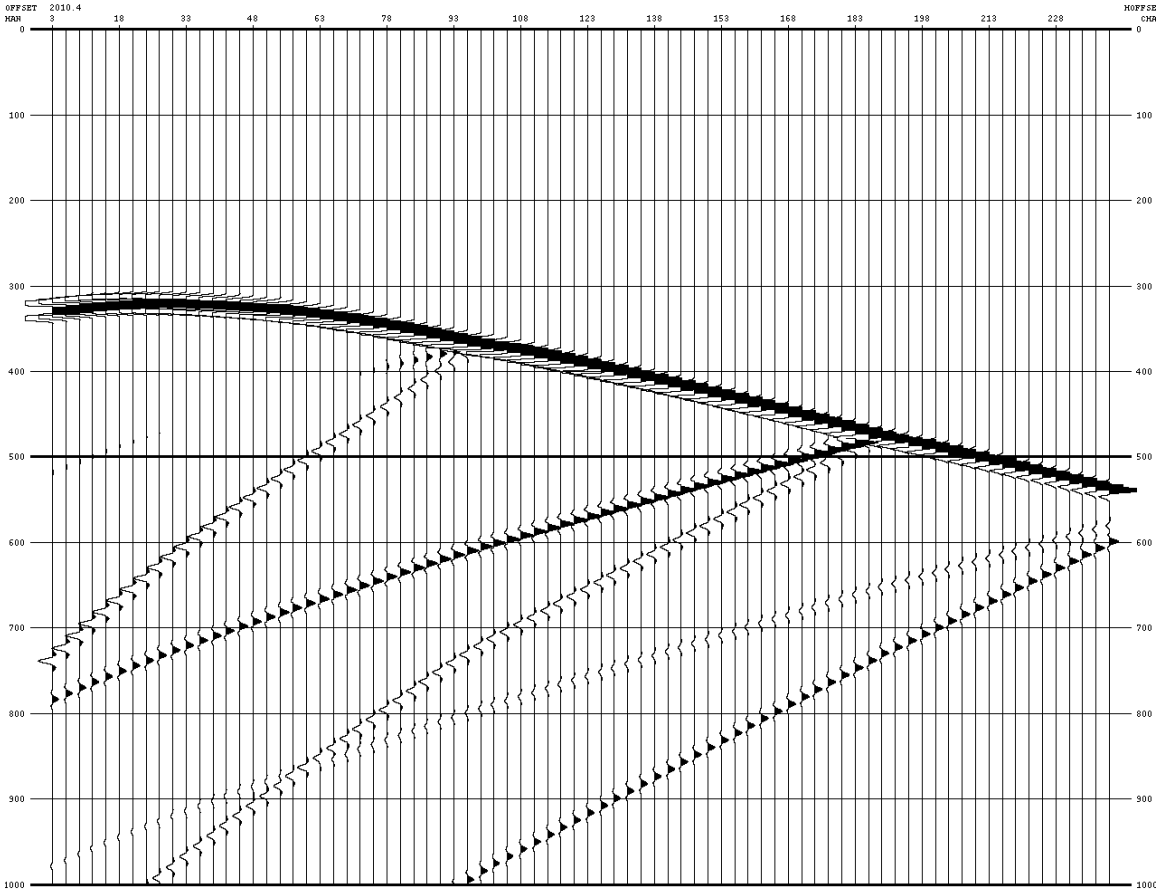

Figure 24 Vertical component of the elastic reflected wave field. Upgoing PP reflections and PS conversions from three target horizons are included.

Synthetic Model 3 San Andres Fault Zone

The 3D model was constructed to generate test data in a 3D VSP layout for the deviated receiver array at the main hole location. Figures 25-27 show various aspects of fault zone illumination that one can expect to extract from the VSP data. Figure 32 shows a sample shot gather from the synthetically generated data. Only the fault reflections and the first arrival are being computed. When all surface shots are processed, we were able to image the fault zones very well, as shown in Figure 28. Both of the faults are steeply dipping, and one of them dips more than 90 degrees away from the receiver well. Finally Figure 29 shows a snapshot of the wave front as it is being computed. Waves originate from a source point, get reflected off of the faults, and are captured into the deviated receiver array.

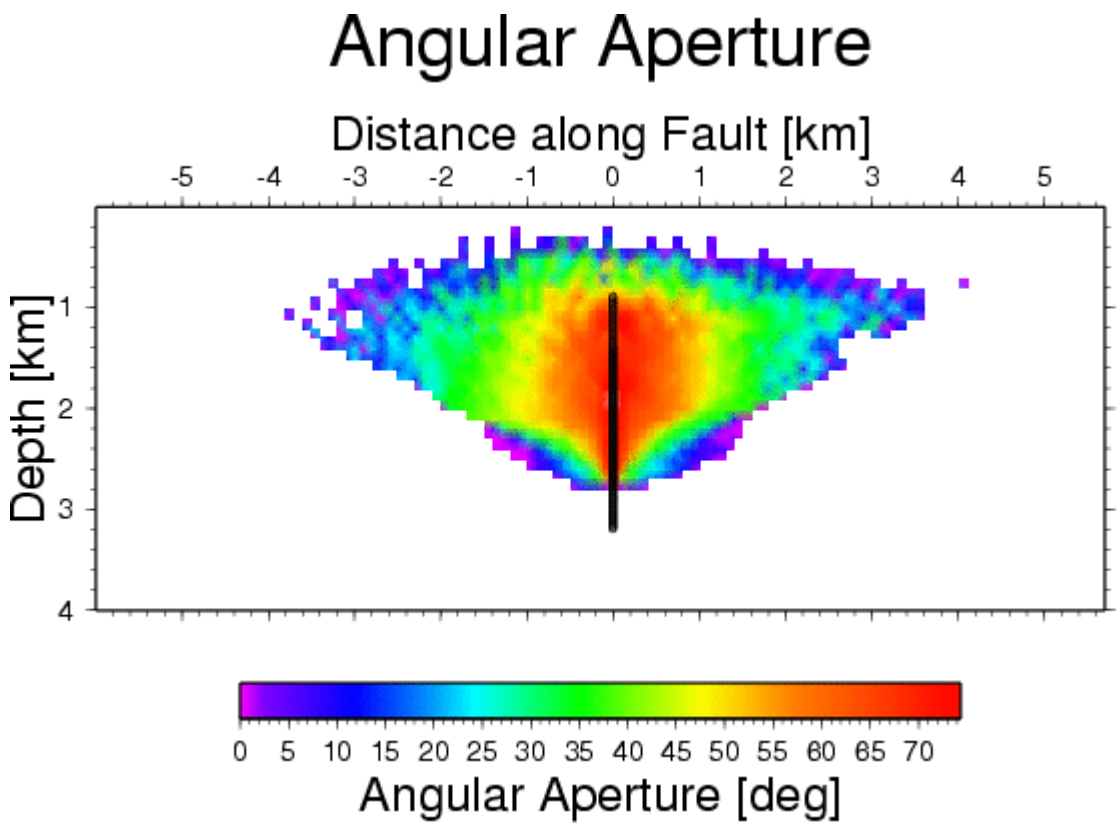

Figure 25 Angular aperture on the vertical fault plane for a 3D shot geometry recorded in a long borehole receiver array penetrating the fault zone..

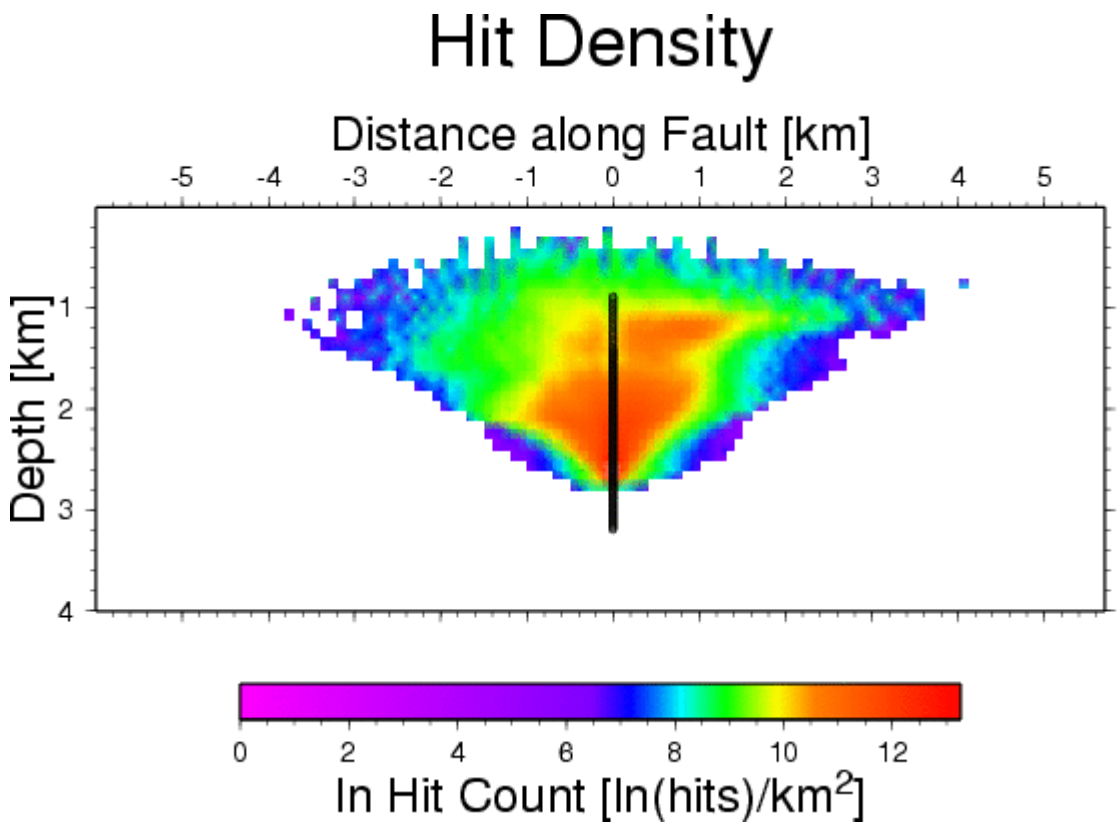

Figure 26 Ray density and illumination estimate for the same geometry.

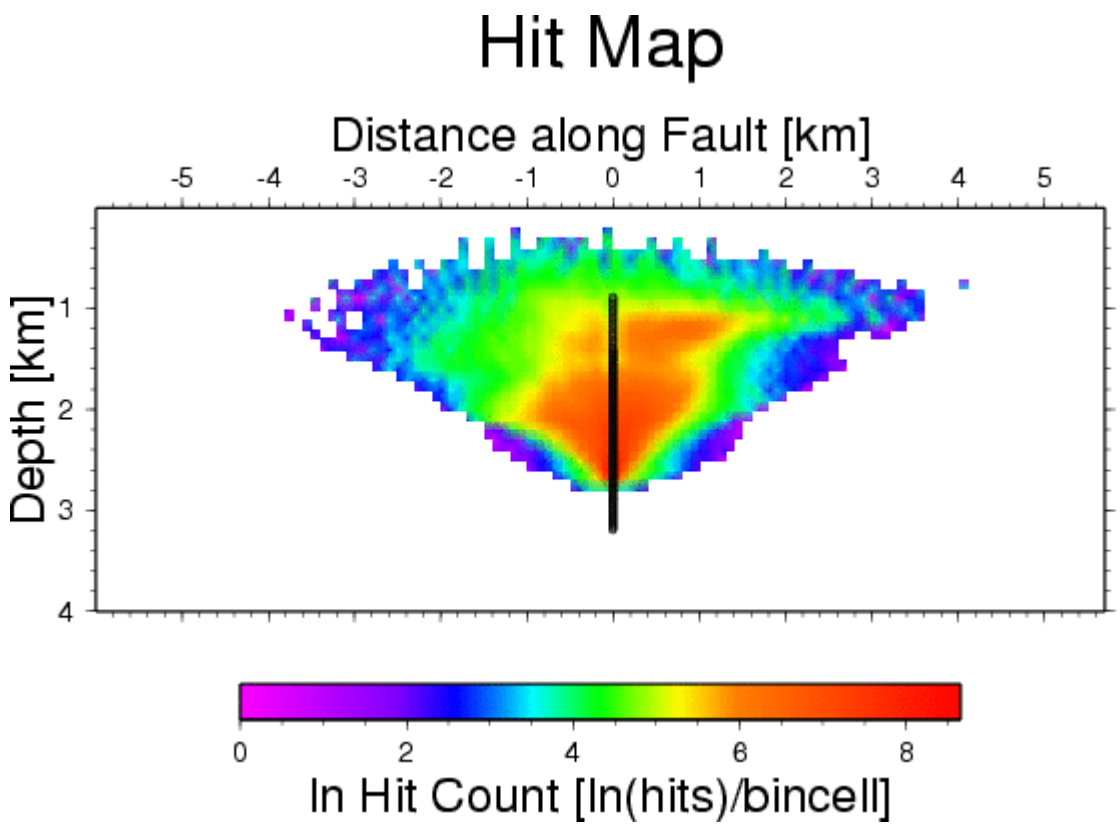

Figure 27 Ray hit count estimate for the same geometry, obtained from 3D ray tracing.

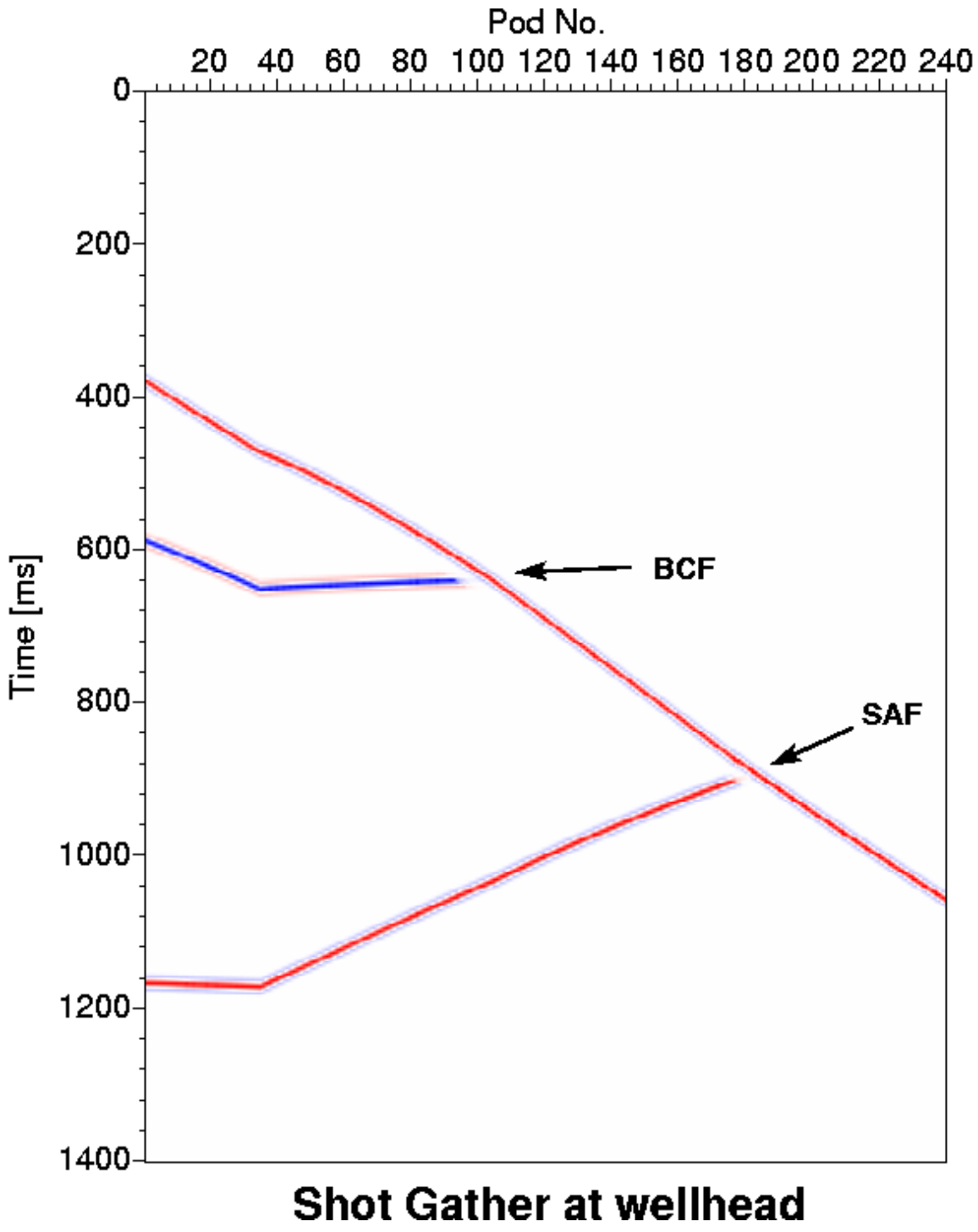

Figure28. High frequency recording of fault zone reflections and first break. The left fault (BCF) exhibits a negative velocity contrast,and the right fault (SAF) is modelled as a positive velocity contrast.

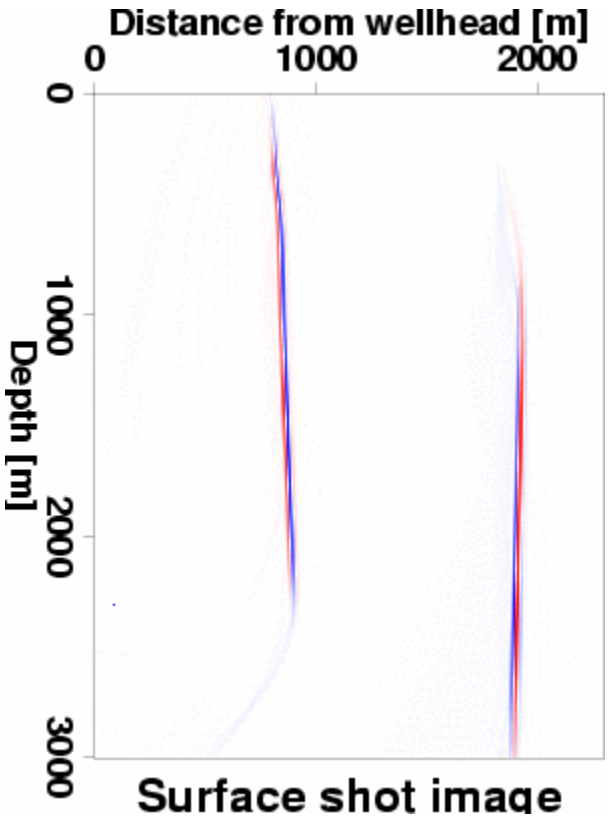

Figure29. Synthetic data after pre-stack migration. The fault zones are imaged very well. One fault is dipping more than 90 degrees away from the receiver well.

Synthetic Model 4.
This very simple model features a horizontal reflector at a depth of 2.0 km and a homogeneous overburden. It is used to establish 3-component polarity standards and to test and validate 3-component processing algorithms. The 3-component response was modeled using ray tracing in order to get a clear and unambiguous benchmark dataset. Figure 30 shows an example synthetic 3-component receiver gather for 3 shotpoints and assuming a zero-phase wavelet. Hodogram responses can be modeled for a variety of different source signatures.

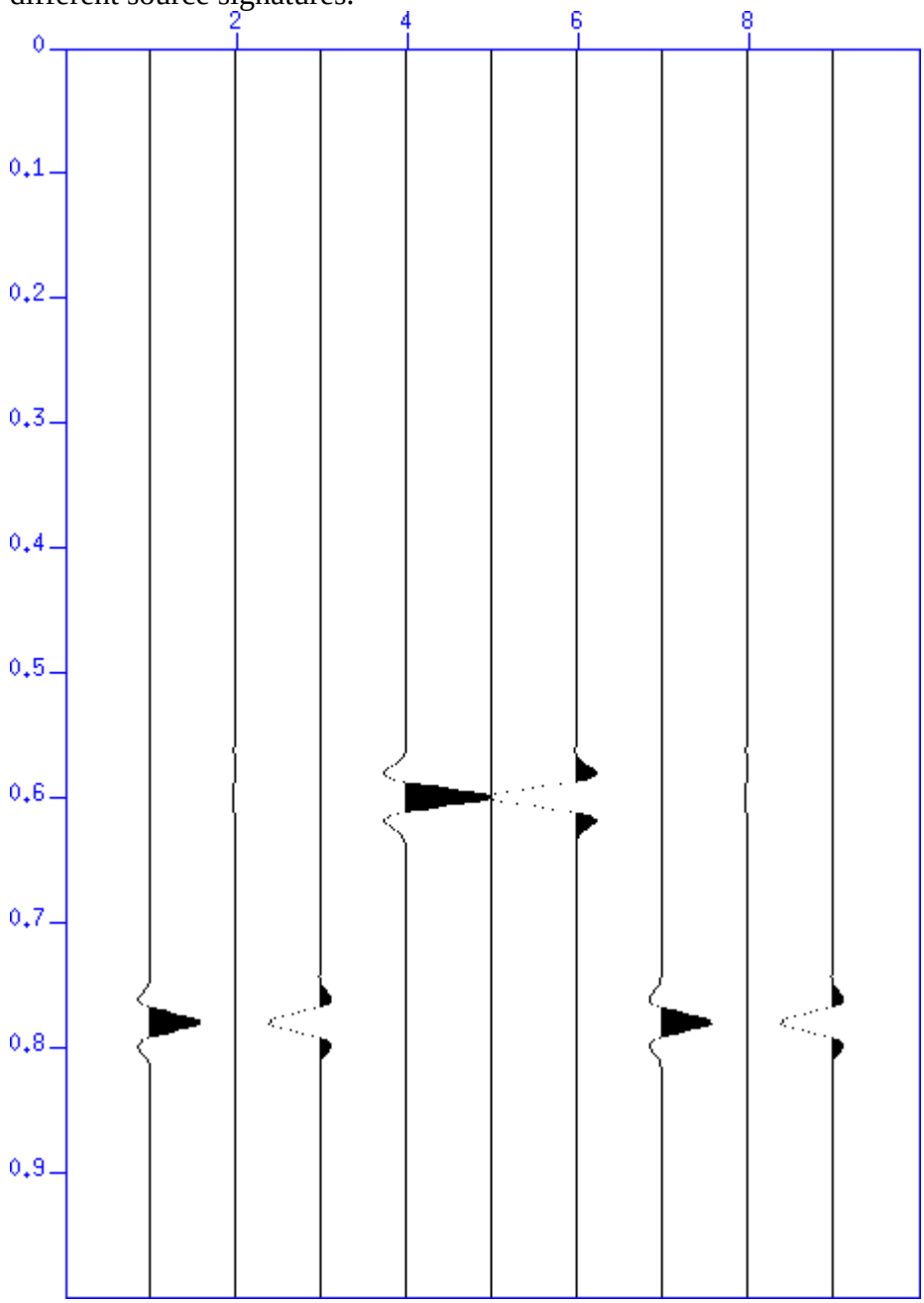

Figure30. 3-component receiver gather for 3 shotpoints using a zero-phase wavelet.

Synthetic Model 5.

This model consists of two target horizons with a moderately steep anticlinal structure. Synthetic data for this model was created using raytracing of P to P reflections off two target horizons. Imaging of the synthetic data allowed us to quantify possible artifacts near the edge of the illuminated area on the anticline that can be caused by the imaging algorithm. Methods to mitigate imaging artifacts can be tested and validated using the synthetic data.

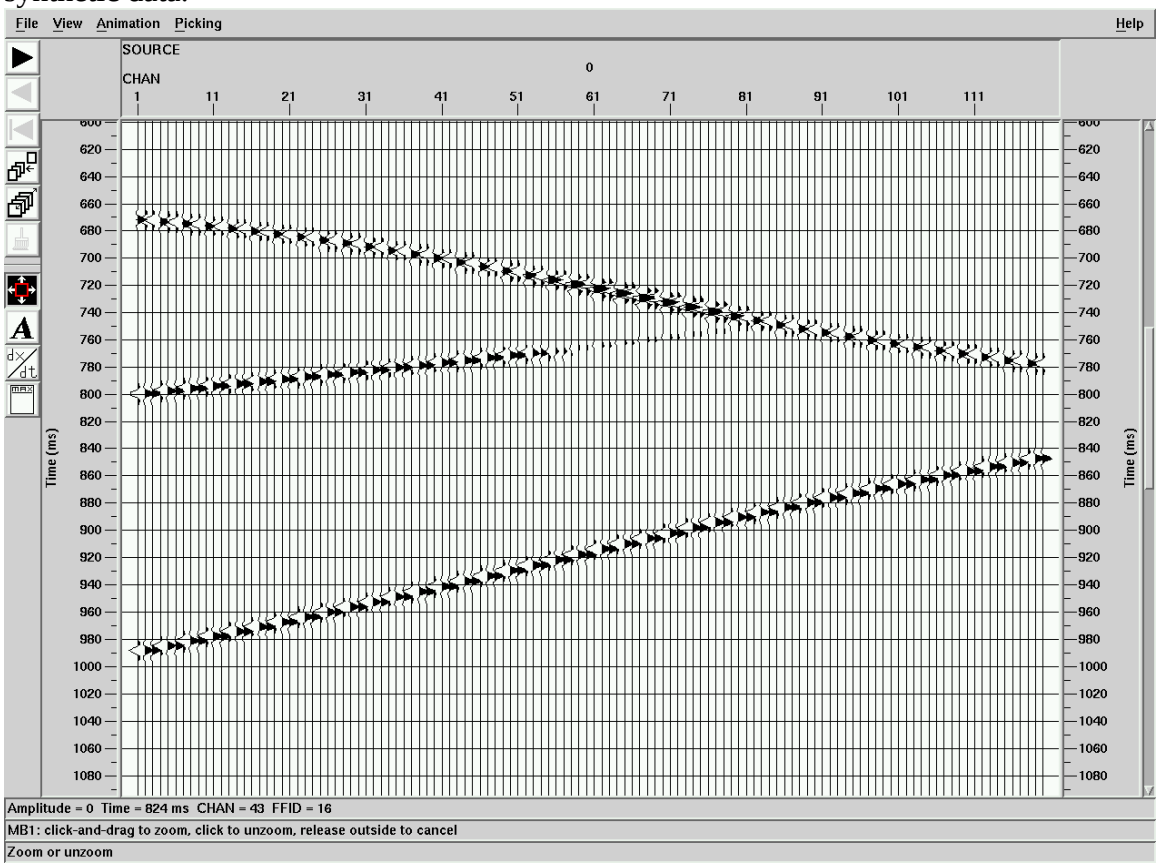

Figure31. Example 3-component shot gather showing the direct P arrival and two P to P reflections from the two target horizons. Amplitude effects due to geometrical spreading as well as phase effects due to caustics are included in the synthetic data. The data id displayed with an AGC to better visualize the upgoing reflected energy.

Synthetic Model 6.

This model is used to test illumination and imaging effects that are imposed by the length of the receiver array in the borehole. In a first step, illumination modeling using 3D raytracing was performed. The resulting fold illumination maps (Figure 32) show the difference between a 20-level receiver array and a 160-level receiver array in the same borehole. The angular aperture on the target horizon, i.e., the difference between the minimum and maximum incidence angle of specular rays at a depth point is a direct measure of the quality of the depth image: The wider the angular aperture and the wider the imaging operator, correspondingly, the better the final migrated image will be. This is shown in Figure 33 for a 20-level array and a 160-level array in the same borehole. Note the very narrow aperture below 10 degrees for the 20-level array that would not allow obtaining a reliable depth image of the hummocky target horizon. In contrast, the angular aperture for the 160-level array goes up to 45 degrees which allows a sufficient operator width for depth migration so we can expect to image also the steeper parts of the escarpment on the horizon. Figure 34 shows example shot gathers of the raytraced synthetic data for the 20-level array (left) and the 160-level array (right).

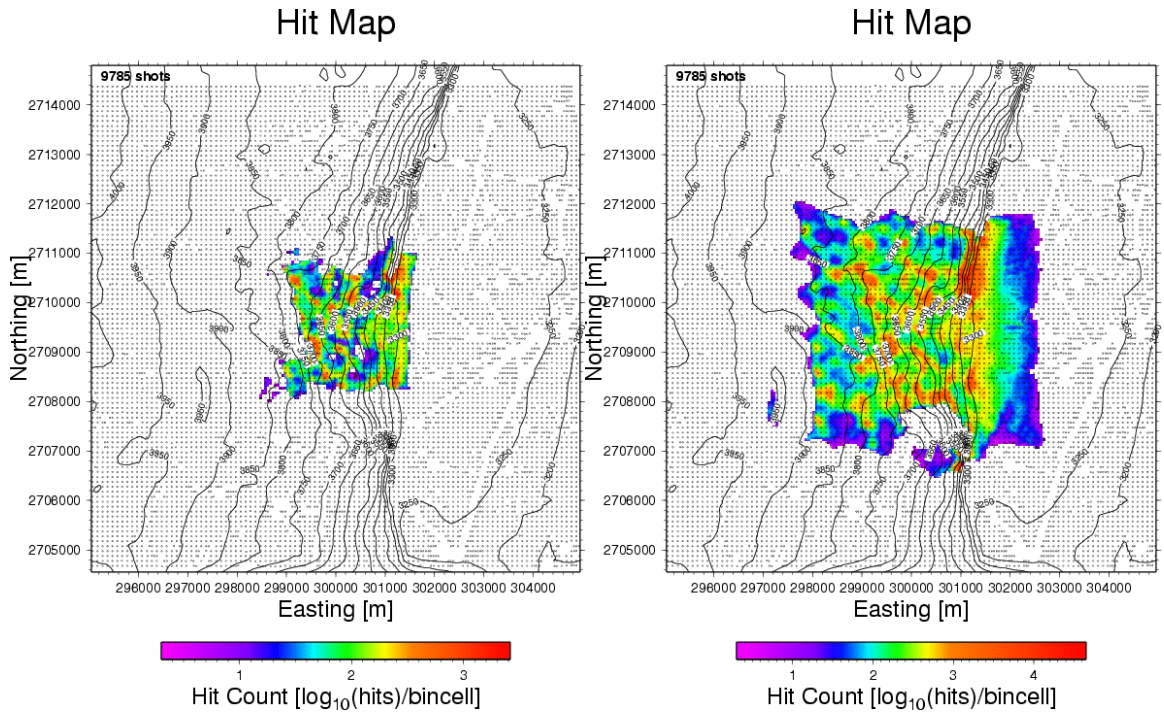

Figure 32: Illumination map on target horizon (indicated by black contours) for (left) a 20-level array hung high above the target and (right) a 160-level array filling the entire borehole.

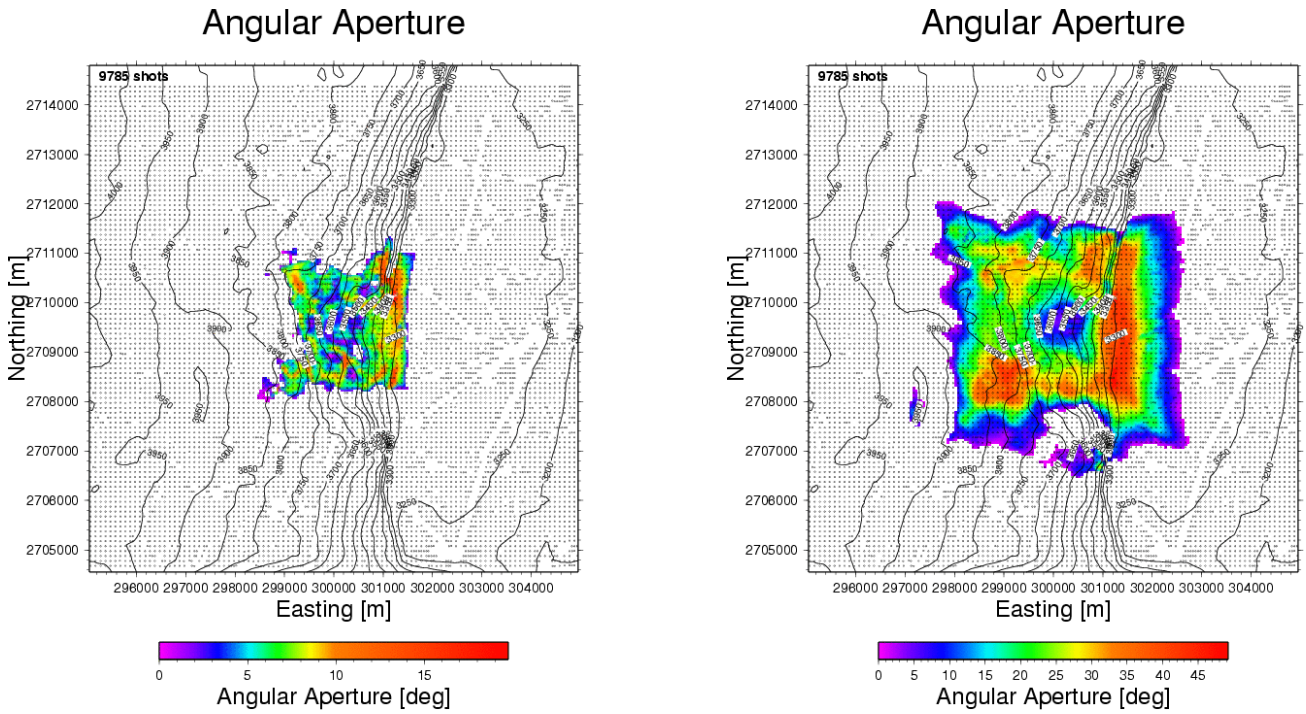

Figure 33: Angular aperture maps for the 20-level array (left) and a 160-level array (right in the same borehole.

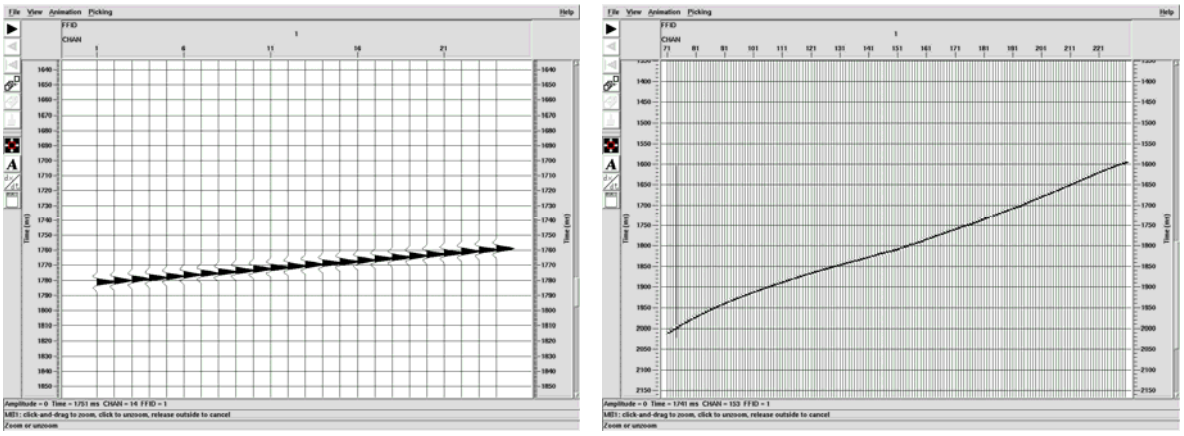

Figure 34: Example shot gathers for a shot into a 20-level array (left) and a shot into a 160-level array (right) which essentially fills up the entire borehole.

Task 4

Document data selection and model generation, archive synthetic borehole seismic data.

Geologic models and seismic data files that are deliverables of this project are listed in Appendix A. They include velocity grids and SEGY-formatted data files of the synthetic data for Synthetic Models 4, 5, and 6.

Task 5

Collect the basic data types that will be displayed in the 3D framework. Examine specific display and functionality requirements for each data type.

Many basic data type classes were used and re-designed. These include such things as physical property models and seismic volume definitions, 2D maps, source and receiver locations, three-component seismic traces, well log surveys and log curves, and ray paths. Below is a partial list that is representative of the breadth of the data classes that were used in this effort.

3CSeismicTrace
AnisotropyModel
AxisInfo
AxisTransform
CoordSysInfo
Contour
FBPicks
GridVolume
Horizon
ImageMap
Mesh
RayPoint
RaySet
SeismicTraceData
SrcLocation
StaticSolution
StructuralModel
SurfaceGenerator
Tomography
VelocityModel
WellInfo
WellLog
WellLogCurve

Many low-level data type classes were also used and re-designed as part of this project. These include for example, classes to handle basic drawing capabilities, on-screen menus and widgets, seismic data processing, lists, and math functions. More discussion on examples of the higher-level seismic data processing aspects is presented in the Task 15 section.

Task 6

Design and document the multi-component display framework by analyzing the data flow and functionality requirements. Select software building blocks that are portable and widely available.

Overall System Architecture

Our overall system architecture is based upon open standards that provide reliability, portability, and ease of use. In particular, we employed three low-level toolkits in our software development. OpenGL is recognized as the industry standard for high performance graphics. It is vendor-neutral and available across all operating systems, and known for the ability to handle demanding graphics displays. OpenInventor is a higher level graphics toolkit that essentially sits on top of OpenGL. It too is available across a wide variety of computer systems, and very widely used in the software applications that are graphics-intensive. These toolkits simplify our graphics programming efforts by providing a rich set of display capabilities. Finally, QT is a cross-platform toolkit that provides utilities for building graphical user interfaces. These and the tools that were available in the already existing P/GSI framework provided us with a solid extensible foundation upon which we were able to build tools specific to our needs in presenting, processing and manipulating 3D borehole seismic data. Figure 35 shows an overview of the software architecture. The three red areas indicate software components that were added as part of this grant.

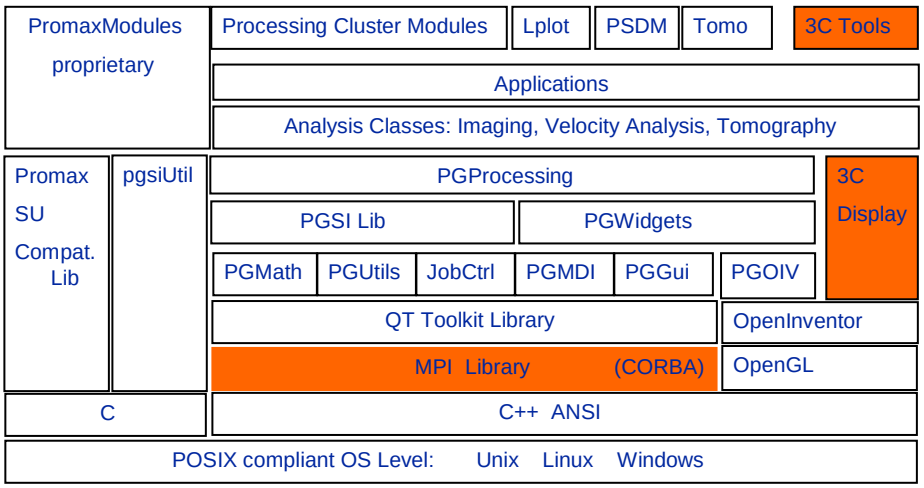

Figure 35: Software architecture overview. The three red areas indicate software components that were added during this project.

The Display Framework

Figure 36 shows the relationship of underlying framework components. Having these components configured in an optimal way allowed to derive from them multiple tools, each with its unique characteristics and tailored to specific user needs, while the basic framework remains unchanged. Figure 37 and Figure 38 show a blank skeleton of the 3D VSP Work Bench tool.

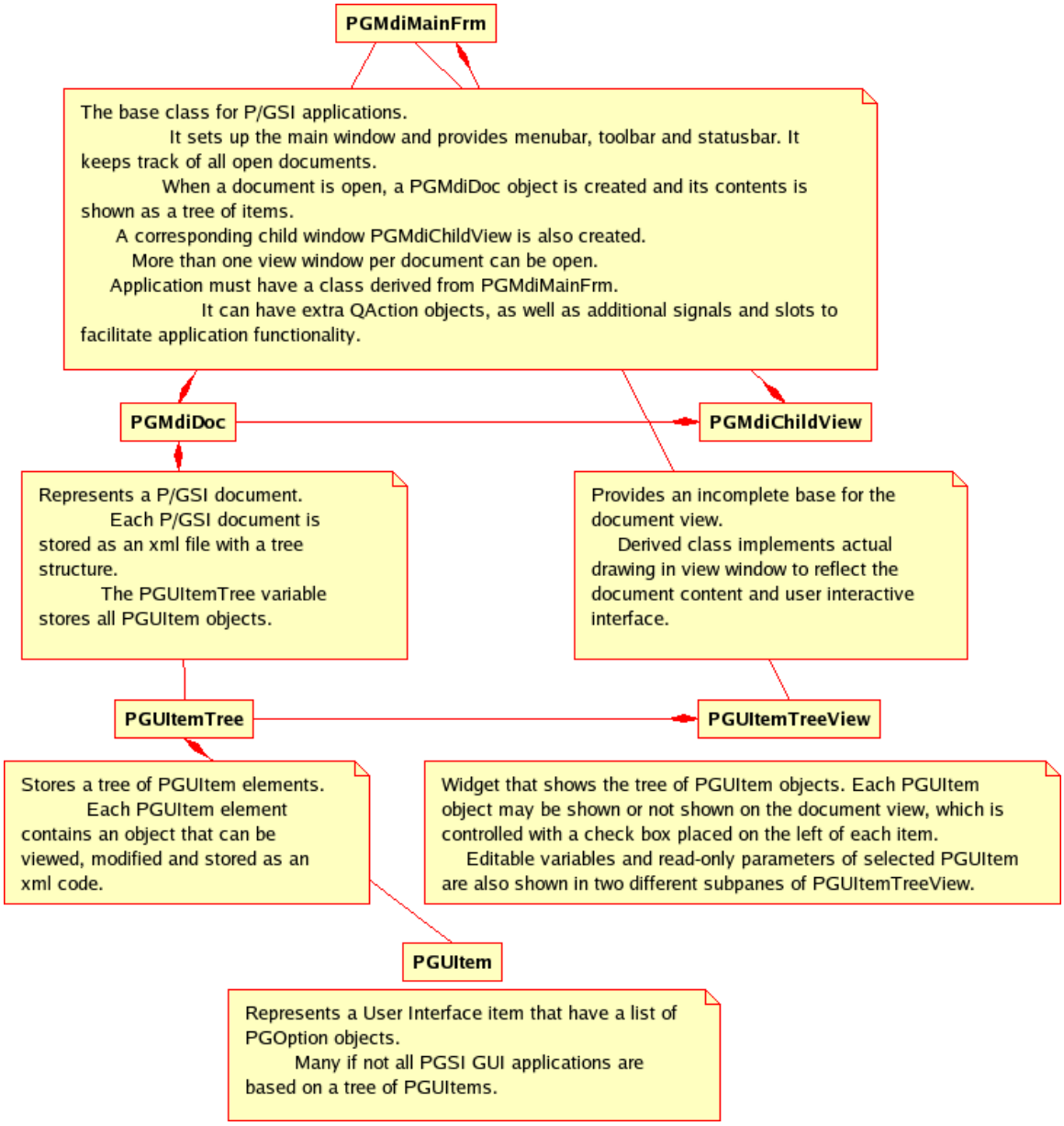

Figure 36: The application template uses this underlying library of classes. The application skeleton is able to incorporate multi-component 3D VSP displays and actions in a common framework.

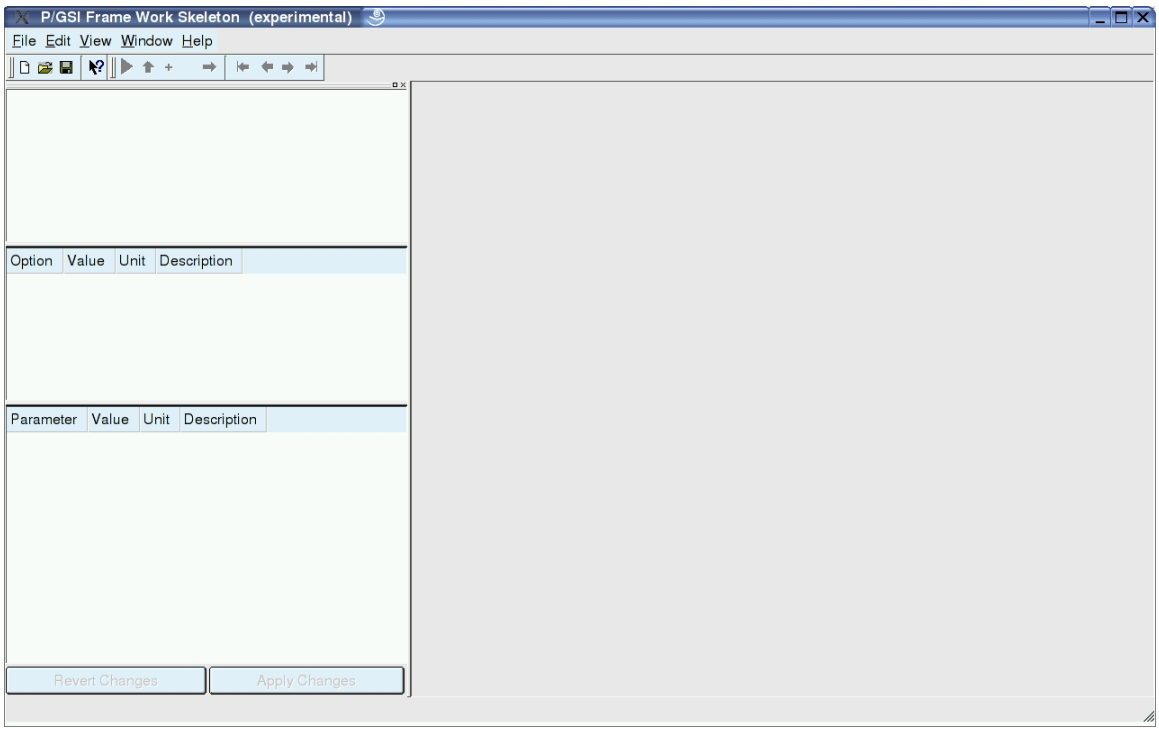

Figure 37 The application skeleton showing the basic window layout.

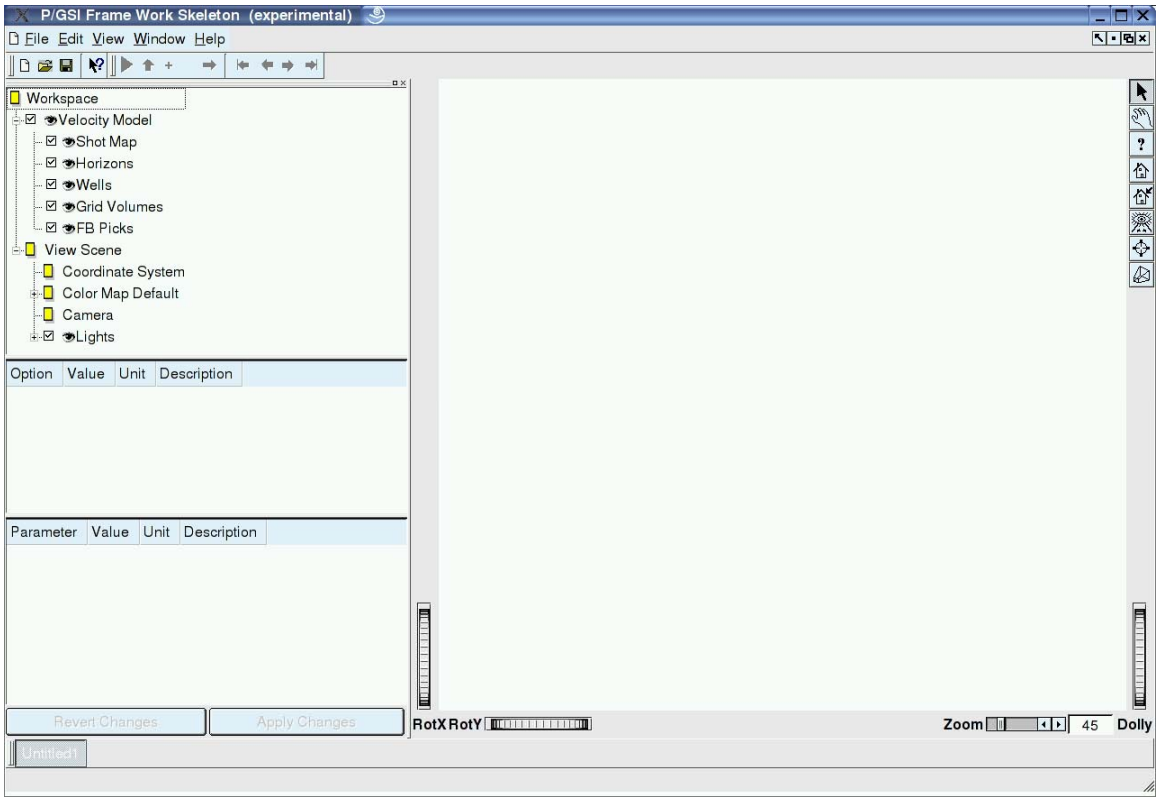

Figure 38 Visual representation of the 3D VSP Work Bench. It shows several work areas that are capable of displaying objects that are needed in the multi-component VSP processing and interpretation framework.

Once a workspace is activated, basic reusable constructs such as a list or a tree of items allow for a versatile set of objects that manage and visually represent the data. By incorporating this design pattern, a user can display simultaneously many views, even of the same data. Figure 38 above shows the workspace components in tree view. The main components are the 3D viewer window(s) and the user navigation area which includes data selection, display parameter controls, and fixed parameters.

Composite Volume-style Displays

Figures 39-46 show examples of composite interactive scenes using the multi-component 3D VSP Work Bench application. These composite displays take place in a single display window. Display items communicate seamlessly within the window and to the controlling main window.

Figure 39 starts out with a First-Break Pick item in the tree view of the main window, while Figure 40 shows a selected point view of the same data item. Figure 41 shows a display of a well log curve with a cylinder type view, consisting of color coded values mapped onto the circumference of the cylinder. The Display Type option in the main window was set interactively to Cylinder by the user. With this display type a correlation between well log data and seismic image volume slices is particularly easy to see.

Figure 42 shows a single depth slice and the bounding sides of a seismic data volume, and Figure 43 shows arbitrary horizontal slices of the same data volume.

Figure 44 shows the power of this versatile system to view a composite of several data objects within the same viewing window. Here we show the 3D VSP source locations, a well log curve, and a depth slice of the seismic volume. Rotating the entire scene and turning on two vertical slices of the seismic volume near the wellbore in Figure 45 overlays the well log curve directly onto the seismic image, confirming the location in depth of a reservoir horizon from two independent sources of subsurface data. Figure 46 shows the back side view of the seismic volume with the well log just reaching the target horizon in depth.

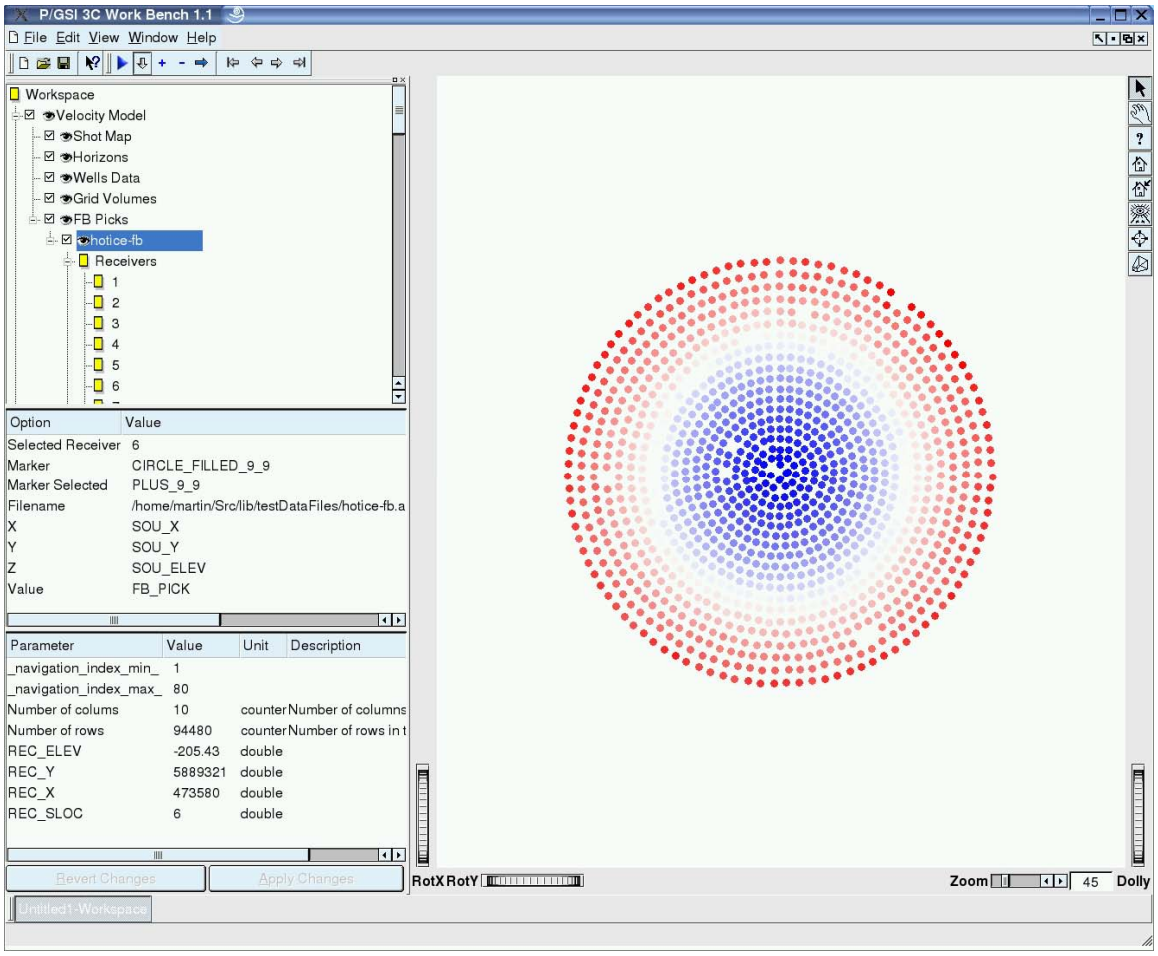

Figure 39. Picked first break display of travel time on the source locations.

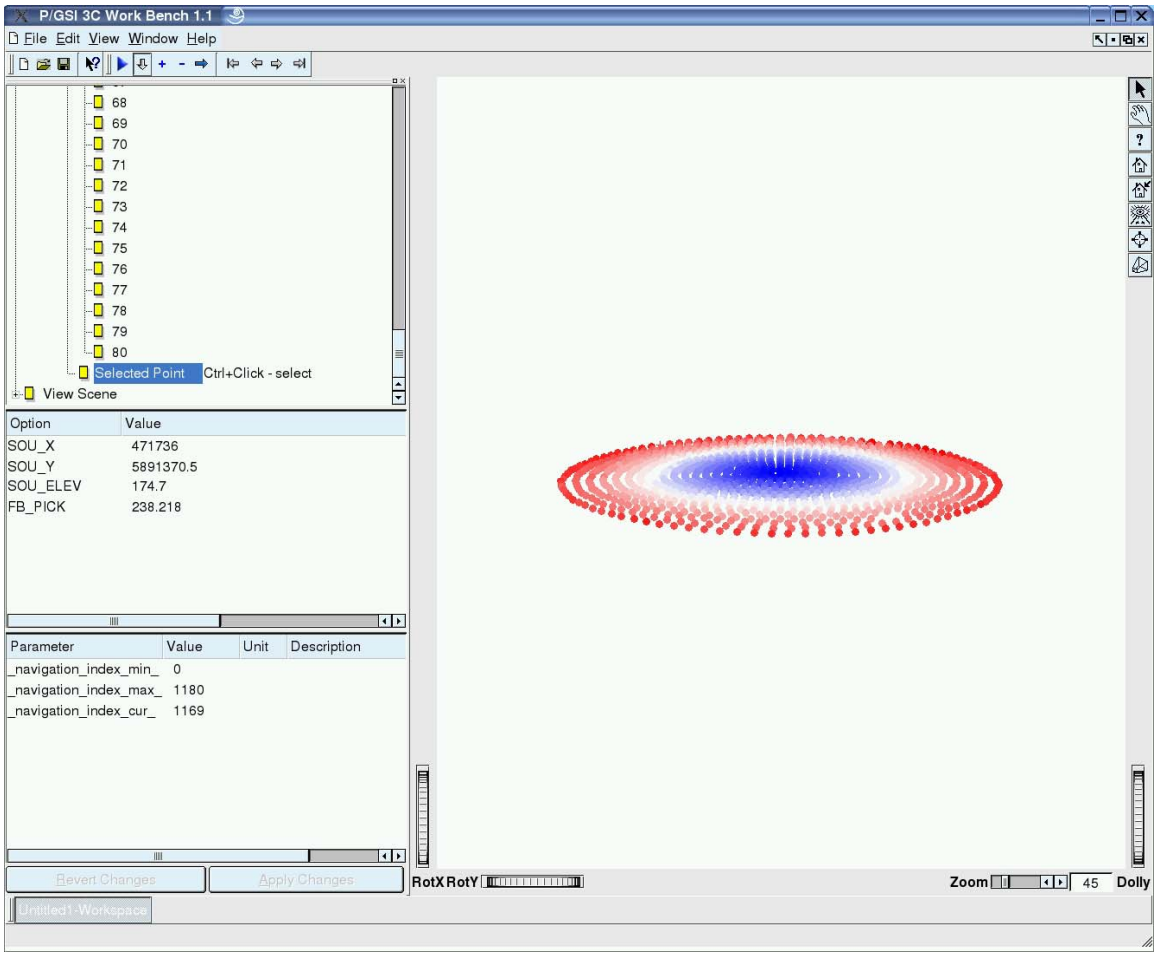

Figure 40. .Picked first break display with point selection enabled, retrieving first break times for selected source locations.

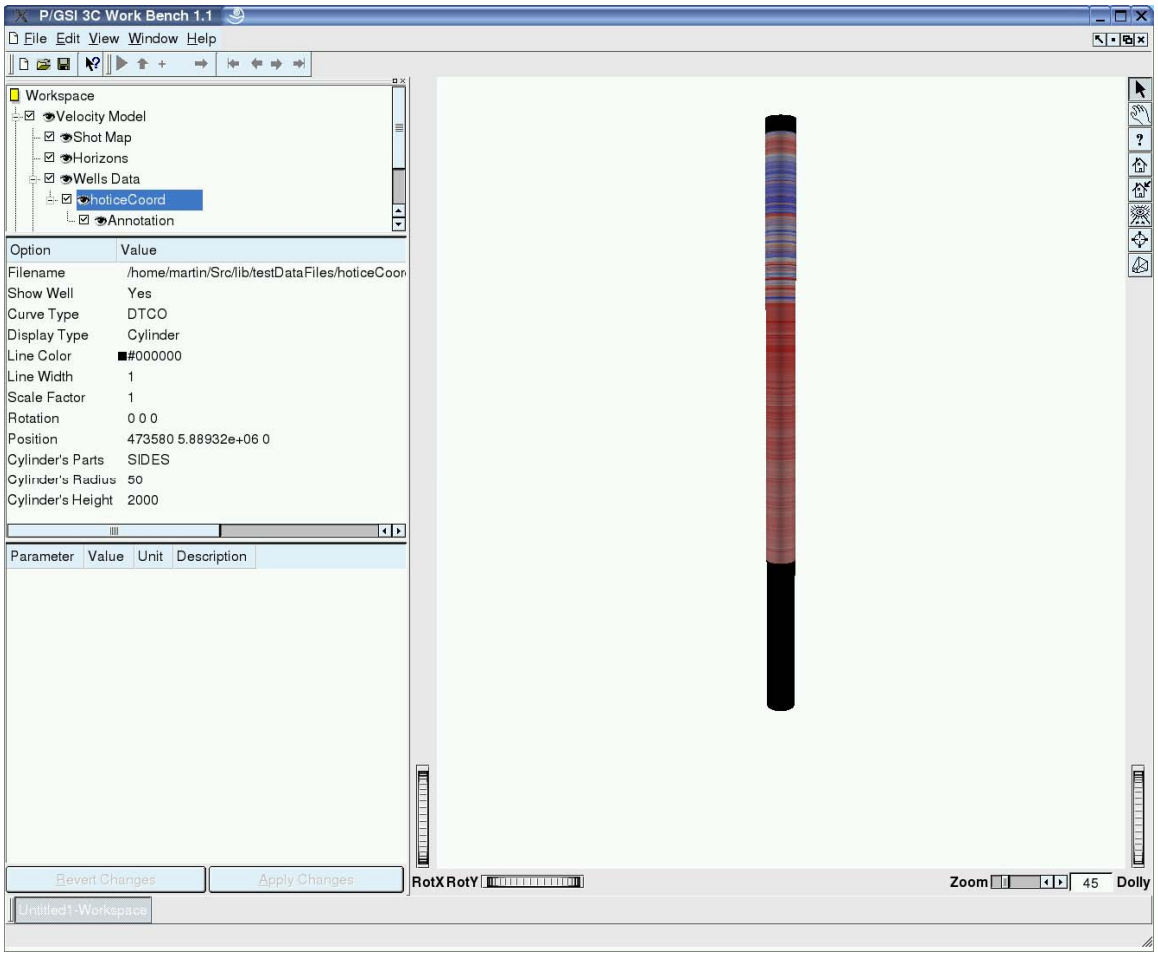

Figure 41. Well log curve displayed as a texture map along the well track.

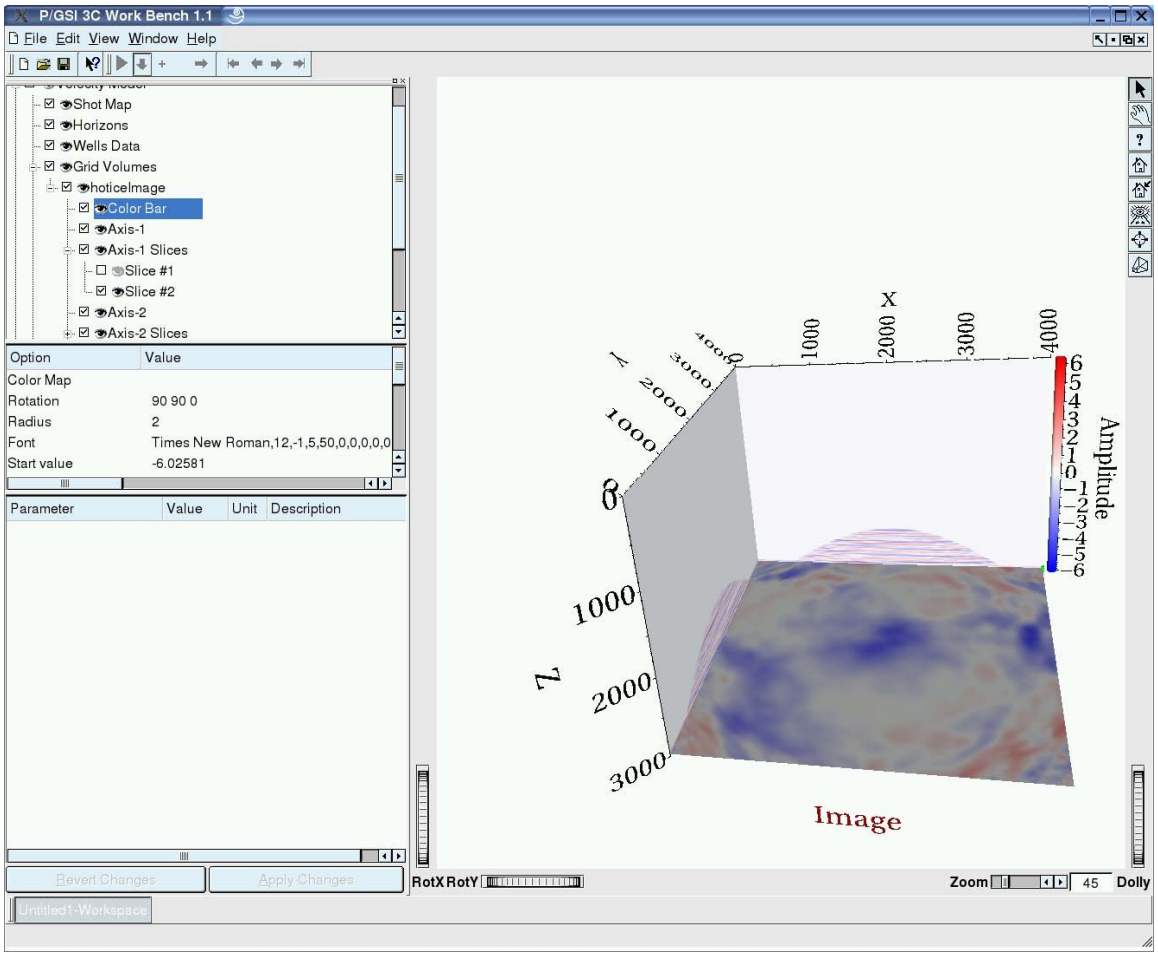

Figure 42. Seismic volume displayed as a deth slice with bounding sides.

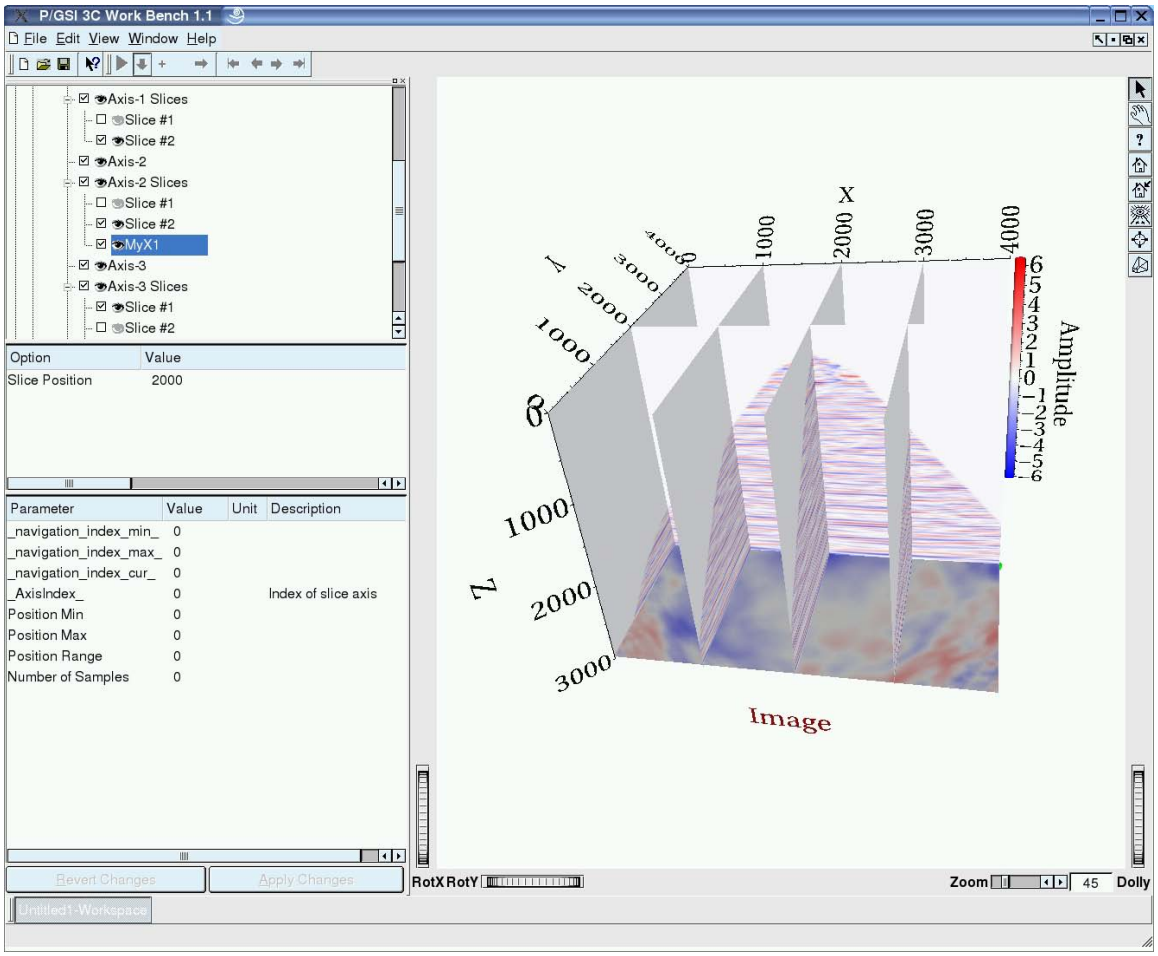

Figure 43. Seismic data volume displayed with various arbitrary volume slices.

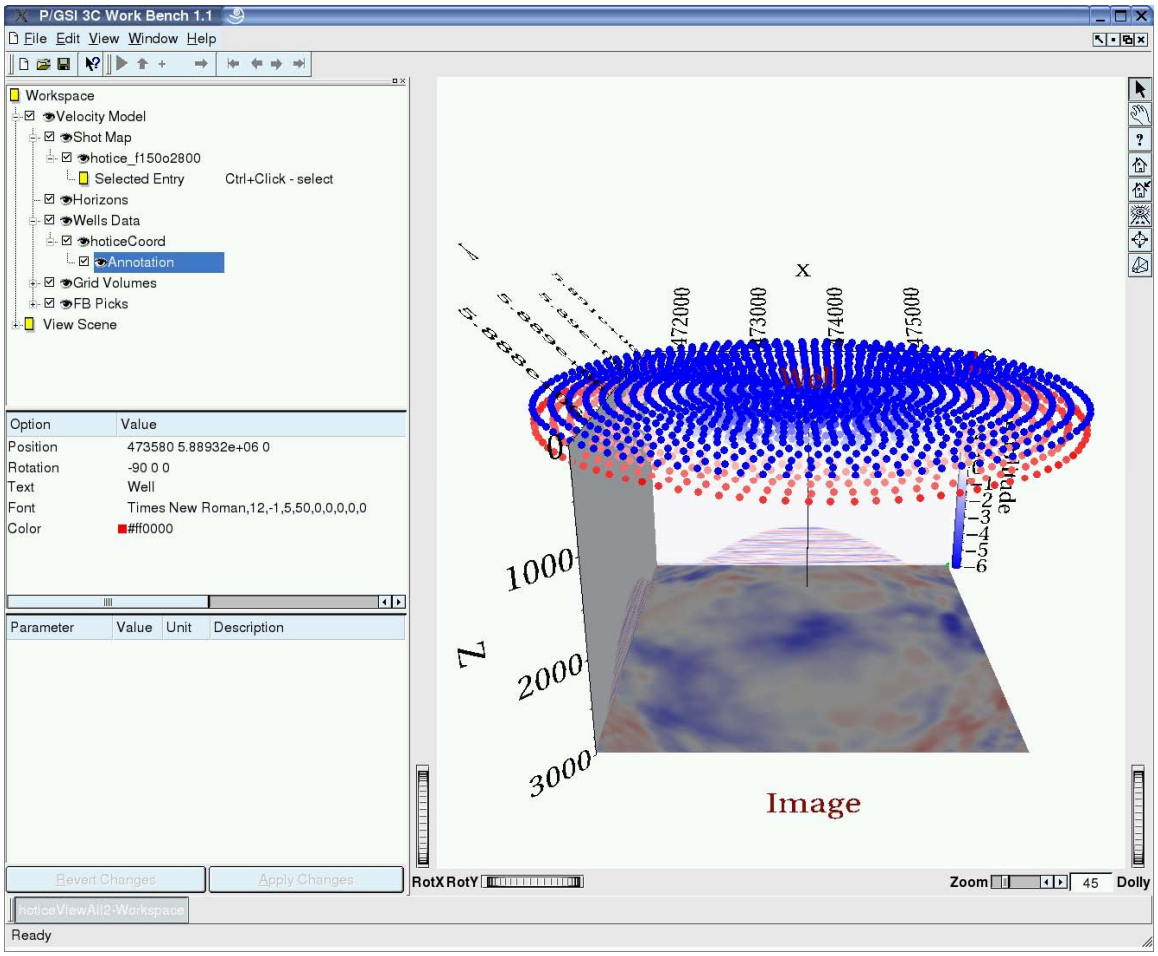

Figure 44. Composite interactive display of source locations, first break picks, a well log curve, and slices through the seismic image volume.

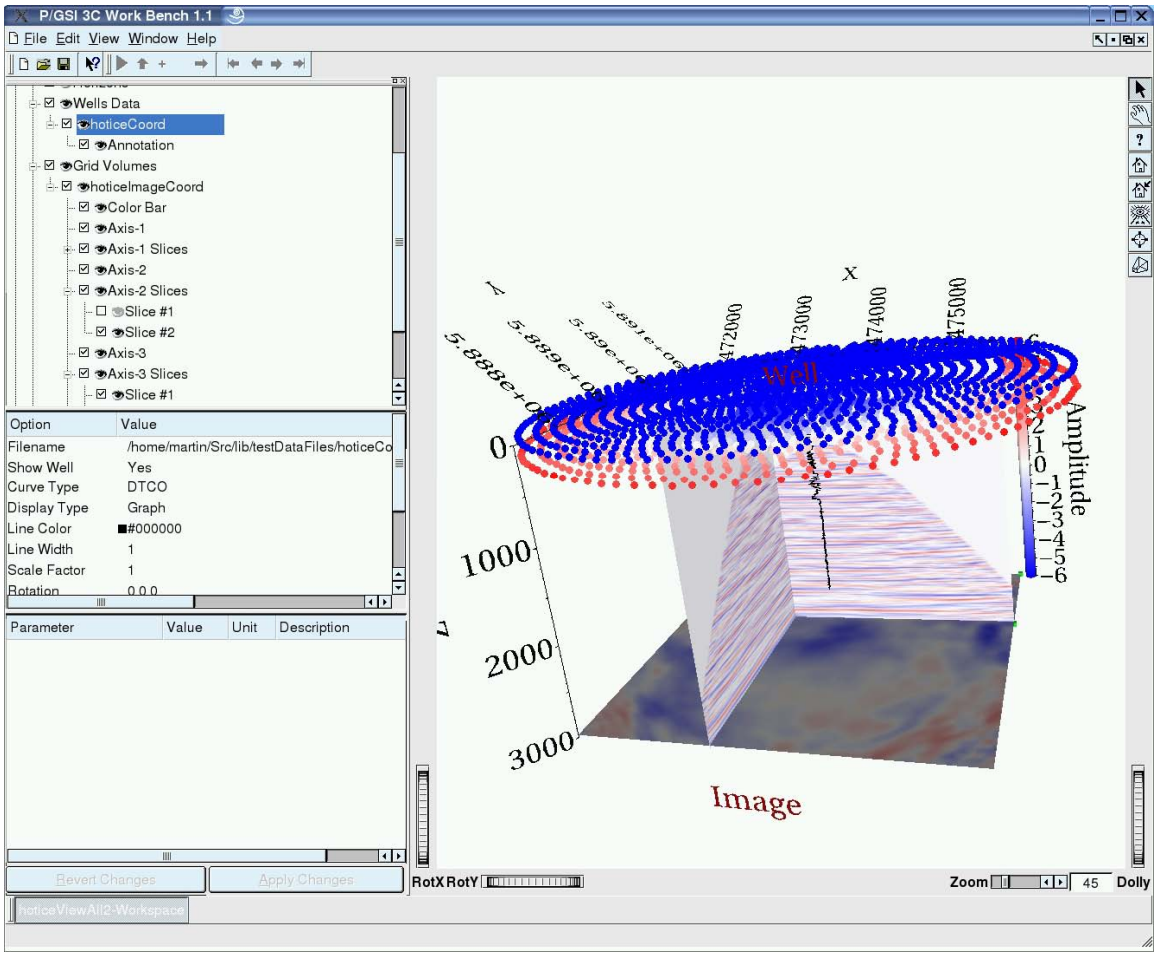

Figure 45. Animated view of the composite interactive scene.

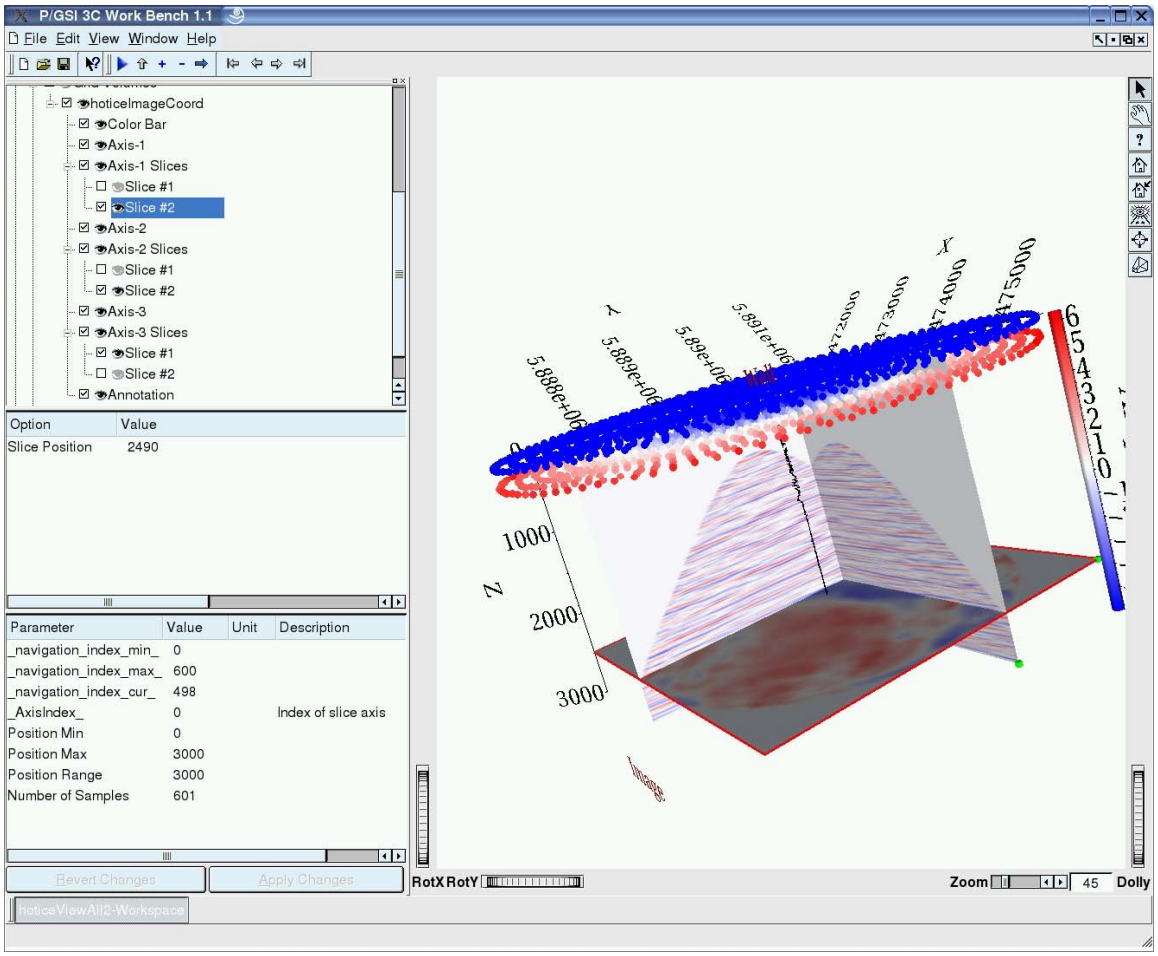

Figure 46. Back side view of the composite scene, well log curve superimposed on the seismic volume slice.

The Multi-Component Work Bench

The 3D VSP work bench application is composed of several high level objects. The most important ones are the User Interface item (PG-UItem) and the Display Item (PG-DItem). The application framework library manages lists of such items. The PG-UItem tree includes things such as ray tracing, seismic data items, annotations, well logs, and multi-component related features. The PG-DItem tree includes things such as data grids, cubes, traces, and pointsets. PG-UItems are displayed on the left hand side of the work space. The PG-DItems are visualized on the right hand side of the display windows. Figure 47 shows the basic relationship between those two items. Both item types communicate through direct method calls or through a signal and slot mechanism, discussed in more detail in Task 14. This clear separation between data management and visualization allowed us to separate development tasks in an efficient manner. The user can modify either PG-UItem or PG-DItem. Actions initiated on either side are communicated instantaneously to all objects through the main application.

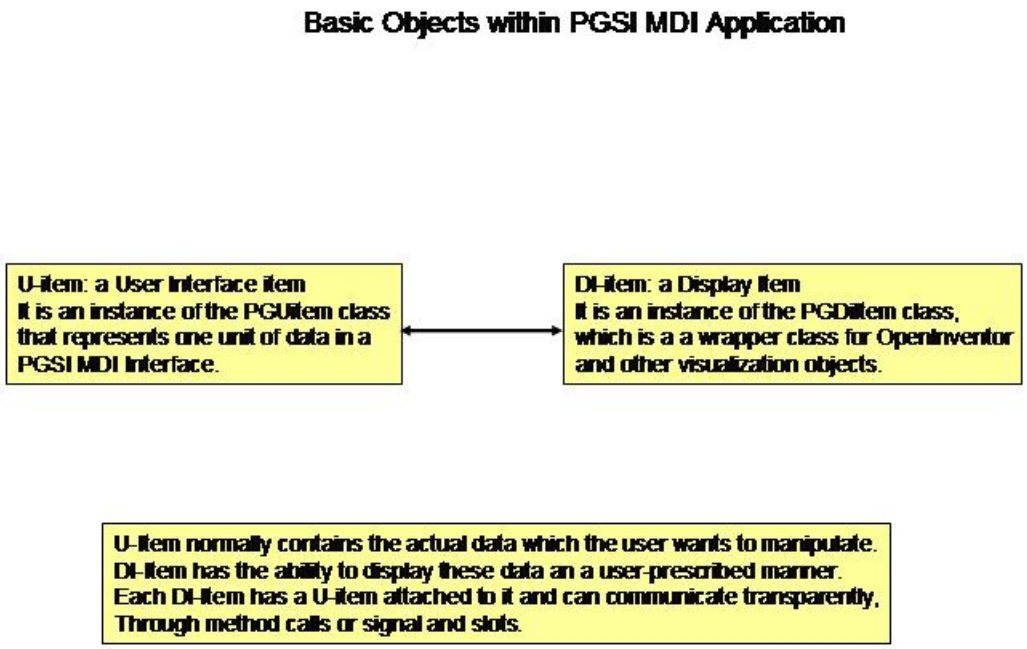

Figure 47. A MDI application consists of several basic objects that are managed transparently through direct function calls or a signal and slot mechanism.

From the end user perspective, one moves through a simple set of steps to create a work space. The user can create a new document within the 3D VSP Work Bench, and this will open a work space in which several categories of data items are displayed. Right clicking on those items shows a list of possible actions; load, save, delete, open a window, and so on. In this manner the geophysical data objects are attached to the PG-UItem, which completely hides the loading or the creation process from the user. Depending on the type of display and the data that are requested, a list of configurable and fixed parameters are displayed on the left hand side of the application. The options are displayed in the parameter viewing area, and the user can edit those options. Upon hitting the “Apply Changes” button all changes are propagated to their respective recipients and evaluated by the PG-DItems. These display items then work through their internal algorithm and update the visualized scene accordingly. The PG-UItem list is visualized as a nested tree structure, with items logically grouped and ordered. Figure 48 shows the top-level work flow from a user perspective.

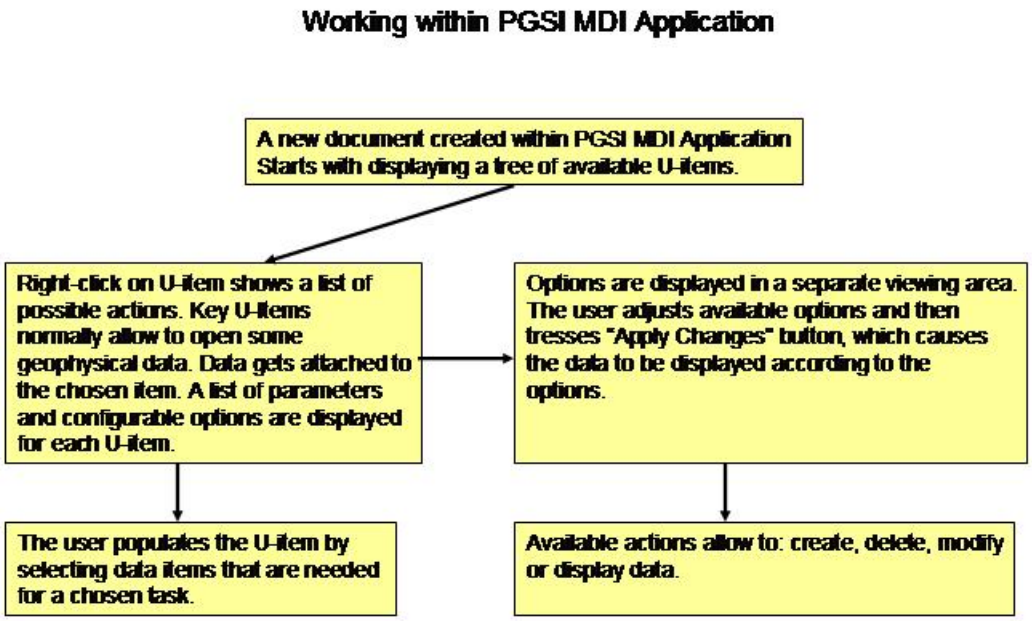

Figure 48. The top-level work flow from the user perspective. Each item has its unique set of options, choices, actions and visualizations.

Using our vendor toolkits and the underlying data and display capabilities that we developed, we then built a skeleton high-level application Work Bench tool suitable to incorporate the project specific display and interaction needs for the integrated multi-component processing and interpretation framework for 3D borehole seismic data.

Starting from the skeleton tool, we created a complete multi-component 3D VSP Work Bench application. We used real and synthetic 3D VSP data to test the application in real-world situations and work flows.

Task 7

Build prototype pieces of the multi-component display framework.

The efforts in this task lead to the development of a number of higher level capabilities that make up the multi-component 3D VSP Work Bench application. The Work Bench consists of tools, also referred to as widgets, that are used to display and manipulate maps, volumes, point sets, seismic traces, well log curves, and sets of seismic wave propagation rays. Here we will give some examples of the capabilities of the 3D VSP Work Bench.

In Figure 49 a shot map and an entire topographic map have been loaded and displayed. The visual representation is shown in the 2D Viewer window on the right. The map shows a particular location of a borehole seismic survey. The well location is indicated with a red dot, while the source area is outlined with a red circle. Lakes, streams and topographic information are shown in the map itself.

Although this is a 2D map view, the display can be manipulated in 3D and visualized together with other information. In Figure 50 some additional 3D VSP source location data have been loaded. By checking the box in front of the item in the left-hand tree view, the source location item is displayed on top of the location map. The source locations are indicated by filled circles. The color of these circles indicates the source id, essentially a quality control indicator, since the sources are designed to be activated in a circular manner.

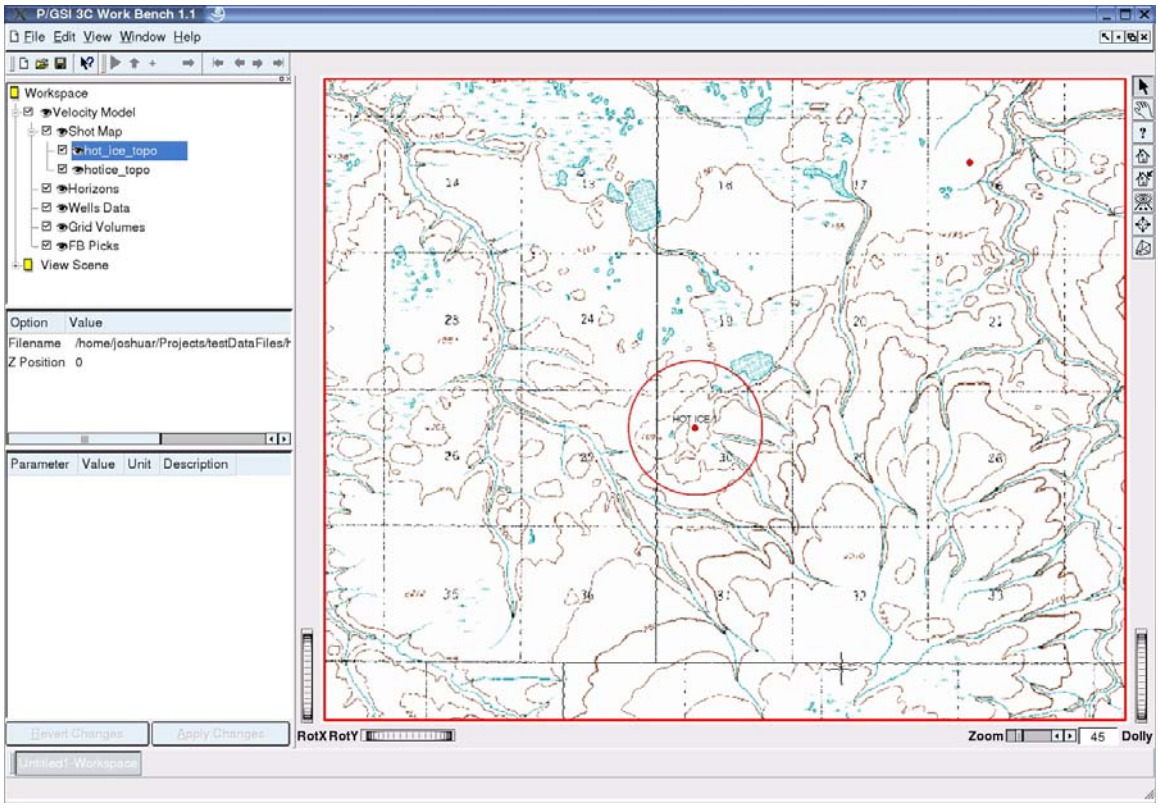

Figure 49 A shot map item has been read in, which displays the topographic map using a particular display item.

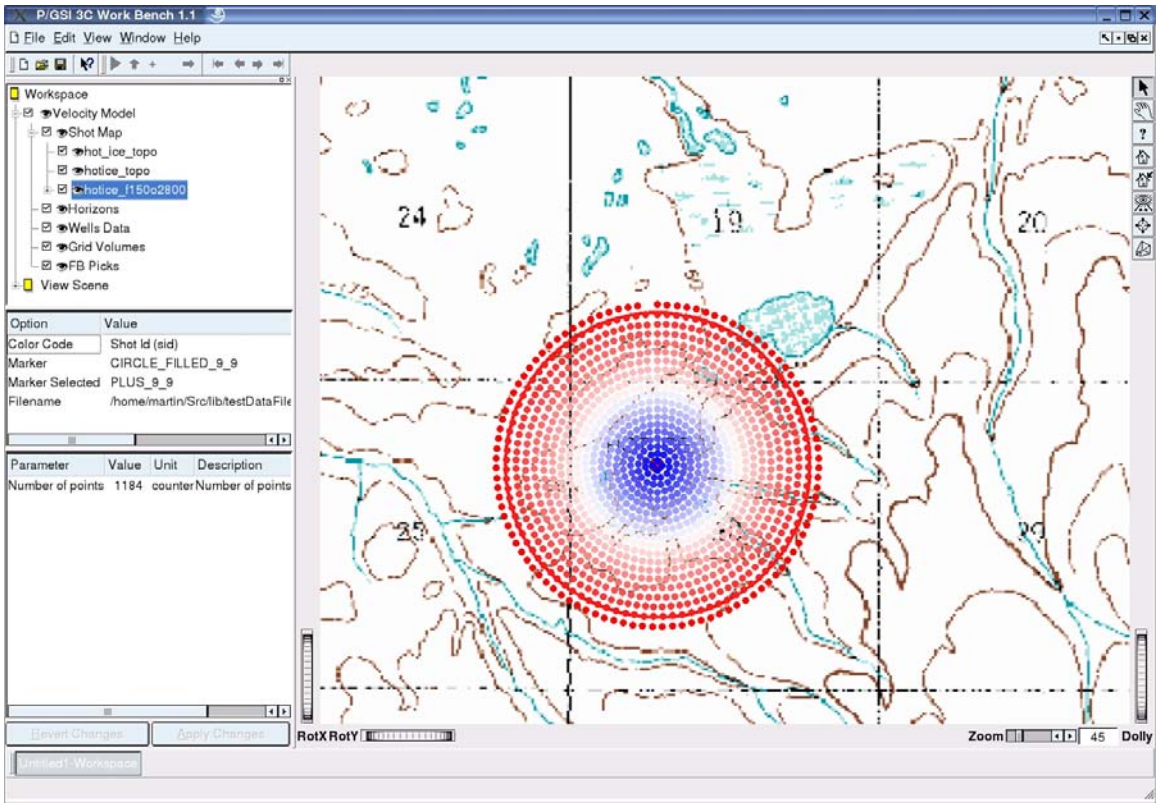

Figure 50 Actual source points and the location map are co-visualized in the right-hand window.

In Figure 51, the same data are displayed from a perspective view. This is extremely useful to spot abnormalities in the 3D VSP source location information during acquisition and processing. The source locations can be animated, and the actual survey progress visually observed by animating specific source location symbols. Each individual source point can be selected in this viewer window and its properties displayed in the option list. Right clicking on the data item in the tree view shows all the possible actions that can be taken with this data, including loading, saving to disk, or launching a series of processing steps to apply to the data.

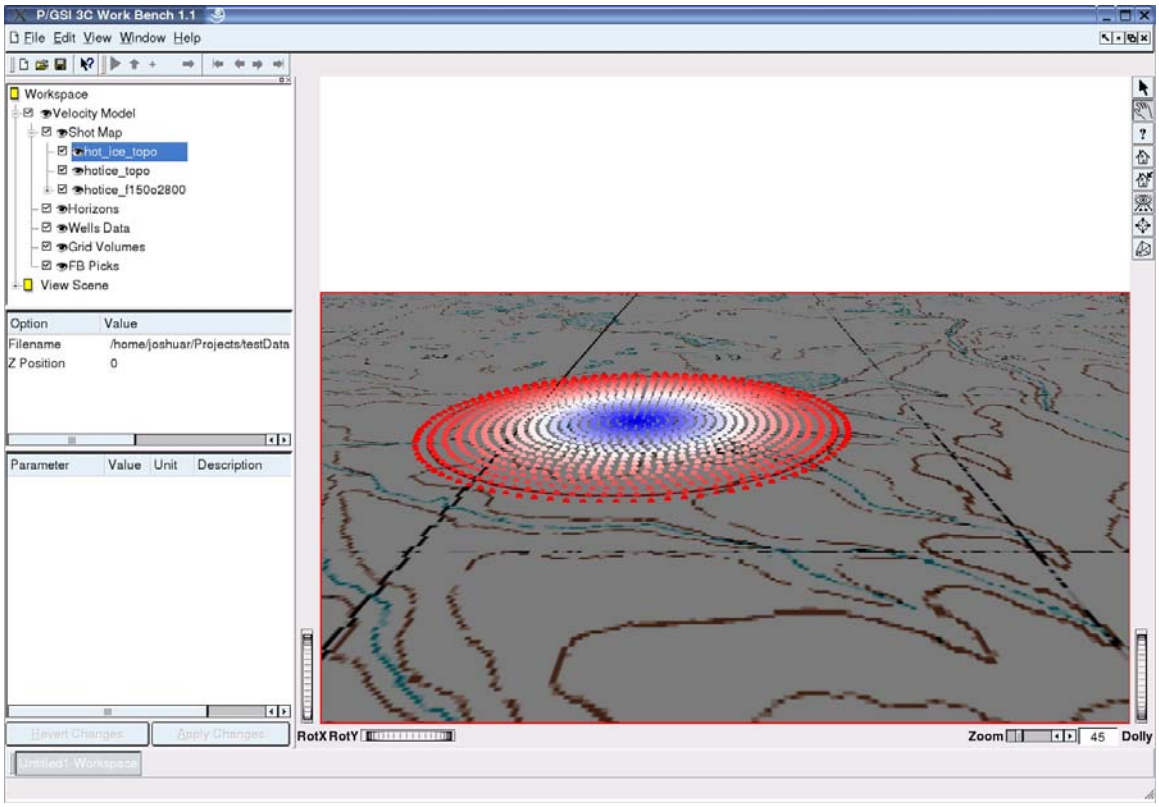

Figure 51 Perspective view of source locations on the topographic map.

In Figure 52 we zoom out to compare the entire map extent with the actual borehole seismic survey area. Several tree items are active in the left-hand tree view window.

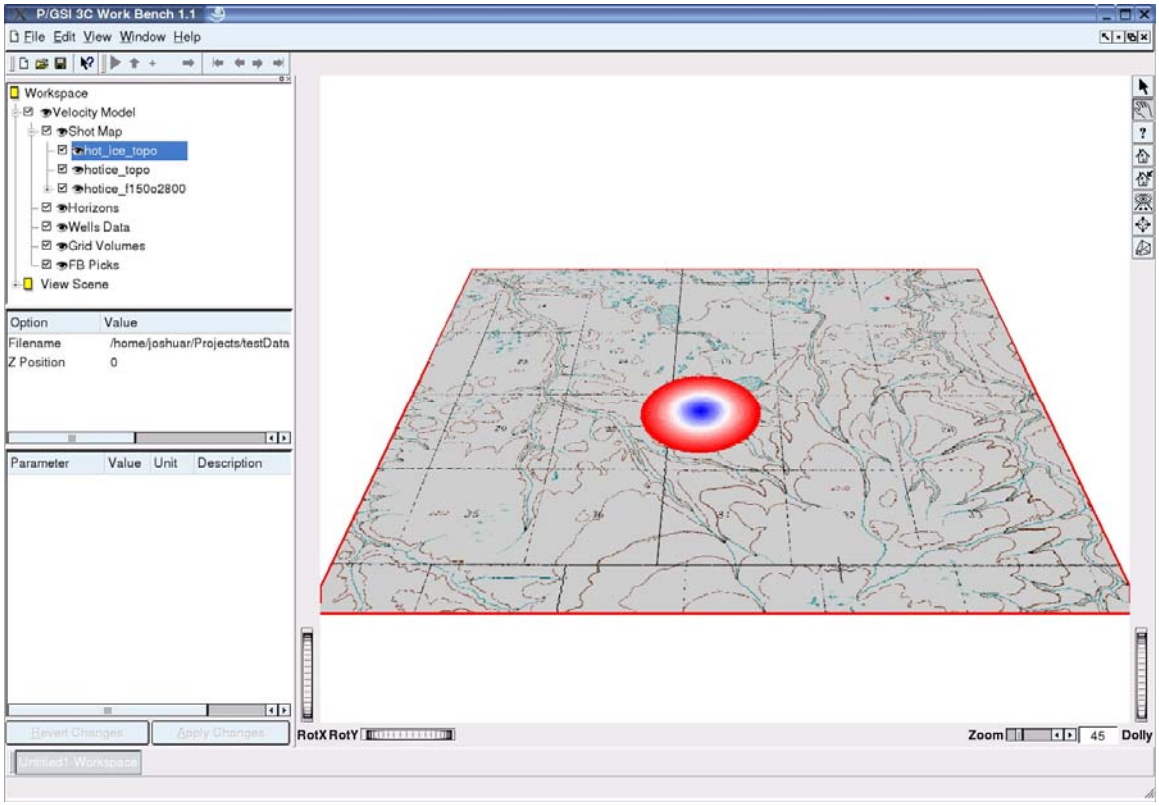

Figure 52 Zoom out to capture the large scale area of the 3D VSP survey.

In contrast, Figure 53 shows the visual representation of a well log as a curve. The depth axis is vertical and data values are plotted along the horizontal axis. In the work space a sub-item handling the well related information is activated and shown in the item tree. The well data has read in an entire LAS data file. In the option view beneath the tree, several options are listed. The content of these options is dynamically retrieved from the data file or from default settings. The values of these options can be changed by the user interactively by clicking on the option fields. In this example, the user has selected the curve type DTCO (corrected sonic log) and has chosen a black line color and the curve type to be a simple graph. All other settings such as position, scale and line width are not modified and taken from default values.

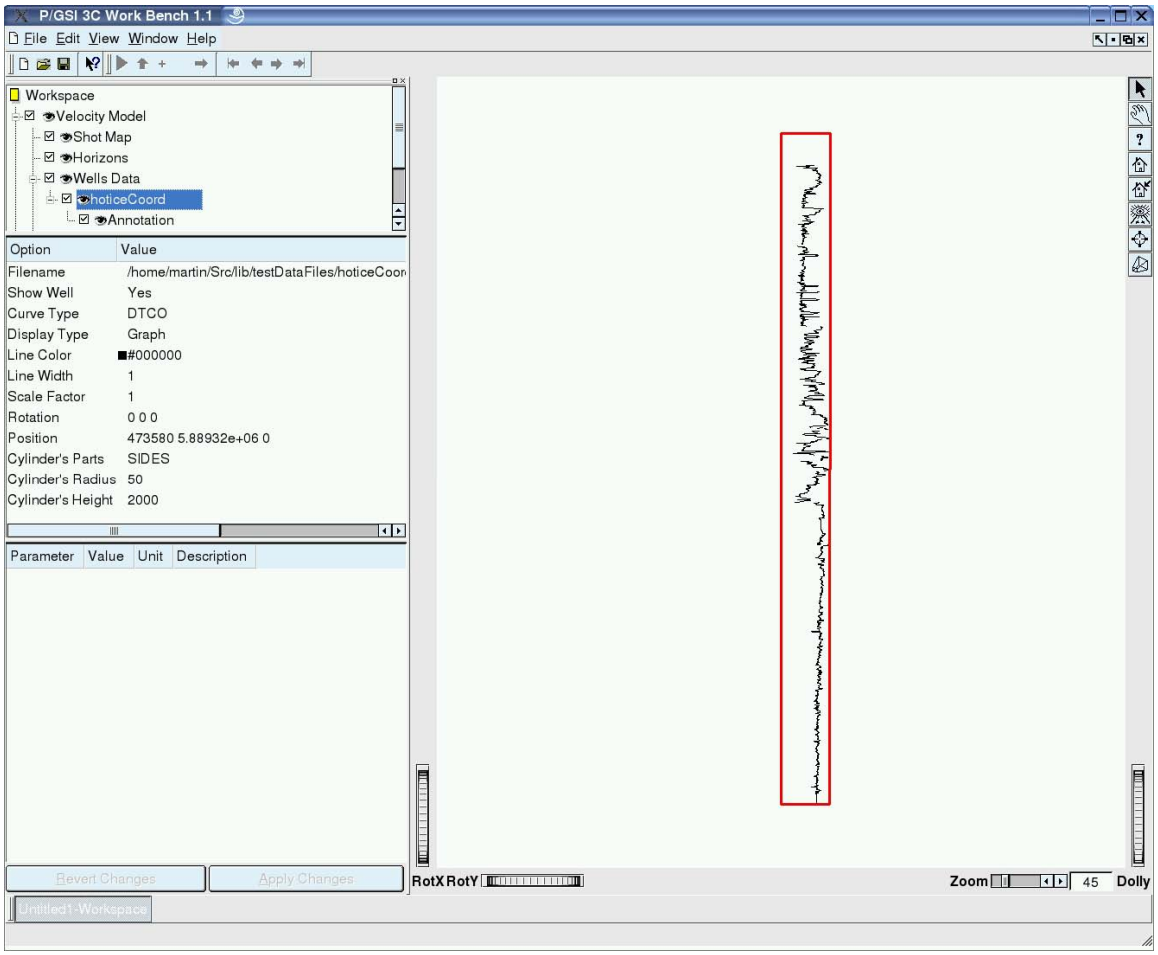

Figure 53 Well log data have been read in and the data present in the well log curve are shown as a display item.

Figures 54-57 show some of the display and manipulation functions that have been developed for working with data volumes. Here we show for example our most widely-used type of volume, which is a seismic image cube. The item tree is now expanded, showing a multitude of sub-items that are activated automatically on reading in a volume. Each and every sub-item can be interactively changed. In Figure 54 we have selected to display a horizontal, or depth slice at the bottom of the volume. We have also selected several vertical slices along the x and y-axes to be displayed. The option view shows the selected slice position of slice number 2 on the x-axis. The parameter view beneath the option view shows the parameters that the user cannot change, representing various pieces of information about the volume slice position. These numbers change dynamically once a slice animation is activated from the tool bar. Seismic amplitude values (an attribute of the seismic volume) are displayed using a red-blue color scheme which is detailed by the color bar on the side of the volume, indicating a range of values from -6 to +6 and the meaning of those numbers denotes amplitudes.

Figure 55 shows the interactive addition of slices for detailed analysis of the image and Figure 56 rotates the original view to examine side and back view of the volume. Figure 57 shows the final selection of volume slices to be displayed, consisting of vertical and horizontal volume slices. The scale and meaning of the volume axis is indicated by text annotation and tick-mark numbering along the edges of the volume.

The entire document including view details can be saved to a file in xml format. Reading in such a saved file will produce the same identical view of the data. Mpeg movies and still pictures can be captured and saved.

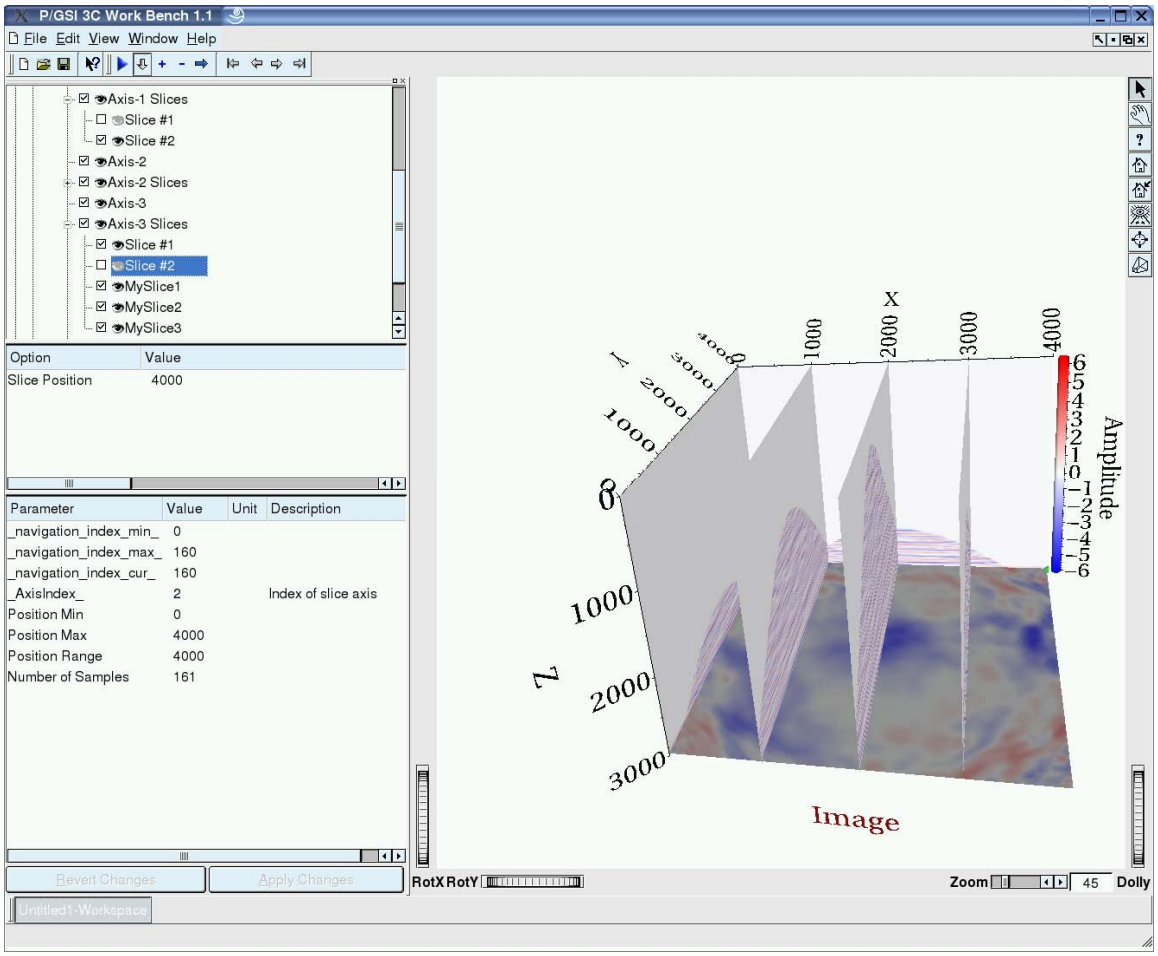

Figure 54 A seismic data volume has been loaded into the Work Bench, and slices of the volume are displayed in 3D. The user can manipulate the view in many ways including rotation, zoom, and translation. Slices can be randomly selected and animated.

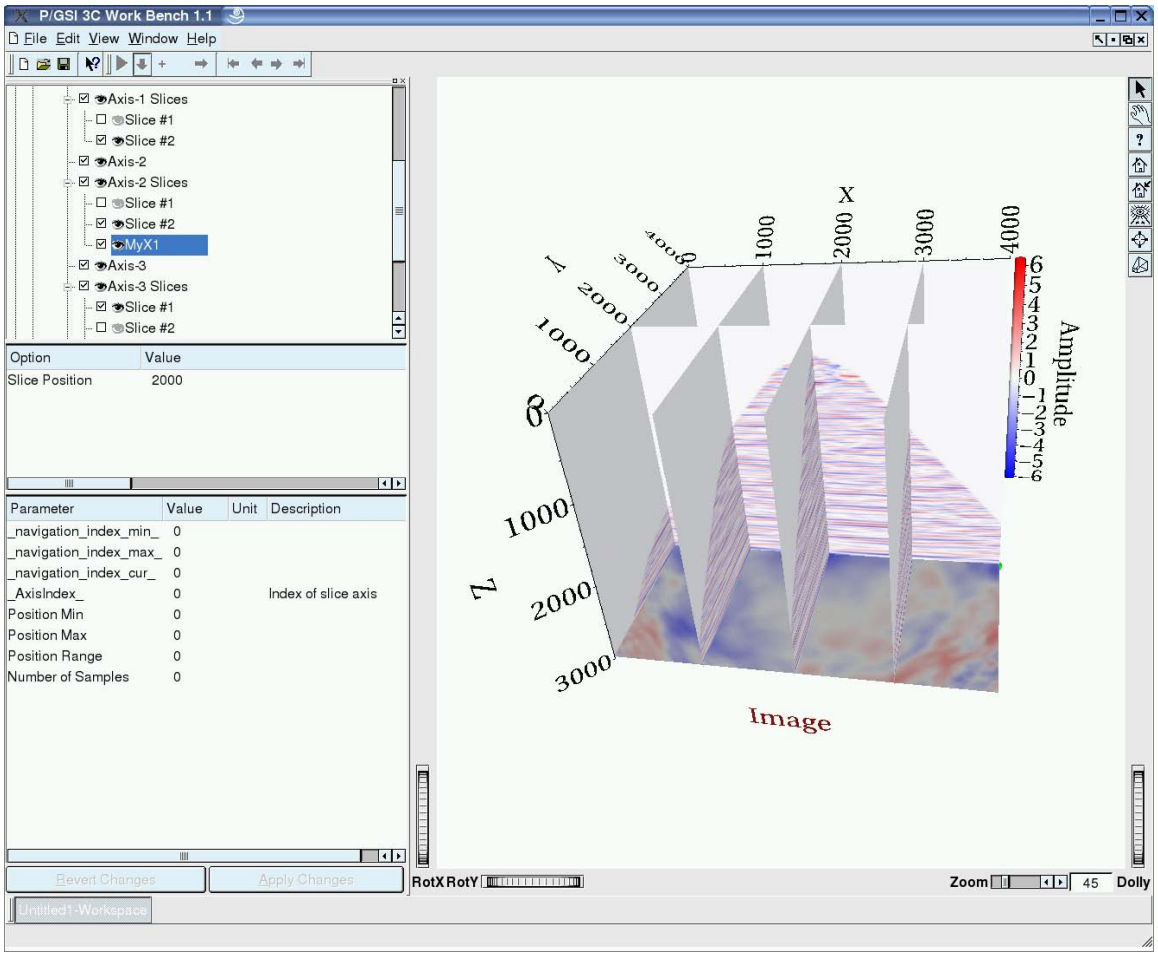

Figure 55 Adding more slices to the view.

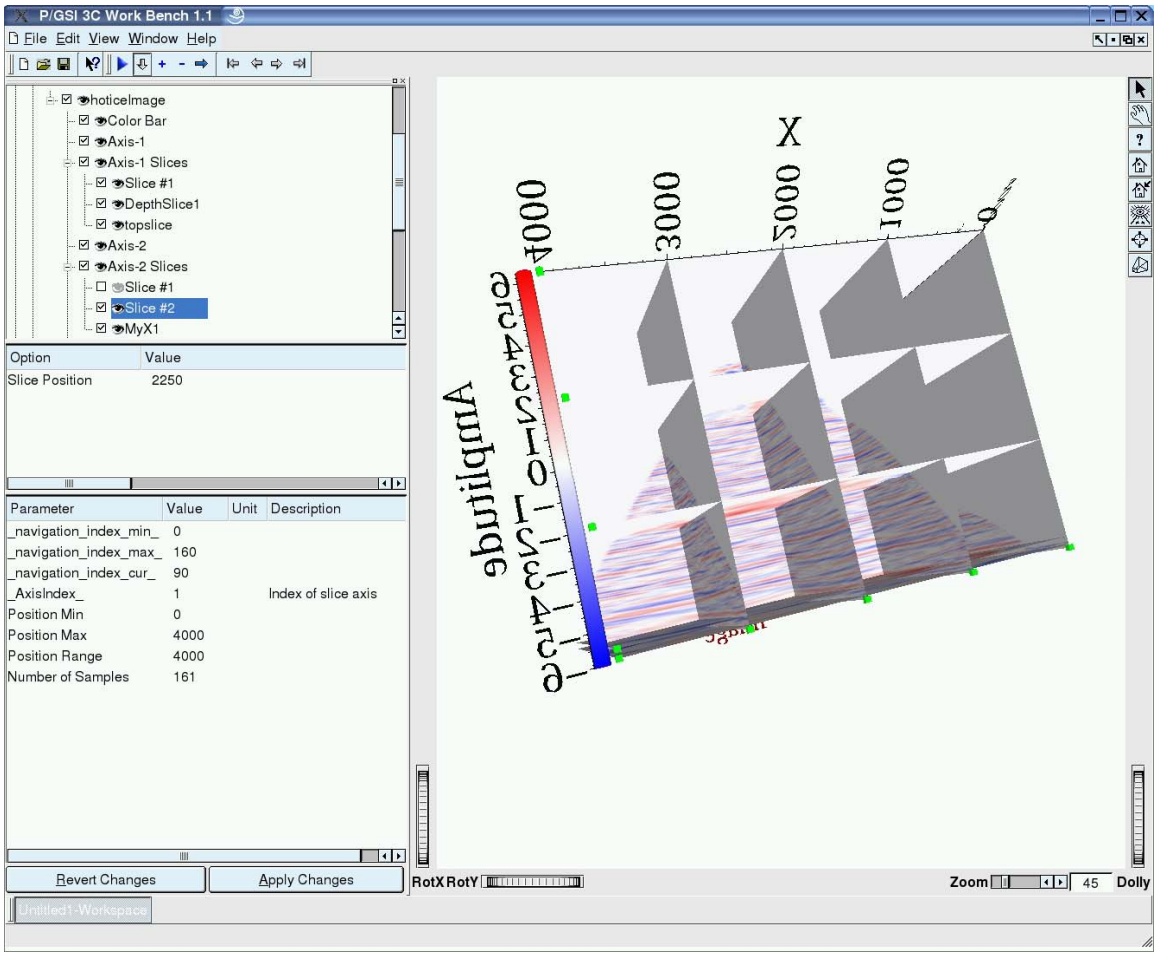

Figure 56 Adding more slices to the view and rotating the volume for analysis.

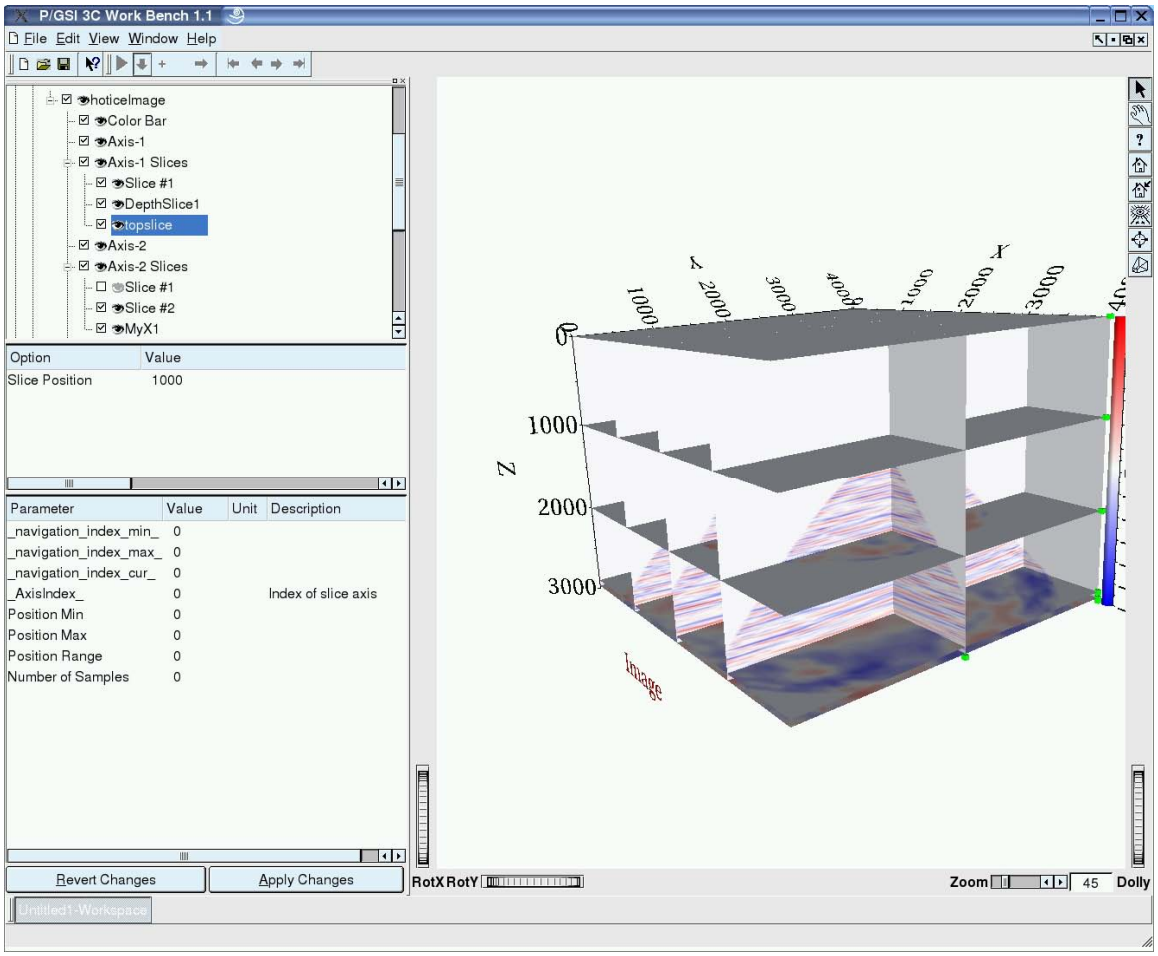

Figure 57 Adding slices along the depth axis.

Figure 58 demonstrates the capabilities we have implemented to display and manipulate first break times. These functions are contained within the FB Pick sub-item in the workspace. Users can read in files containing picked first break times into the Work Bench, and plot them at their associated source location in the 3D viewer window. Source points can be selected and actual numerical values displayed in the option view. The travel times are color coded, allowing quick quality control and sanity checks on survey progress or picking problems in the seismic data. In this example, the 3D VSP source locations are in a semi-circular pattern, along preferred lines. The receiver well location is in the center of the circle at the intersection of the three dense source lines.

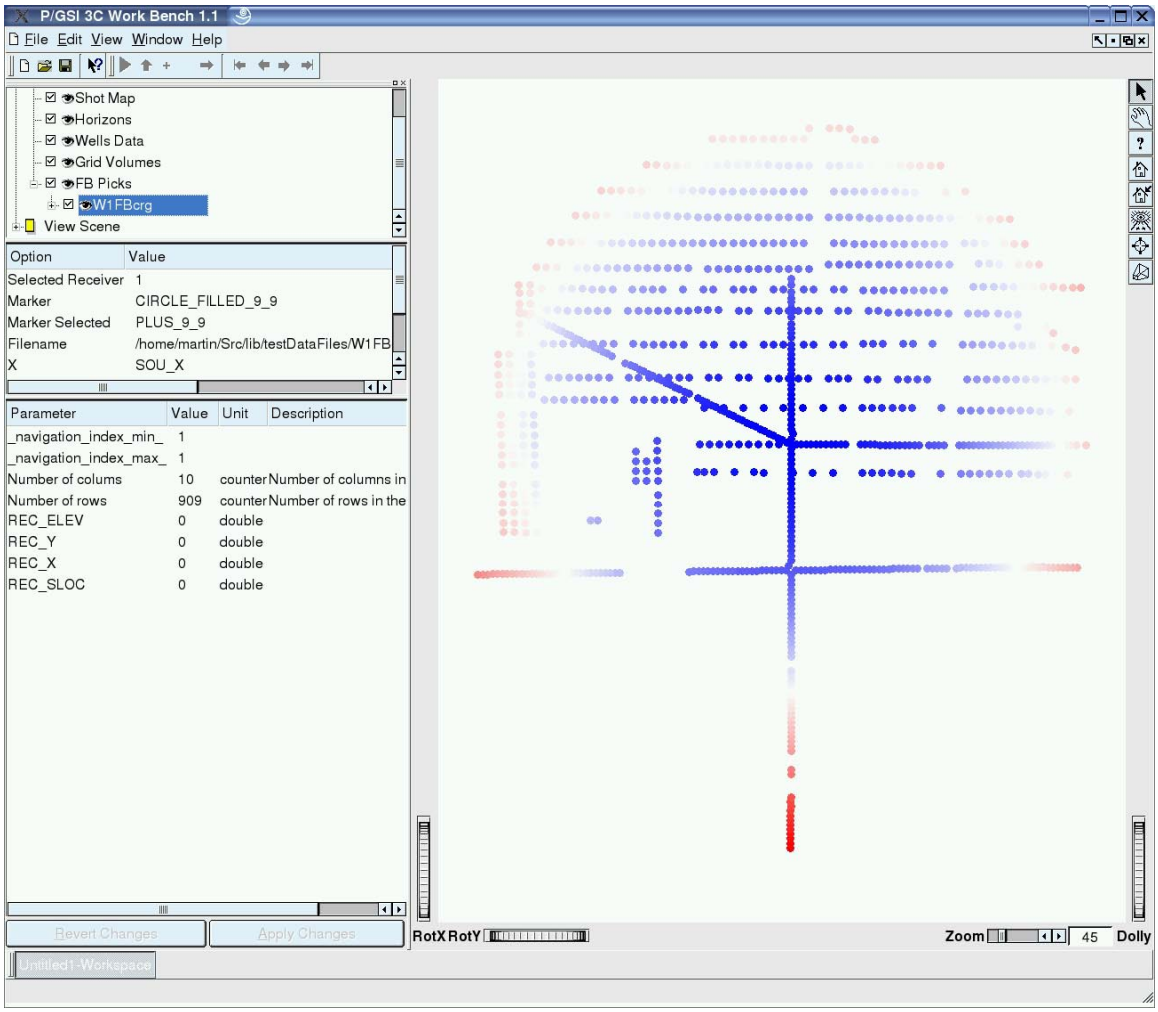

Figure 58 First break picks have been loaded into the Work Bench from a multi-well survey. The dots are source locations, colored with two-way travel times.

Figure 59 and Figure 60 highlight some of the functionality available to work with horizon data. Horizons, or 2D surfaces, can be displayed in many ways. Horizon information is loaded into the work bench in Figure 59. The viewer window shows a 3D representation of the horizon, which is colored in opaque red. It clearly shows the dominant dip orientation and variability of depth along the horizon. Option and parameter views show horizon-related information taken from the input file as well as from the default and user defined settings. User controls include such things as transparency, color, and the Z-axis datum. Fixed settings include the number of triangles that make up the mesh surface, and since this surface is a regular grid, the number of points along the X and Y axes. This surface is displayed as an open mesh.

In Figure 60, a different surface is displayed as a closed mesh. This is useful if a region of seismic or velocity volume data is selected and needs to be manipulated in the space confined by this closed surface.

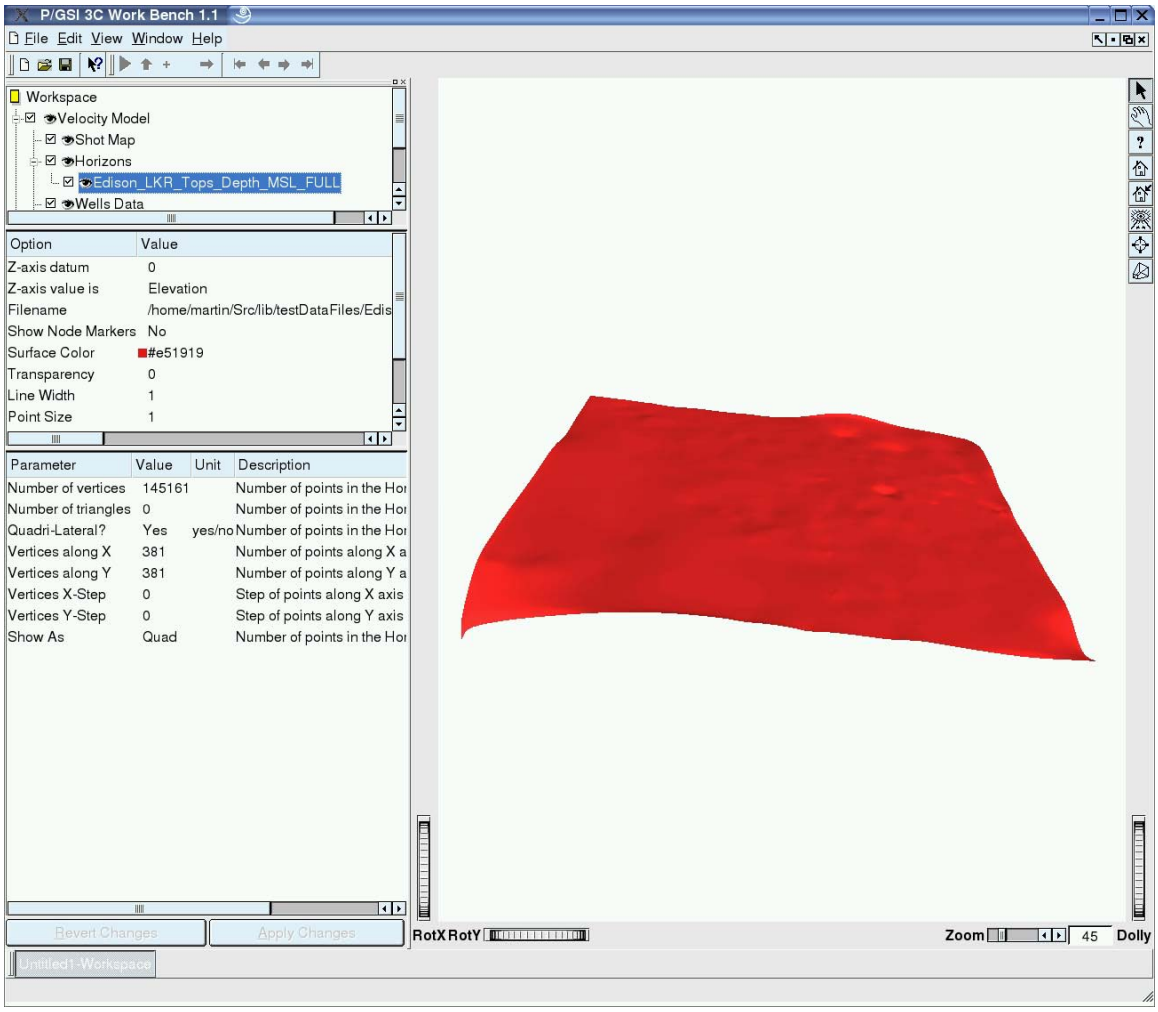

Figure 59 A horizon has been loaded into the Work Bench and is displayed as an opaque surface in three dimensions.

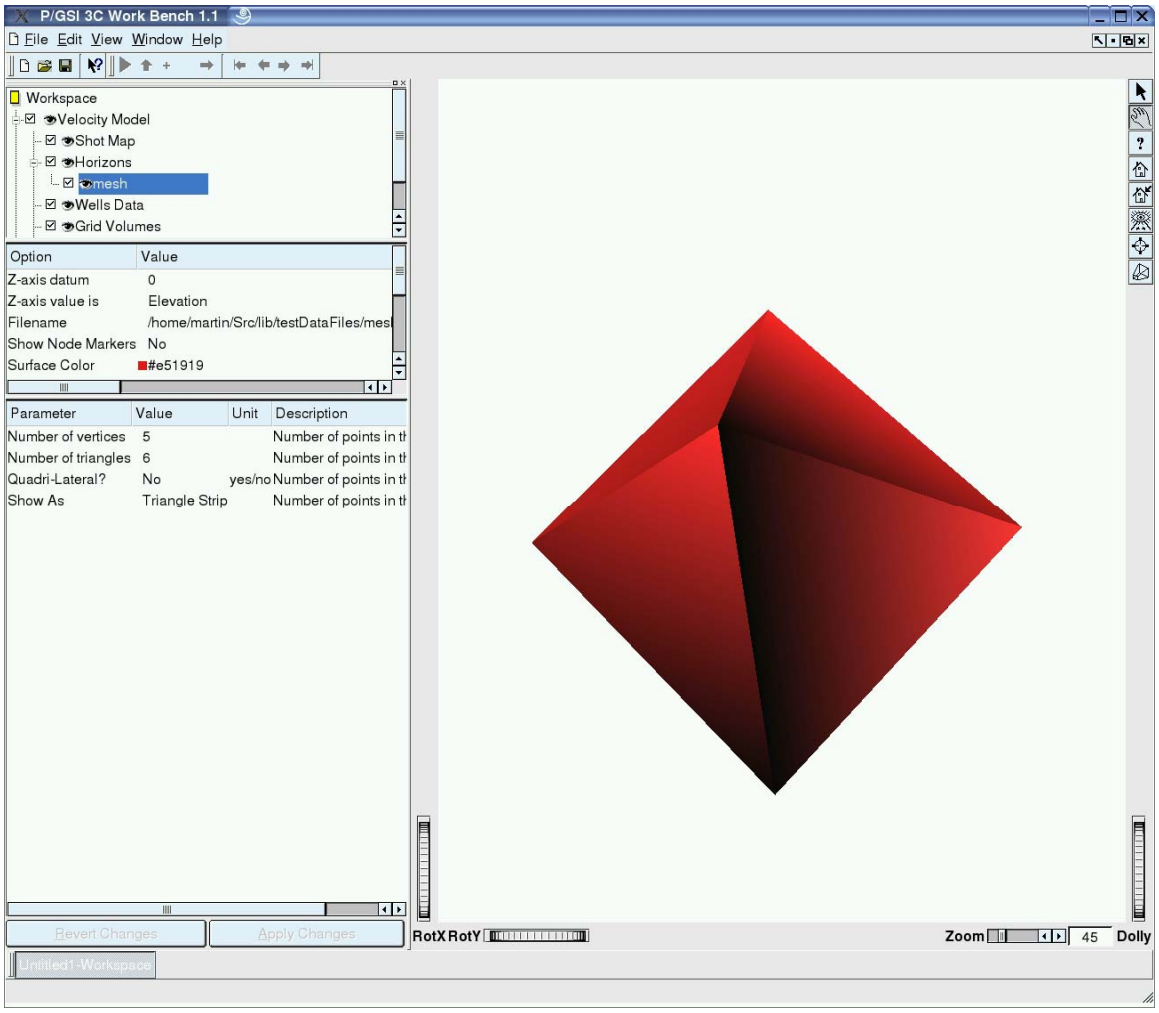

Figure 60 A different 3D surface has been loaded, which resembles the shape of a pyramid. In contrast to the horizon, this surface defines a closed volume..

Figure 61 and Figure 62 show seismic volume displays for a multi-well VSP image volume. The image volume in this case is not a cube, but a narrow corridor. The green boxes indicate interactive draggers which allow the user to interactively slice the volume. A color bar calibrates the seismic amplitude information.

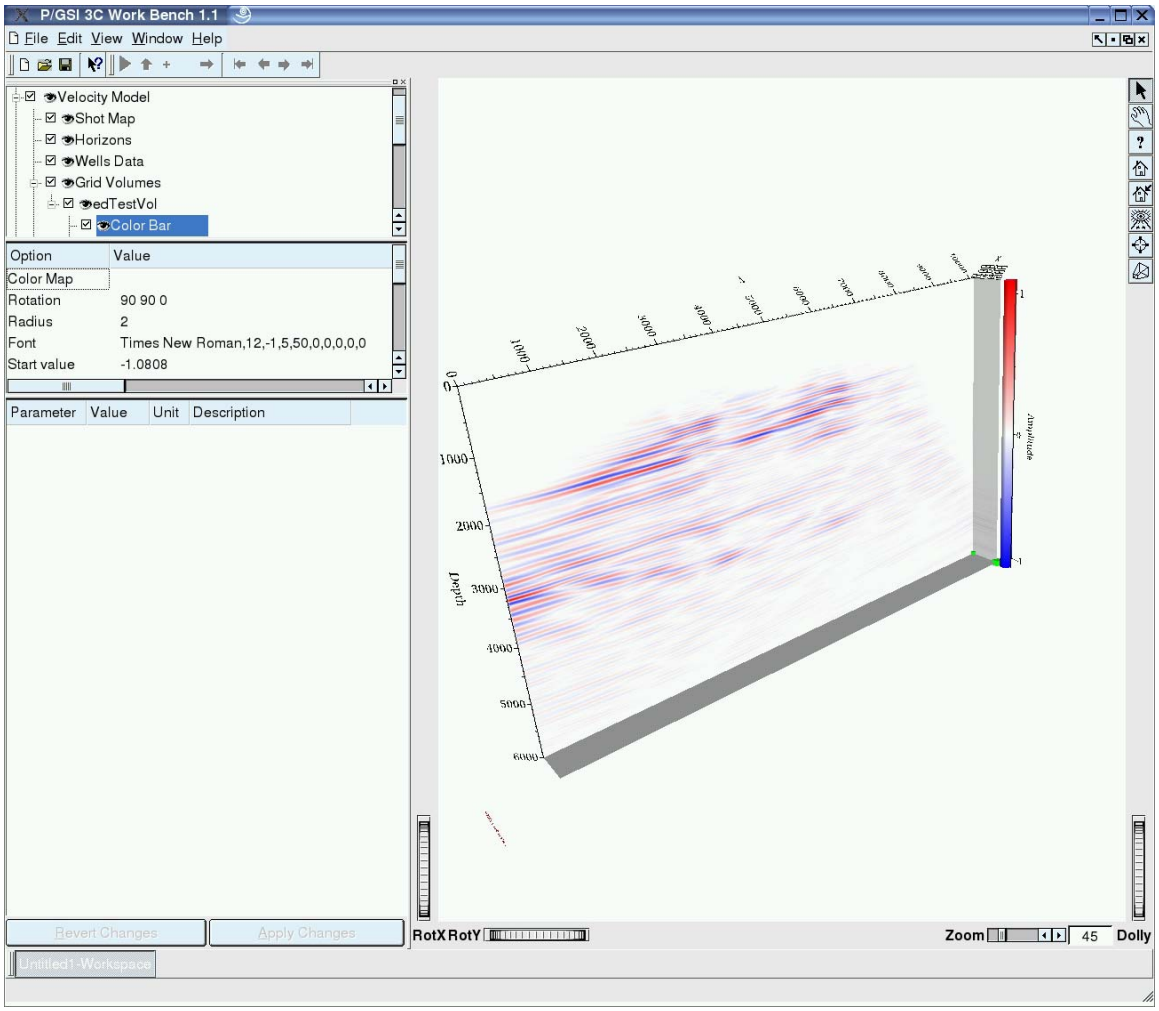

Figure 61 A multi-well seismic volume loaded into the Work Bench. The volume consists of a narrow corridor; color is seismic amplitude.

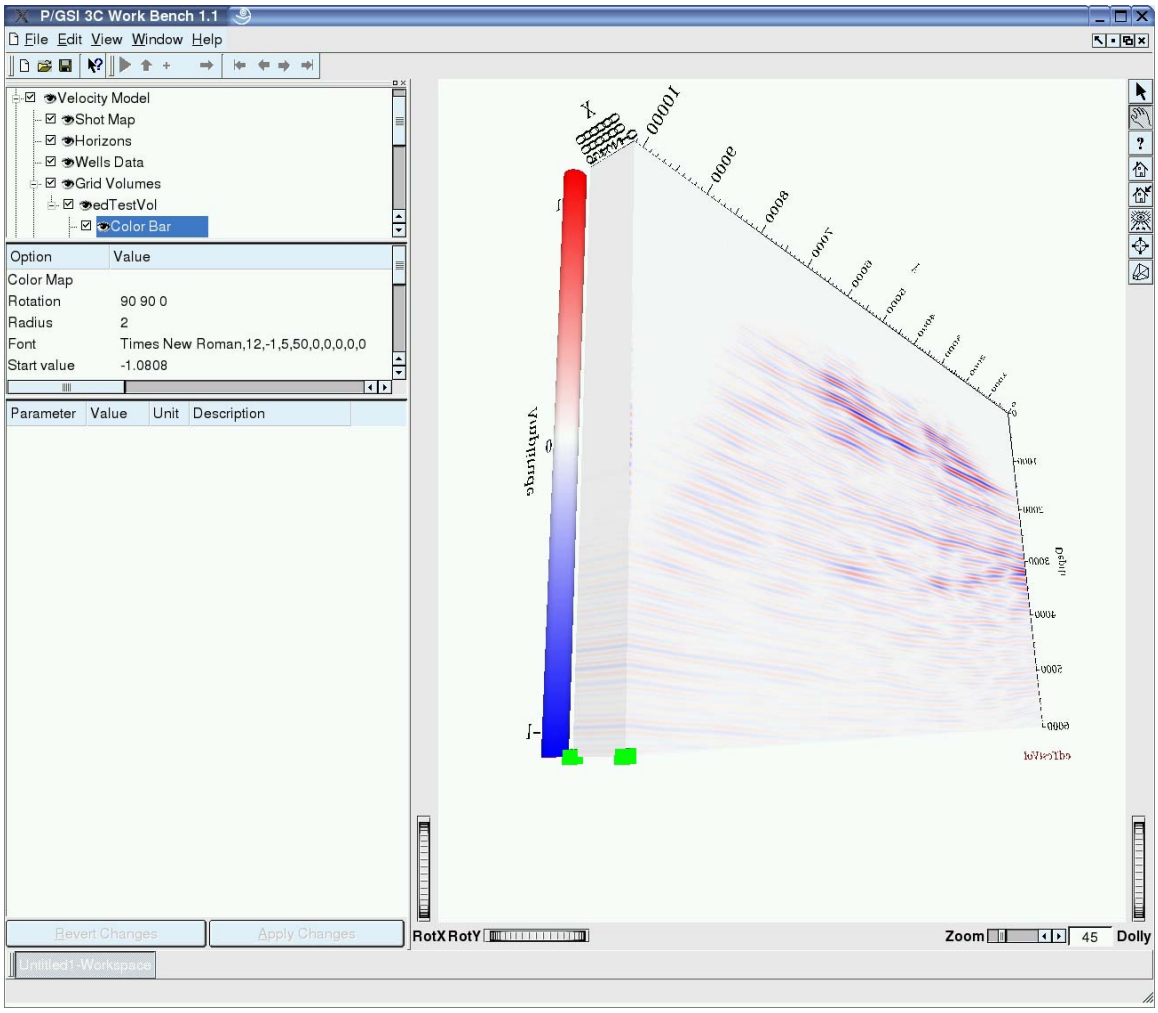

Figure 62 Back and side view of the multi-well seismic cube, shown by rotating the volume in 3D.

In Figure 63 and Figure 64 show some of the features that are useful when looking at displays that combine disparate data types. Figure 63 shows a seismic volume together with three distinct horizons. Slices of the volume confine a space which is illuminated from the top and front. Figure 64 rotates the entire view to visualize the intersection of the horizons with the volume slices for a detailed interpretation of the image volume. Conformity of the horizons with the seismic image can be judged easily, and the user is able to perform quality control checks to see whether the seismic image agrees very well with horizons that have been interpreted from other sources of information. Horizons can be selectively displayed and slices removed and added on demand.

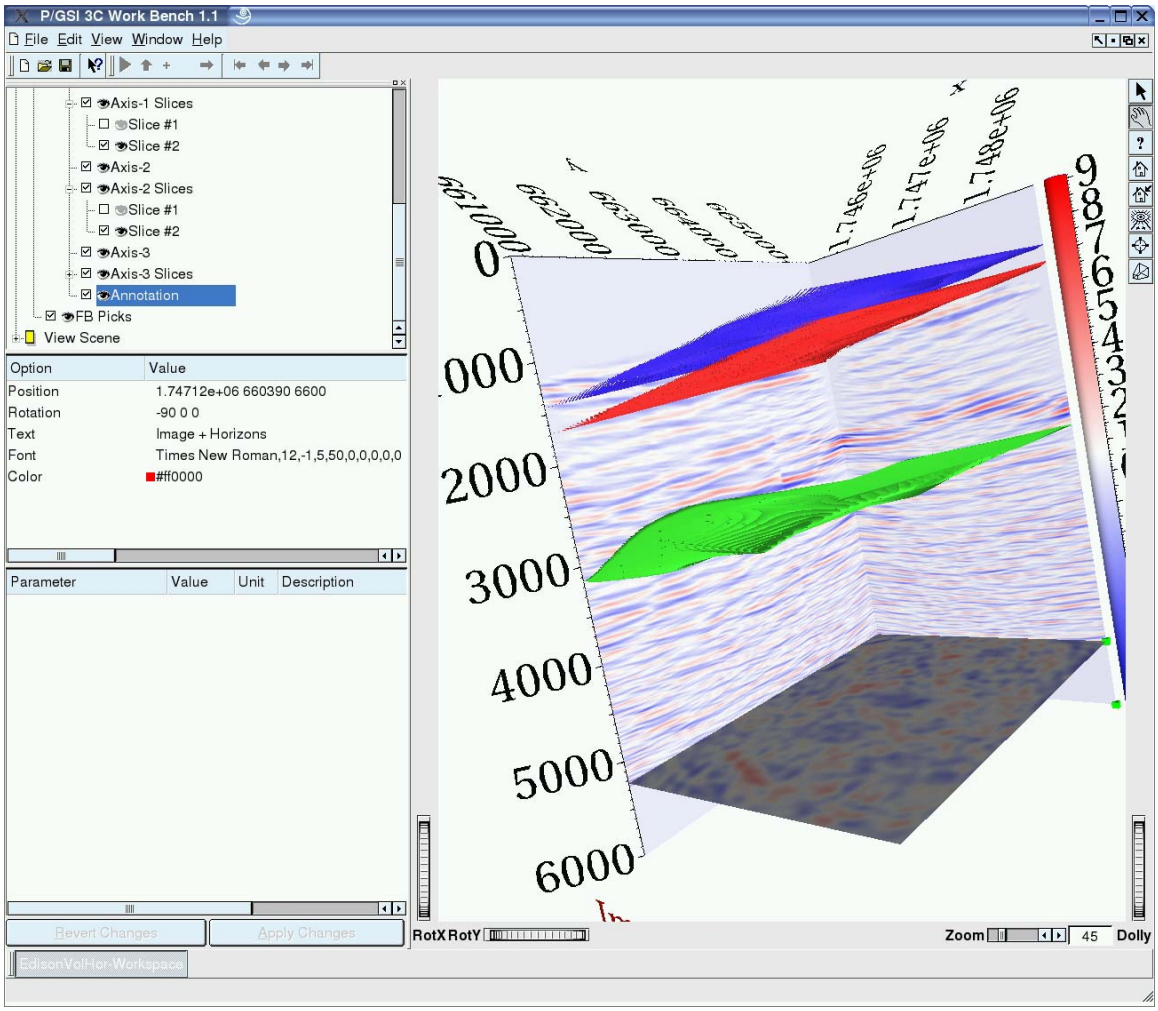

Figure 63 A 3D seismic image volume is loaded into the Work Bench together with horizons. An interpretive analysis can be carried out by correlating seismic amplitudes where the cube slices intersect the horizons.

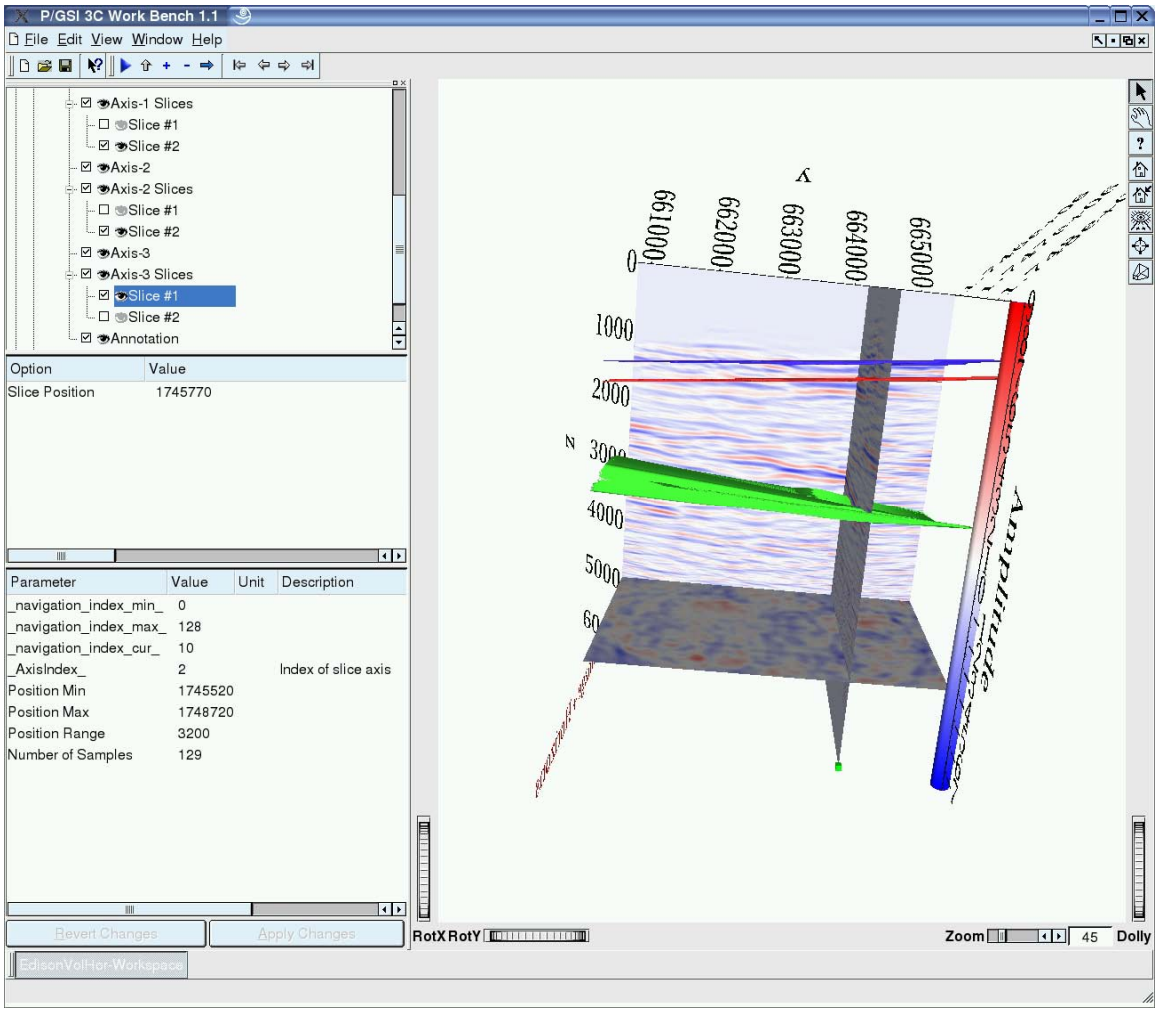

Figure 64 The seismic image volume and horizons are rotated to view the back side of the volume.

We implemented a widget to display particle motion of multi-component seismic data within work bench application. This tool allows us to read in multi-component seismic trace data and display these data in various views. Figure 65 shows the complexity of the hodogram widget, which contains three separate viewing areas. The right most sub-view is a conventional trace display, showing the x, y and z component of the seismic trace for a specific source-receiver combination with a vertical axis of time.

To the left of this view there are two sub-views that display projections of two separate component combinations. One display view shows the trajectory of the projected x-z particle motion, and the other view shows the trajectory of the projected x-y particle motion vector for a set of seismic trace sample points from the first display window.

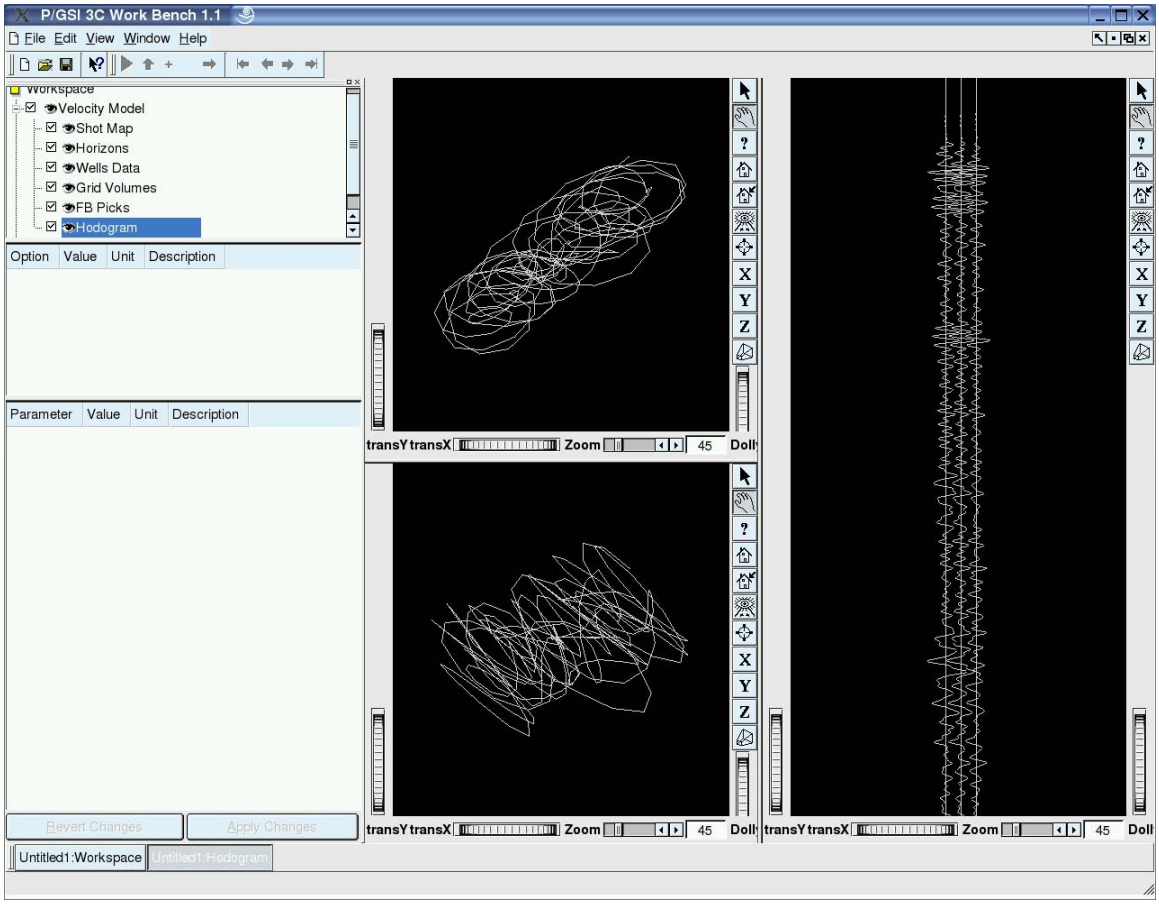

Figure 65 Hodogram display integrated into the Work Bench. Viewers used are x-y plane viewers.

In Figure 66 the sub-views are zoomed to a particular zone of the seismic trace, and the particle motion trajectories in the two planes are zoomed as well. We dynamically switch the viewers of this widget in Figure 67 to full 3D viewers, thereby allowing us to obtain a perspective view of the particle motion projection with respect to time. We are able to rotate, translate and zoom at will for detailed analysis.

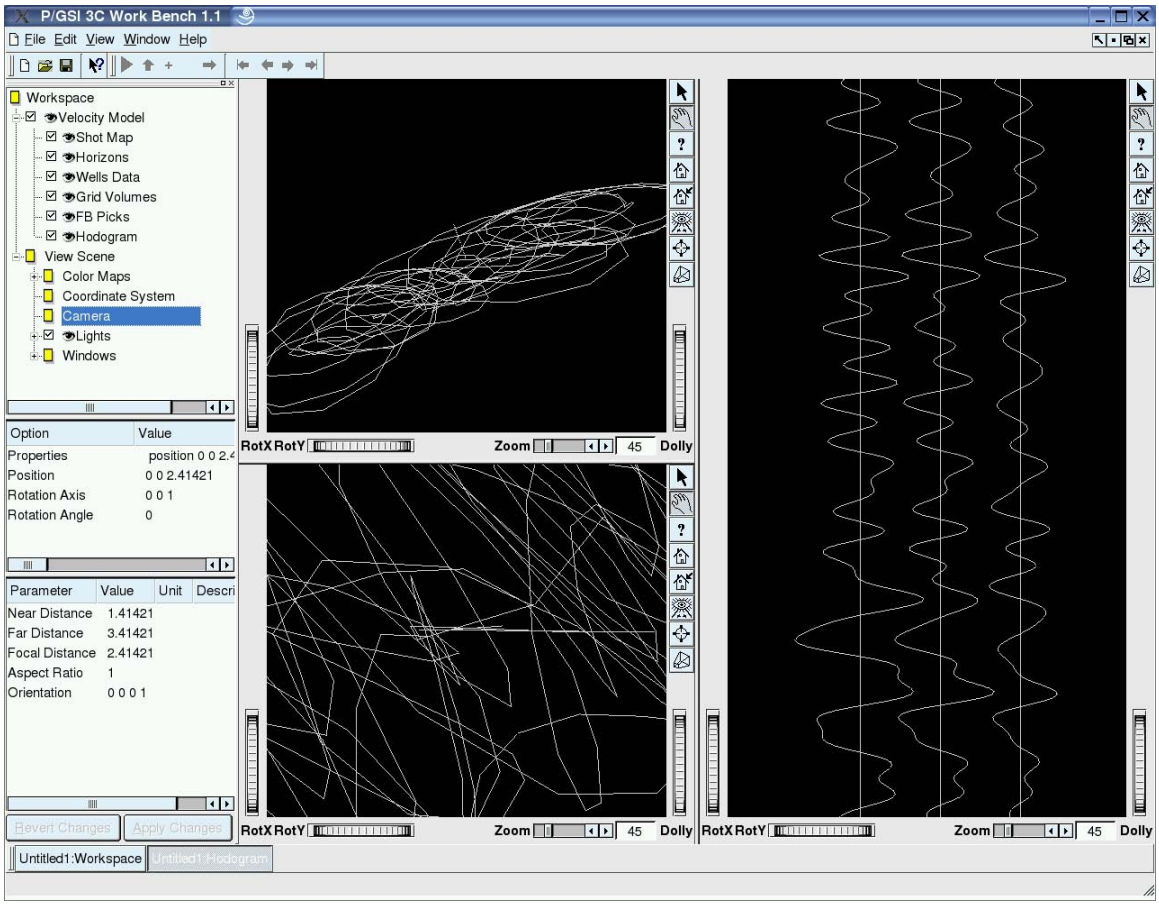

Figure 66 Besides simple 3D viewers, multi-paned widgets and sub-viewers can be integrated. Here they are used to display particle motion information (Hodogram).

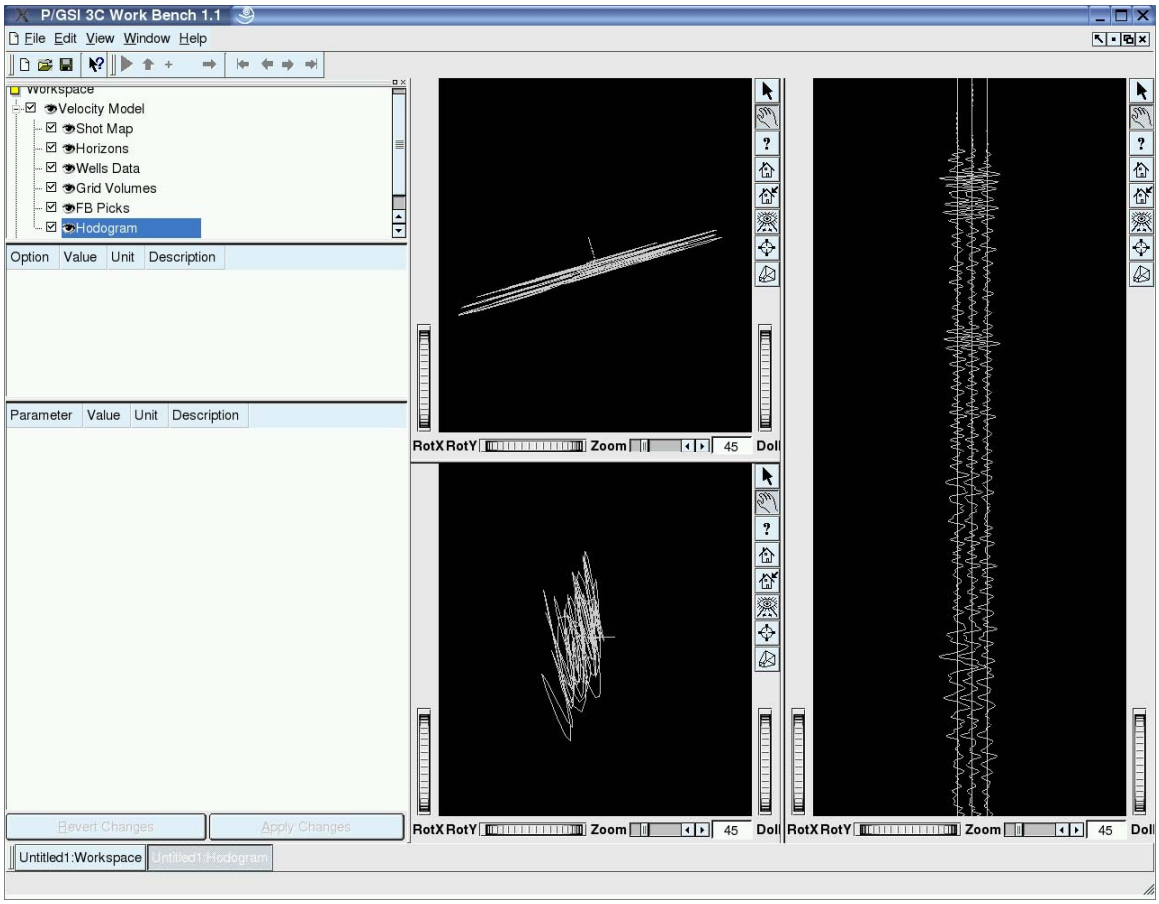

Figure 67 Hodogram display integrated into the Work Bench. Viewers are full 3D, that allow 3D visualization of particle trajectory with respect to time.

One of the key components of the 3D VSP Work Bench is the interactive pre-stack seismic display capability. This functionality allows us to access seismic data sets and load them into the viewer components for simultaneous analysis, with all the other information (velocity model, well logs, horizons, shot maps, first breaks, etc) which is of importance for advanced processing and interpretation tasks such as tomographic velocity model inversion and imaging. Figure 68 shows a corridor gather in a trace display view, and Figure 69 shows a composite view of a scalar corridor gather and a multi-component shot gather.

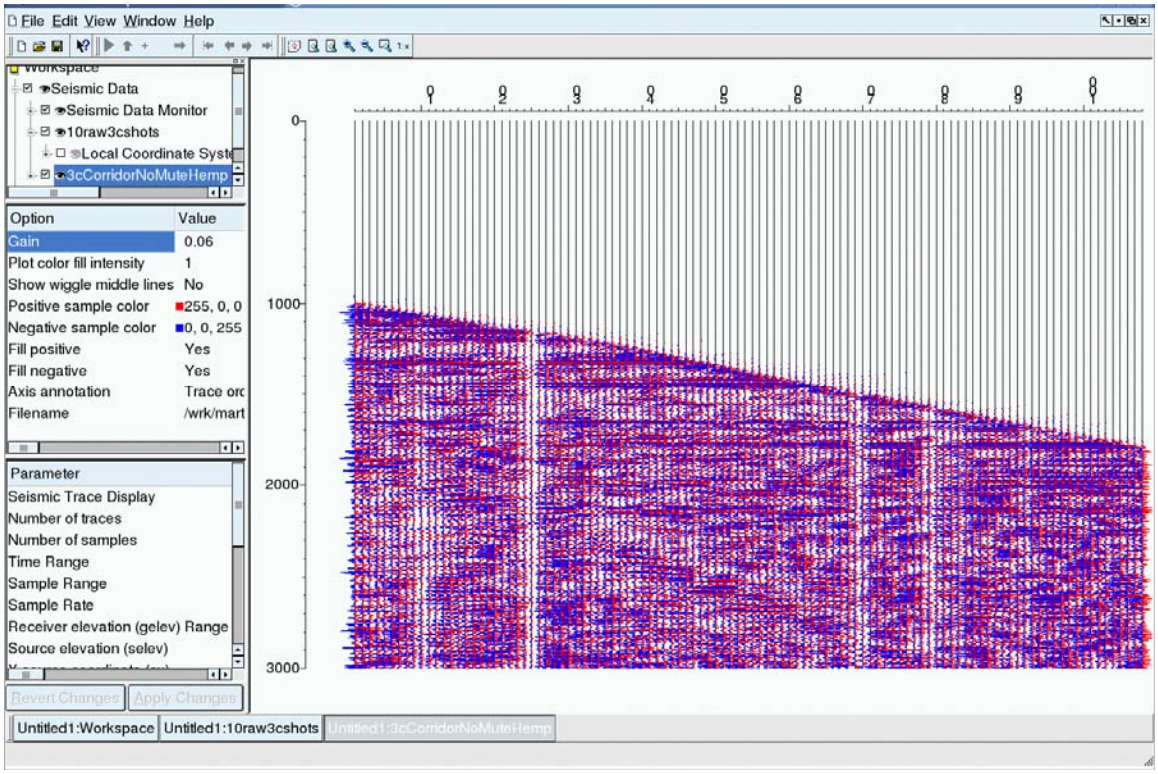

Figure 68 Corridor gather in a trace display view within the Work Bench.

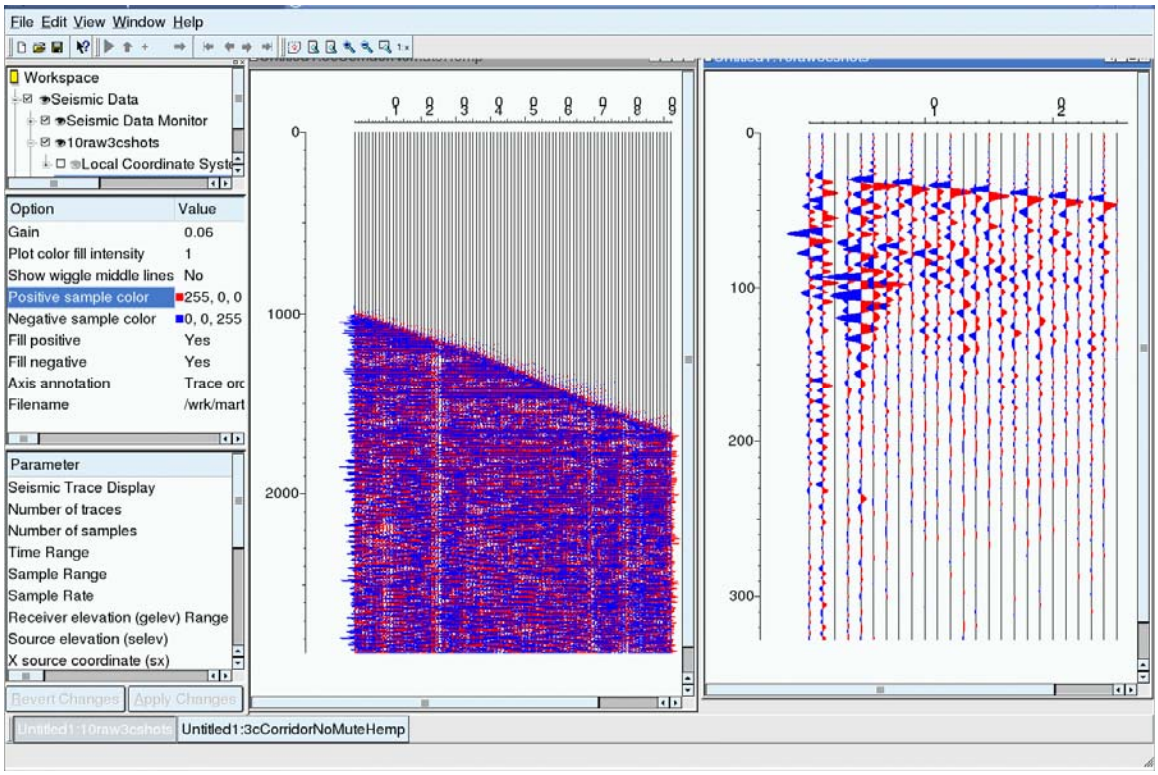

Figure 69 Composite view of a scalar corridor gather and a multi-component shot gather.

Another key component of the Work Bench is the ability to display and manipulate well log curves. Log curves can be displayed for example as lines, as a solid fill, or porcupine display, or in a cylindrical fashion around the wellbore. Figure 70 shows a cylindrical display combined with a porcupine display.

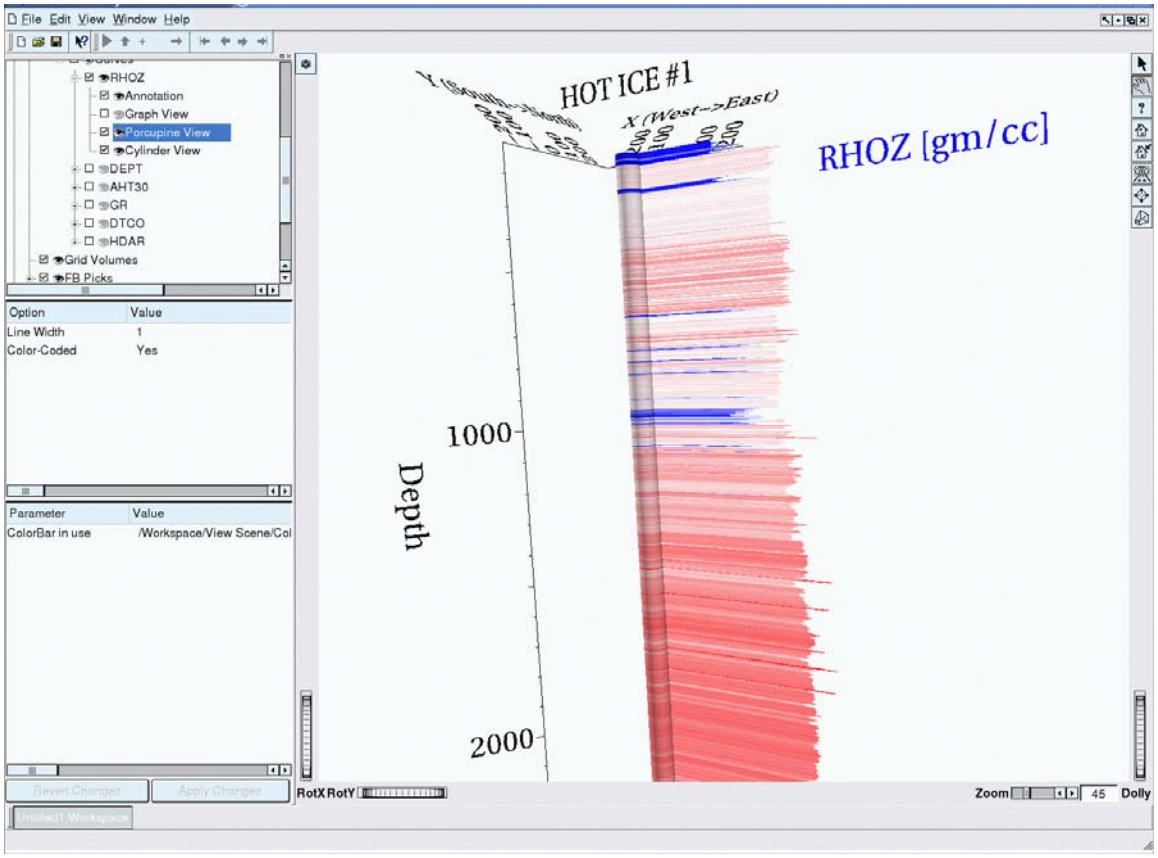

Figure 70 Well log curve cylinder combined with a porcuine display.

Log curve displays can of course be combined with seismic images or surfaces to generate composite views of different data types. Figure 71 shows an example of a well log curve displayed along a slightly deviated well.

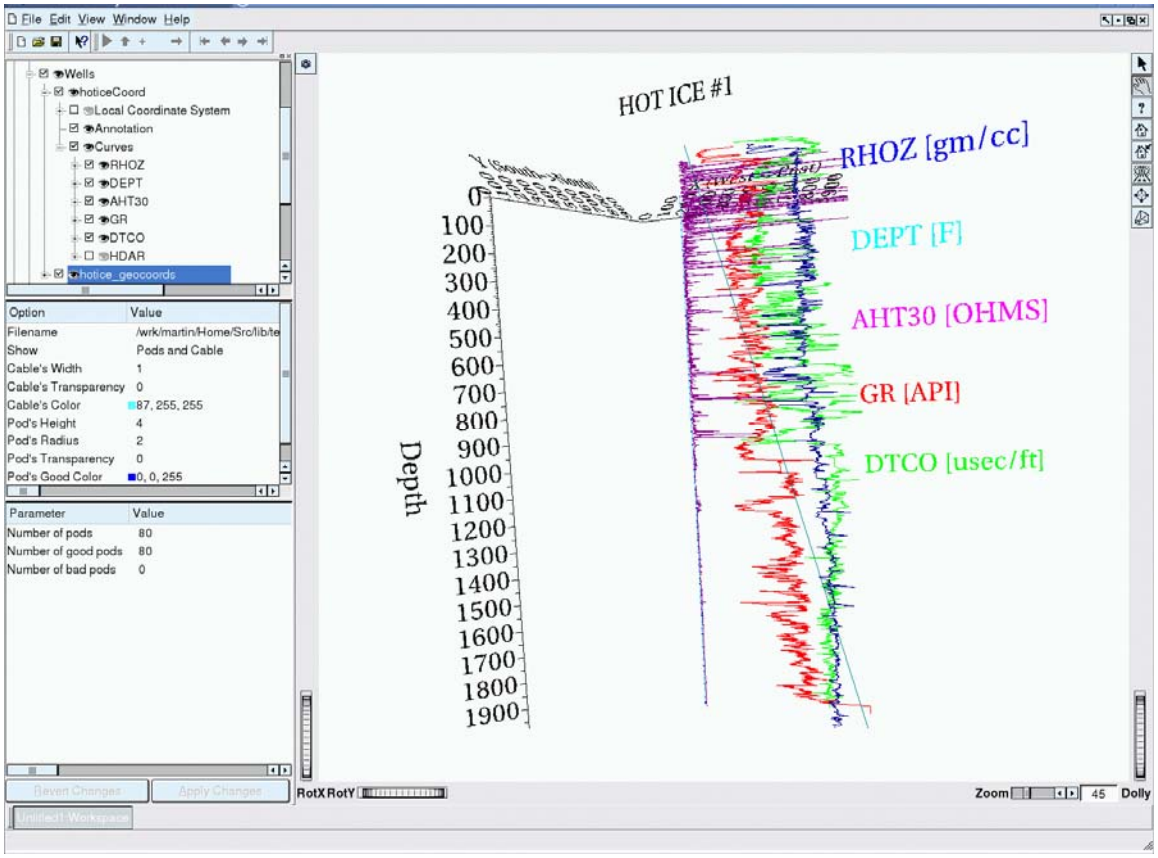

Figure 71 Well log curves displayed along a slightly deviatedwellbore.

As part of our efforts to include functionality for tomographic inversion and ray tracing tools in the Work Bench, we developed a ray path manipualationa and display widget. While incorporating software hooks for pre-existing tomographic analysis modules, we added the ray path capabilities to the multi-component Work Bench. Figures 72-74 show various display options and highlight the capabilities of this widget. Rays are plotted in 3D with information, such as travel time, amplitude, and Fresnel zone width encoded in the color of each ray. Each ray set can be selected and manipulated and tied to other PG-UItems. Figure 72 shows a basic display of ray set lines. Figure 73 shows those ray sets with the seismic amplitude shown in color on each line. Similarly, Figure 74 shows them color-coded with Fresnel zone information.

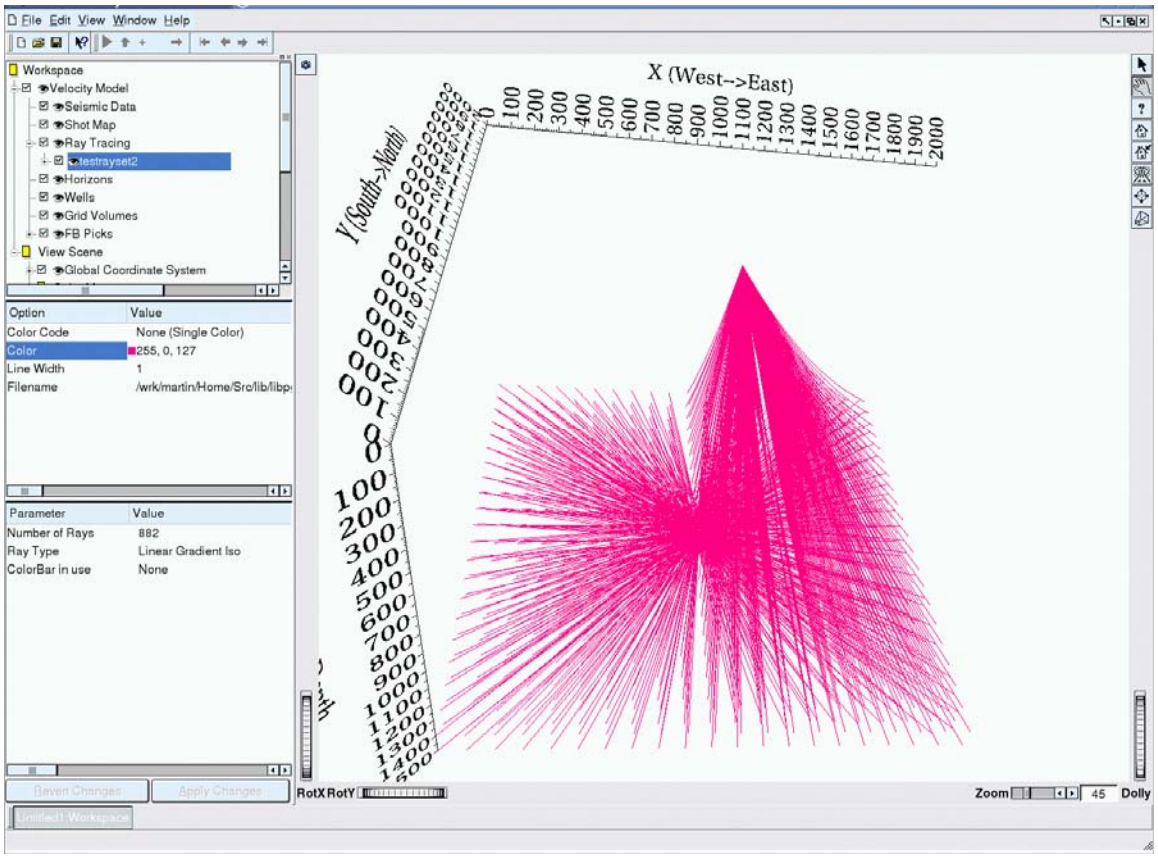

Figure 72 Ray set lines in the Work Bench.

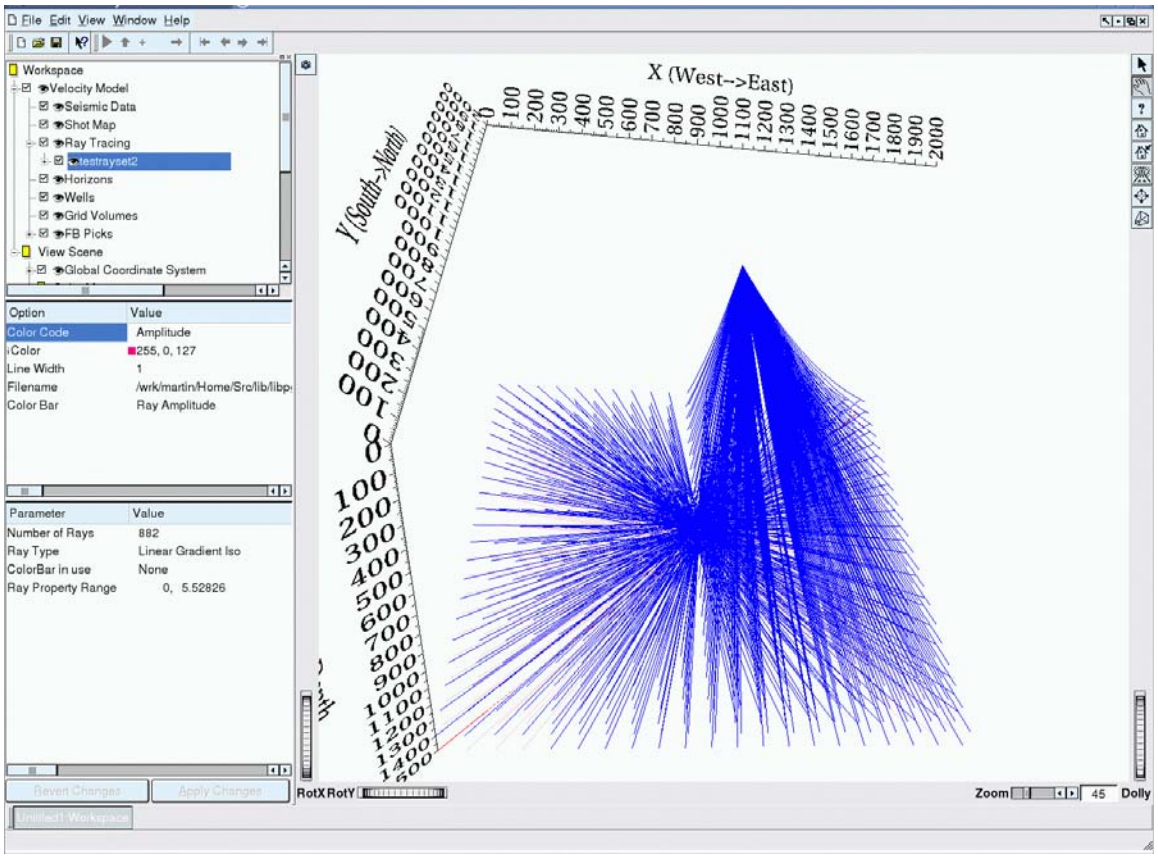

Figure 73 Ray set with amplitude shown in color..

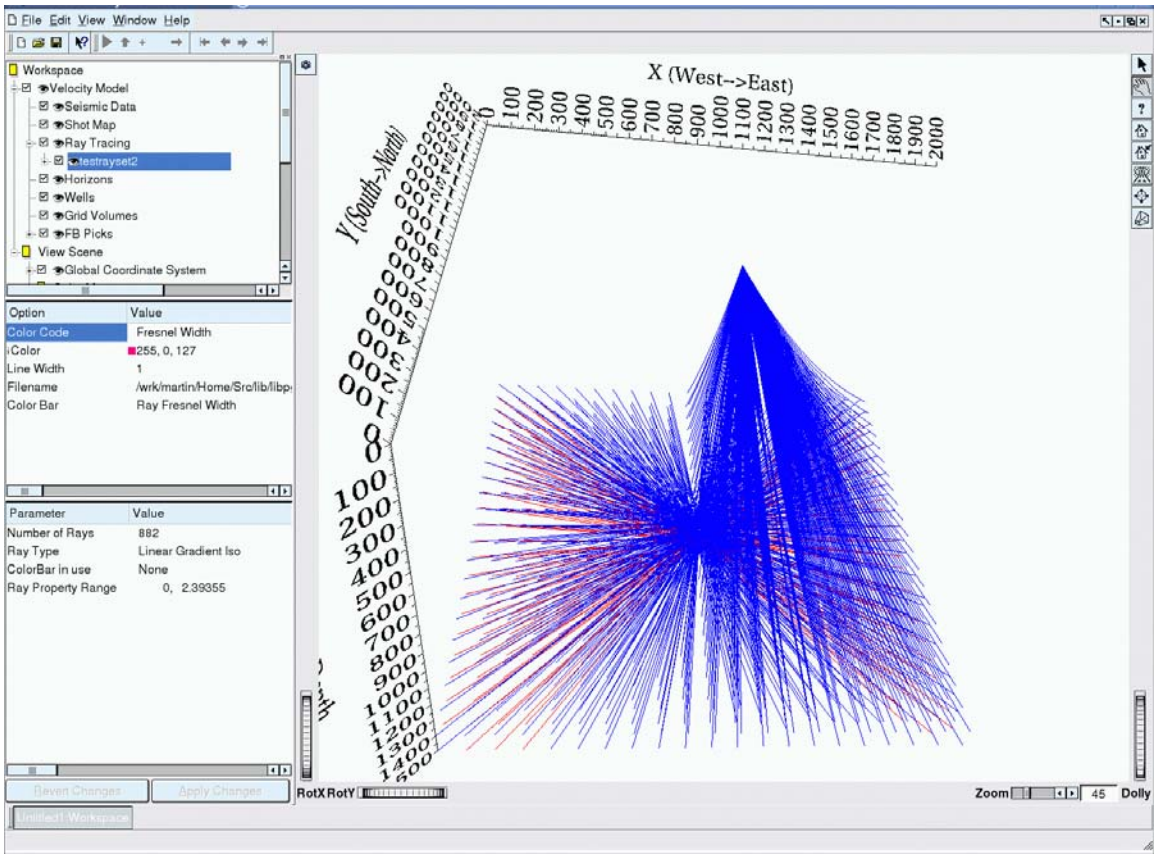

Figure 74 Ray set with Fresnel zone shown in color.

Task 8

Test the prototypes on synthetic and real data. Optimize individual classes and functionality for fast 3D manipulations. Review and modify the user interface to meet the demands of the data processing and interpretation community. The toolkit must be easy to learn and use, and consistent across all display classes.

The need to view several disparate pieces of information together within a single view is well known in the energy exploration and development business. However, it is also important to be able to view individual pieces of information by themselves in order to examine them in more detail. Therefore, we developed the capability to display data components in multiple viewing windows in addition to the composite view. One issue for the user now becomes managing a finite amount of screen space while working with several data types in several views. The problem is exacerbated if multiple display monitors are attached to the workstation. In order to address this issue, we refined the window docking and un-docking features.

Figures 75-78 demonstrate how multiple viewing windows can be created within the Work Bench that contain individual data items as well as and composite views. Figure 75 shows the work bench with the main window containing the data item tree, option tree and parameter tree. In the data item tree various pieces of data have been loaded that are displayed in the work space area. When loading individual data items, the user can select if a new window should be opened. By default the display will go to the already-opened view window. On the bottom of the display are posted the four work space windows that are currently active, entitled: Workspace, Grid Volumes, Wells Data and Shot Map. The windows have been undocked but are still constrained to be within the main work space.

One can clearly see that for certain analyses, it is advantageous to maximize the view of certain display windows while being unconstrained in where to place the sub-views. Figures 76-78 show the individual composite displays in their respective windows. Figure 76 contains the depth slice view only. Figure 77 and Figure 78 display the well log curve and source location respectively, in their own viewing windows.

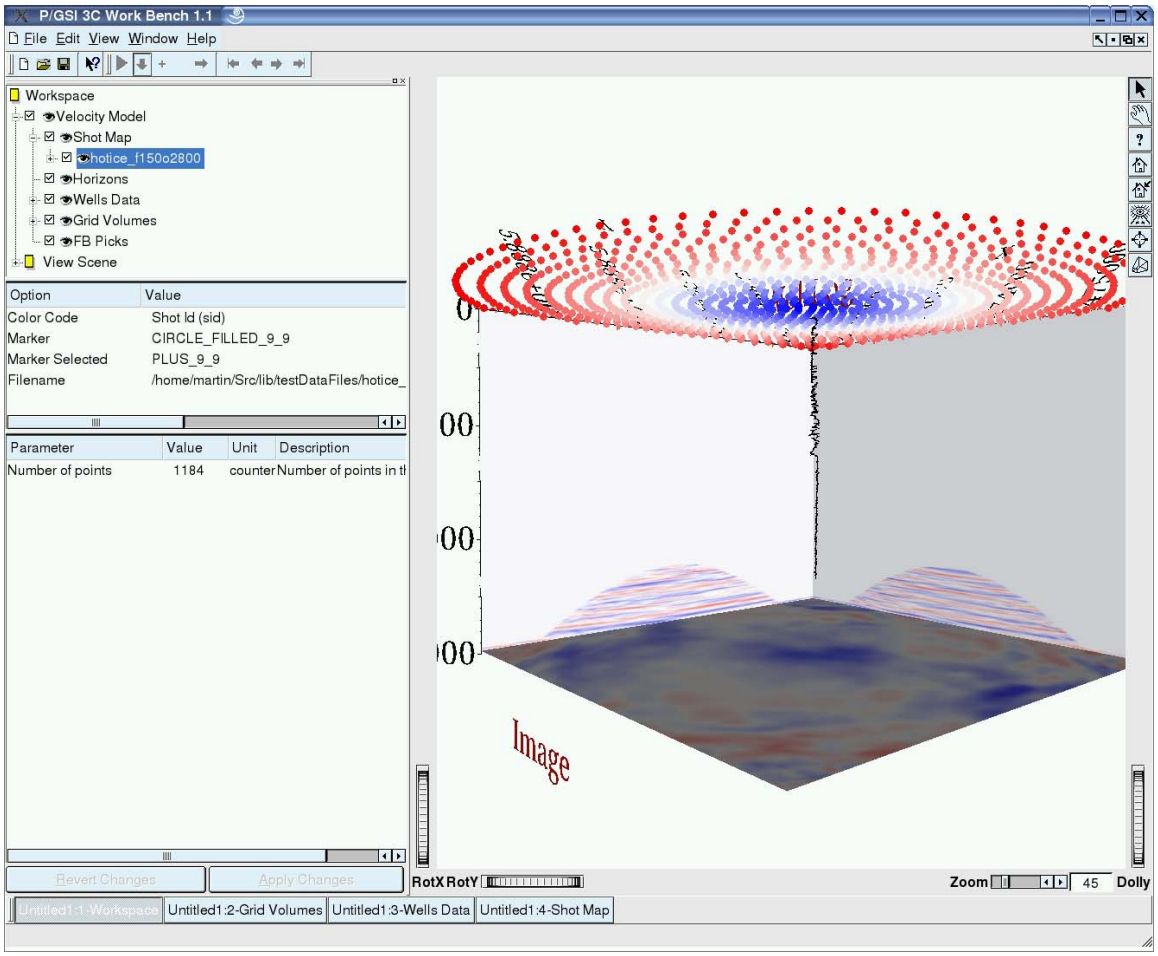

Figure75. View window 1, composite view displaying three different display itema; shot locations, well log and seismic image volume.

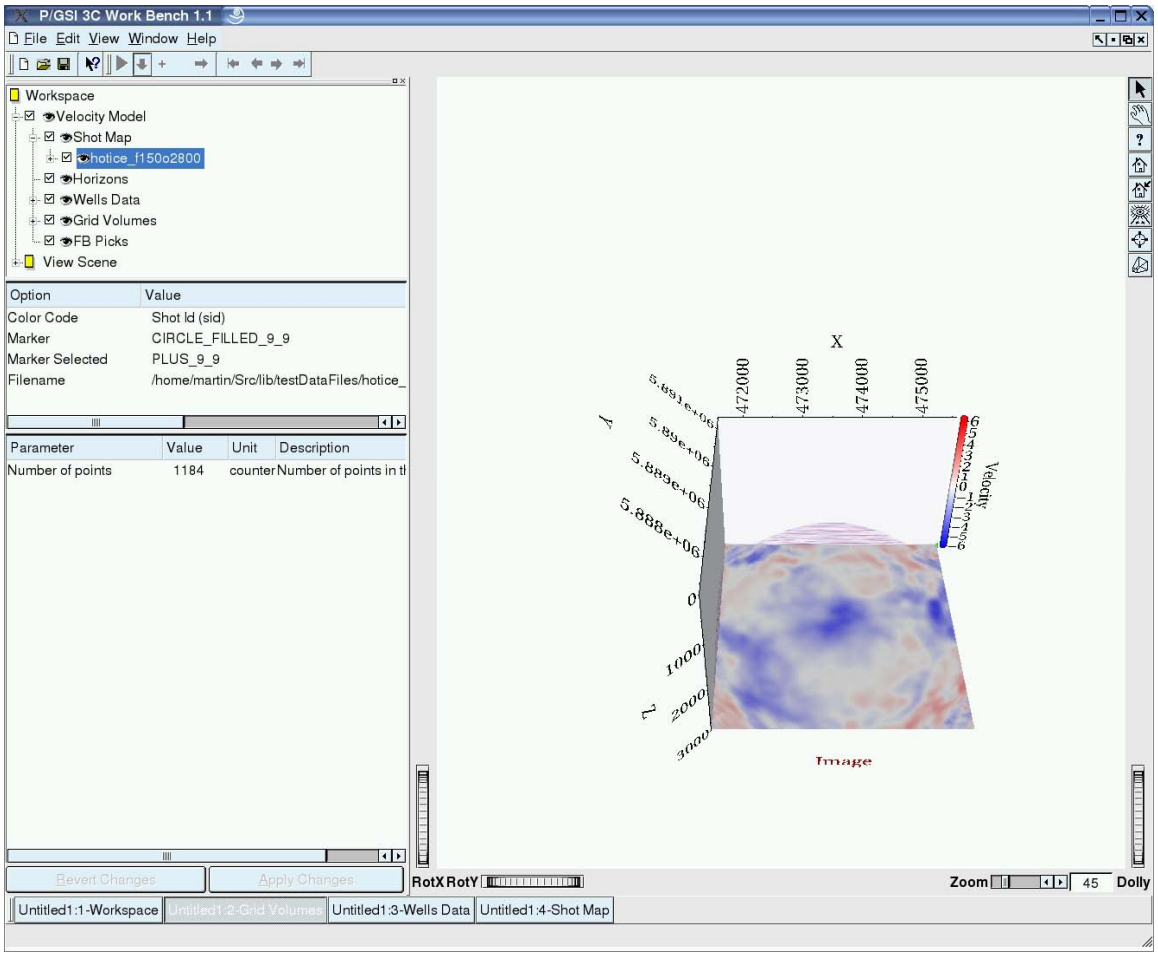

Figure76. View window 2, view displaying seismic image volume slices.

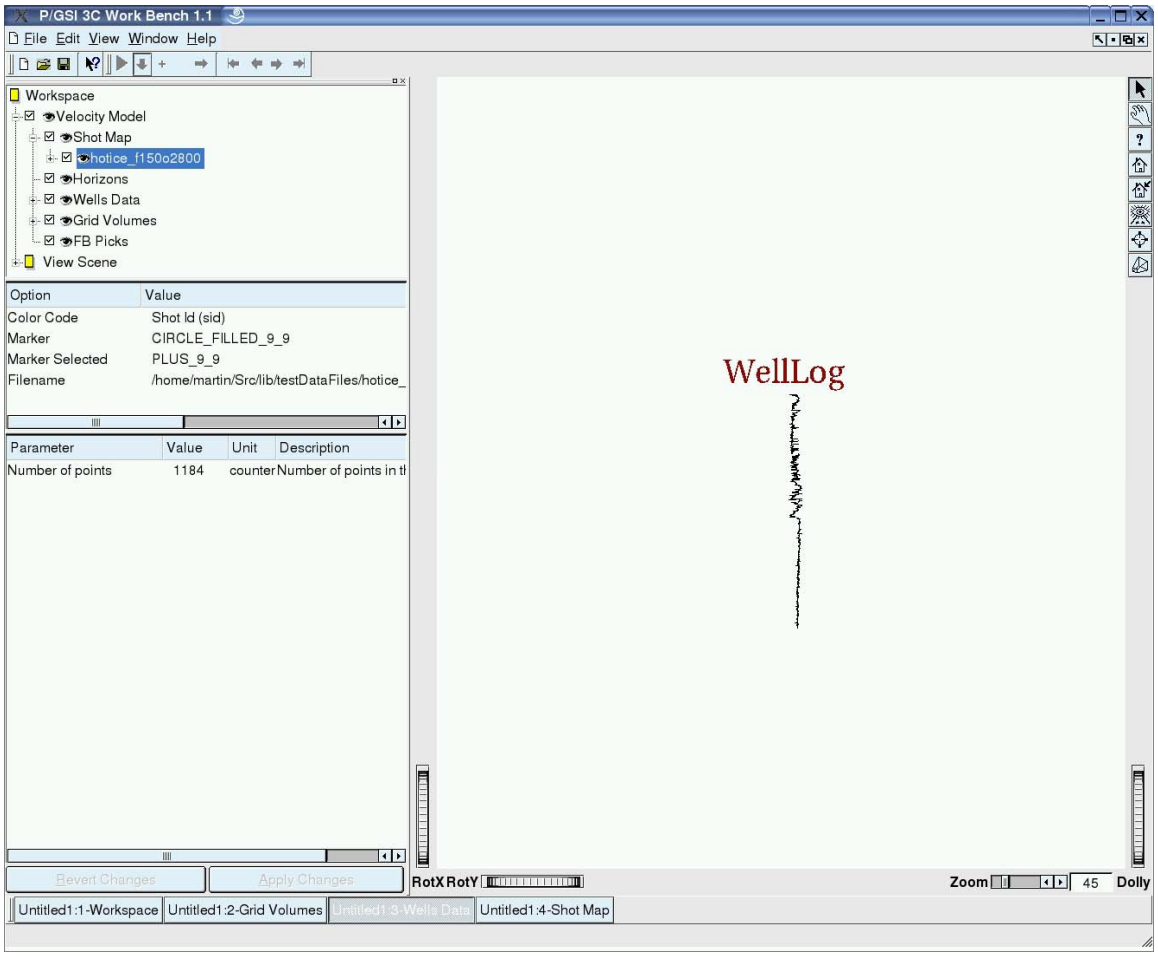

Figure 77. View window 3, display of the well log curve.

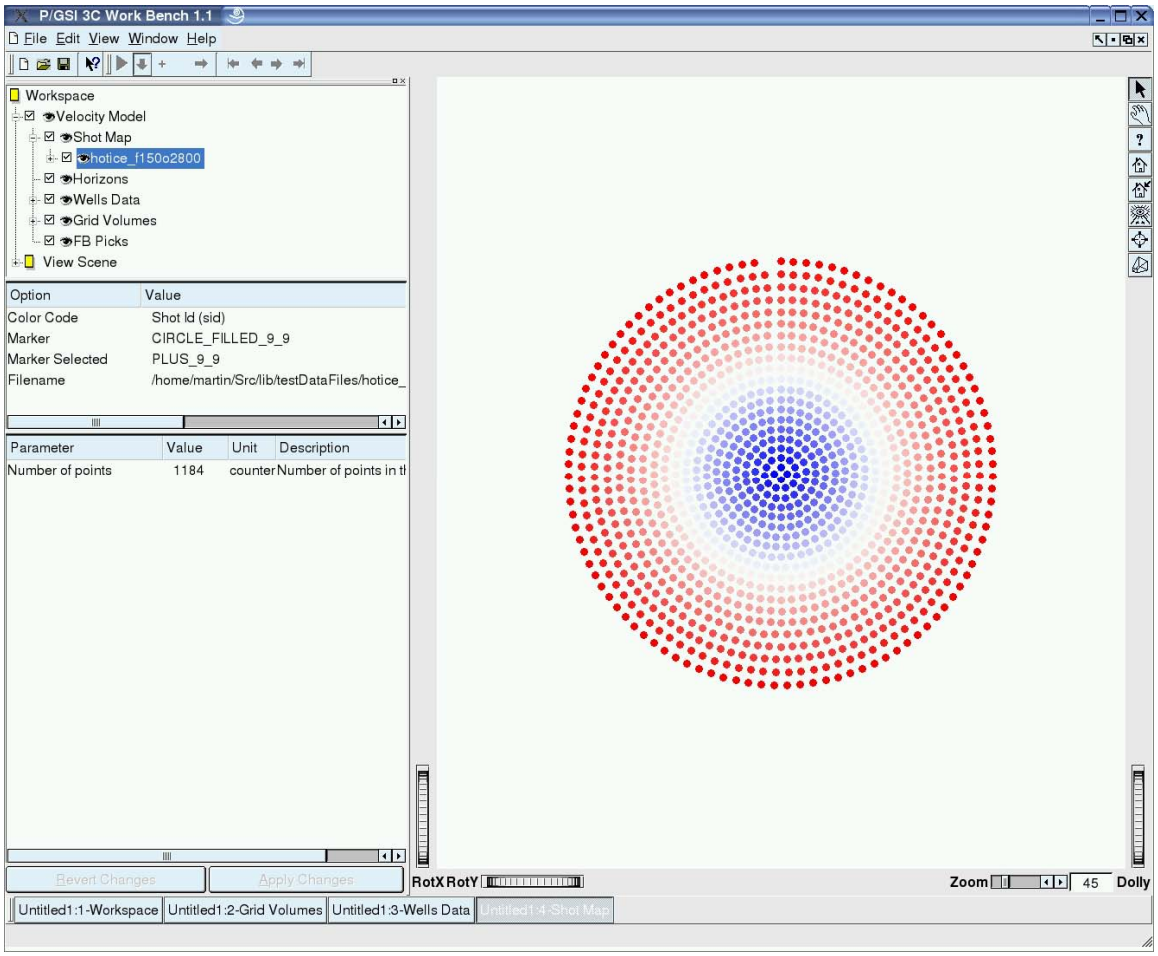

Figure 78. View window 4, displaying the 3C VSP source locations from above.

In the snapshot shown in Figure 79, all of the display windows have been undocked from the main work space window and are free to be placed anywhere on the desktop display. In this way, views can be custom tailored to the needs and requirements of individual users, as well as certain prescribed work flows.

Figure 80 shows the successive state of the composite display arrangement where the user changed the display type of the well log curve in the main window's item tree. Dynamically two sub-view windows got updated and adjusted. The sub-view window containing the seismic image volume slice view has been manipulated at the same time by curser movement in the 3D display window, which in turn dynamically updated the main windows option and parameter view list. Notification is sent from one view window to another if the same data item is displayed in multiple view windows.

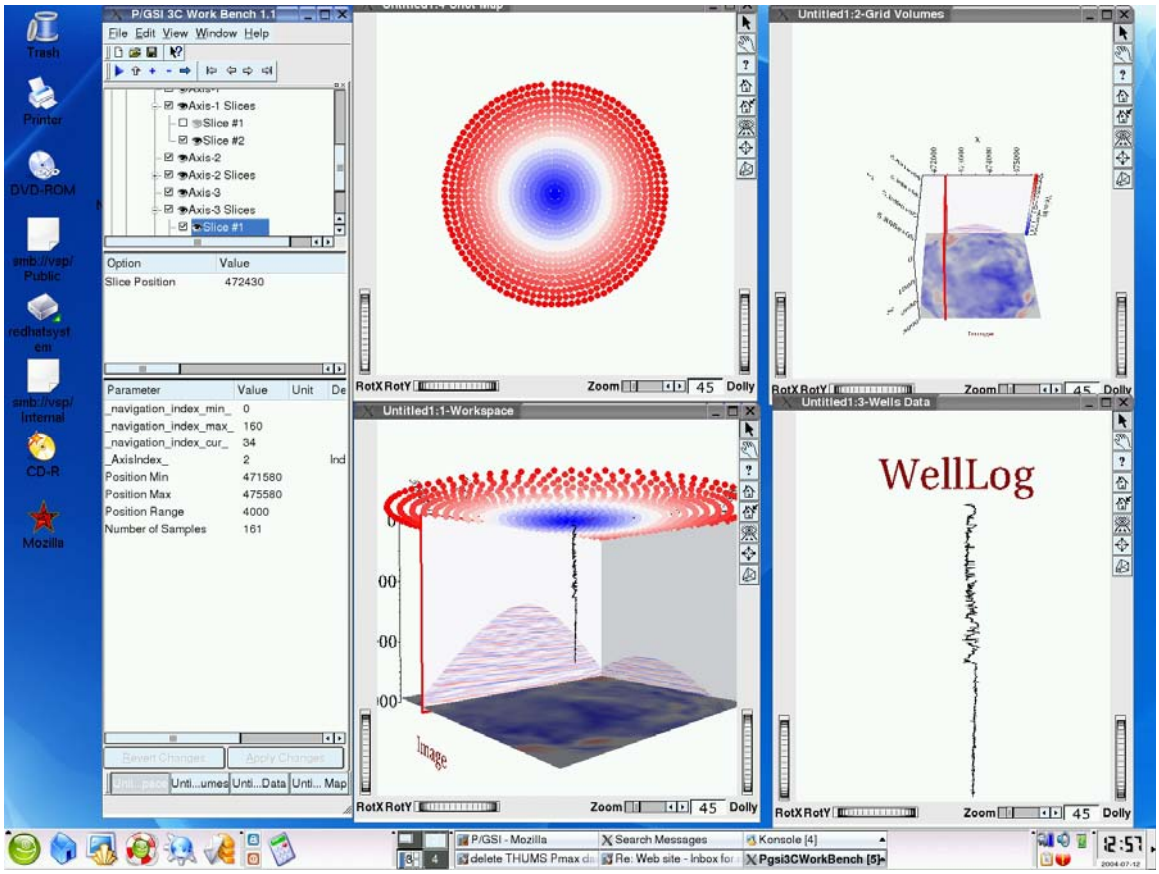

Figure79. Undocked windows of the main Work Bench application and the four view windows, allowing ergonomic use of screen real estate. The user can zoom, compare, and correlate the view windows to evaluate the data.

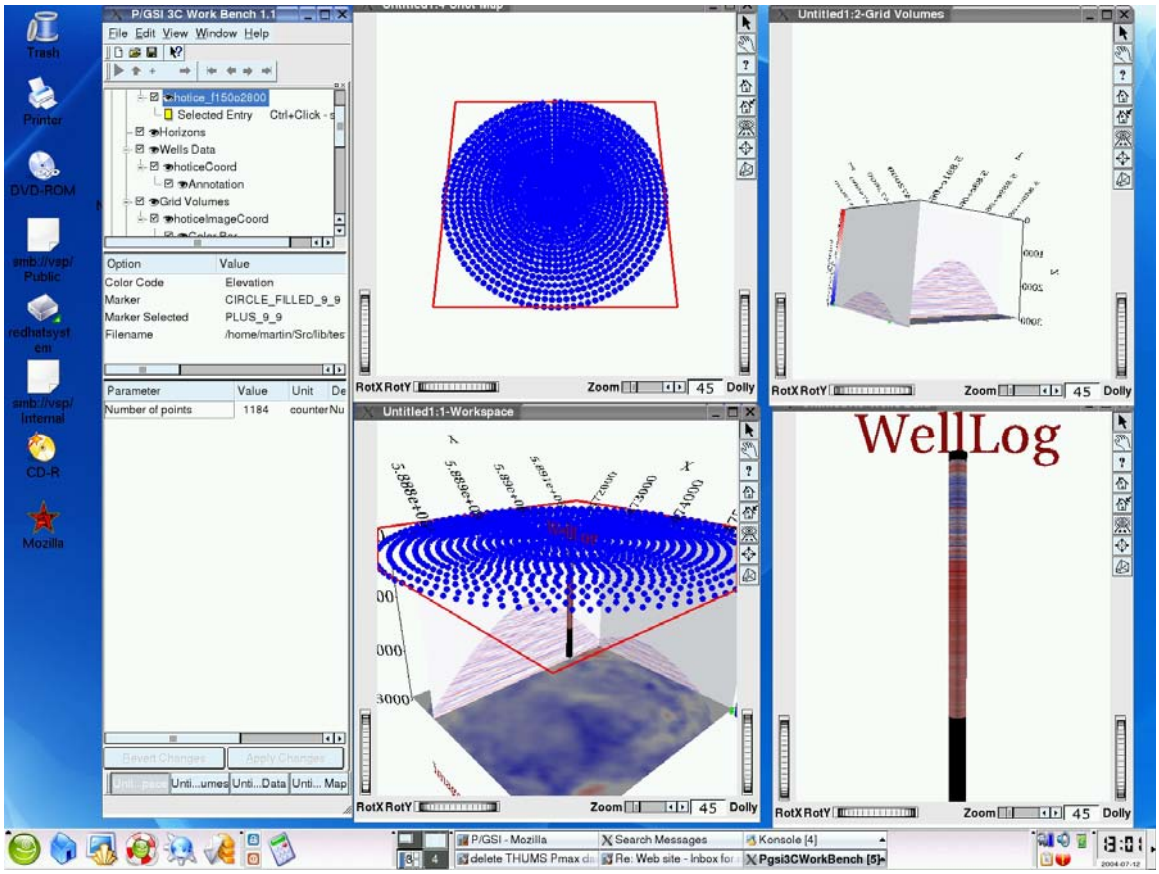

Figure 80 Undocked windows consisting of the main Work Bench and four viewer windows. Each window can be manipulated independently. The ability to efficiently analyze borehole seismic data is greatly enhanced.

The work bench would not be complete without a robust mechanism to transparently convert between local and global coordinates of objects. We added the ability for the user to do this, while remaining in full control of display and labeling aspects. Any widget or PG-UItem object can make use of this feature. The possibility exists to attach and execute underlying processing flows.

Task 9

Analyze the data flow and interaction requirements for specific processing and display functionality. Analyze parallelization and communication needs, and prepare design specifications for these things.

Seismic data are typically represented digitally, as individual traces, and combined into large 2D, 3D or higher dimensional volumes of data. A multi-component 3D VSP survey can range in size from about several hundred MB to several hundreds of GB. Such a large amount of data requires special handling from programmatic point of view. We have re-designed a number of C++ classes to accommodate the needs of efficient large data handling.

We have re-designed and implemented a generalized C++ class called a PGSharedObject. Many different data types, be it well logs, seismic volumes, or geologic horizons for example, can be loaded into the Work Bench from files, and then modified and saved. At this time, there are over 20 different types of shared objects, which include the for example SeismicData for handling seismic traces, and GridVolume, the encapsulation of multi-dimensional data arrays.

As described in Task 6, each piece of data that is read into the Work Bench is encapsulated into a PG-UItem class. Each PG-UItem is a holder of a list of properties in a generalized form, mapping user-friendly names to values of an arbitrary type.

A PG-UItem may or may not have a shared data object attached to it. In either case, the properties of the PG-UItem describe a variety of parameters that are important for the end user. Figure 81 shows the general relationship between the application user interface and the PG-Uitem tree.

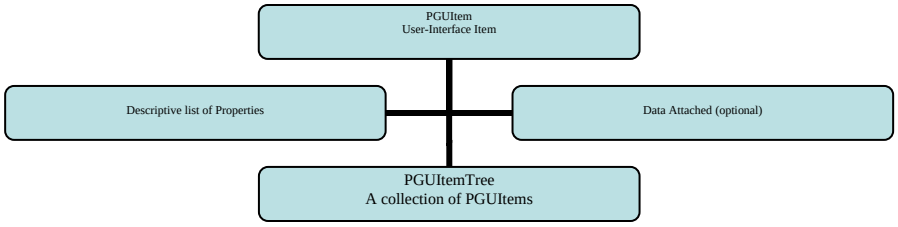

Figure 81. VSP Work Bench design and the relationship between the user interface and the PG-UItem class.

We use are able to use over 50 different types of PG-UItems in the Work Bench shown in this report. A typical example of a PG-UItem without data attached would be properties of a graph axis or plot annotation. If a piece of data is attached, then the PG-UItem has properties describing that data. A collection of PG-UItems is arranged in a logical tree. Each PG-UItem can have a parent PG-UItem and a number of children.

Task 10

Review, select and install communication software for cluster, workstation, and PC processing. Test the communication software for reliability, latency and bandwidth in a single user and multi-user environment.

Consistent with the other low-level toolkits used in this effort, we chose to use the Message Passing Interface (MPI) toolkit to develop interprocess communications for the multi-component VSP work bench. MPI is widely used in the high performance computing community because it is widely available, portable, and easy to use. Furthermore, since MPI was designed for high performance on both massively parallel machines and workstation clusters, it is very efficient. Implementations of MPI are available for free as OpenSource, as well as from third party vendors. We have worked solely with the free OpenSource versions of MPI.

We adapted a suite of classes that are written on top of MPI to facilitate the processing of multi-component VSP data on a Beowulf cluster. However, because of the general design of both MPI and our own class implementations, the identical parallel codes can be run on a single workstation with multiple processors, or on a cluster of single or multi-processor computers.

Task 11

Design the high-level communication patterns among the framework objects, so that a quality of service level is guaranteed based upon the complexity of the multi-component processing and display interactions that are performed.

Intra-process communications are needed so that we can pass key information within the Work Bench tool itself. For example, information must pass from a pop-up dialog box to a function that handles what needs to be done when the OK button is pressed. In addition, this must meet our design criteria of being portable, standard, and easy to use. In a strictly Windows environment, communications of this sort are typically implemented using the Microsoft Foundation Classes (MFC). However, this is not portable across Windows and Unix platforms. A portable set of tools is supplied by the Qt toolkit, with a mechanism called *signals* and *slots*.

Any Qt class can possess one or more signals and one or more slots. Qt objects can emit signals to notify other C++ objects when certain events occur. For example, a signal can be emitted when the OK button is pushed on a pop-up dialog box. A slot is very much like an ordinary member function. Slots are implemented by the application programmer, and connected to signals by the use of the Qt *connect* function. Signals can be connected with any number of slots in any other C++ object. When a signal is emitted, using the Qt keyword *emit*, all the connected slot functions get called.

In earlier days of X and Motif, this type of signaling metaphor was implemented with *callback* functions. The Qt signal and slot design is much more robust, provides a rich set of efficient signaling features, is portable across Windows and Unix platforms, and finally, the slot functions are more reusable than the earlier X/Motif callback metaphor.

Task 12

Implement the high-level communication library.

The VSP processing work flow requires multiple adjustments to the data, mainly to the velocity model, in order to obtain meaningful images of the underlying seismic response. Typically a geoscientist will make an initial estimate as to the velocity of the subsurface, migrate the data, and then view and compare the resulting seismic image with other known information. Where the seismic image differs from what is expected, modifications are made to the velocity model to produce a more accurate seismic image. Thus the data processing work flow is an iterative one, involving many pieces of tangible and intangible information. Figure 82 outlines the data processing work flow in a general sense.

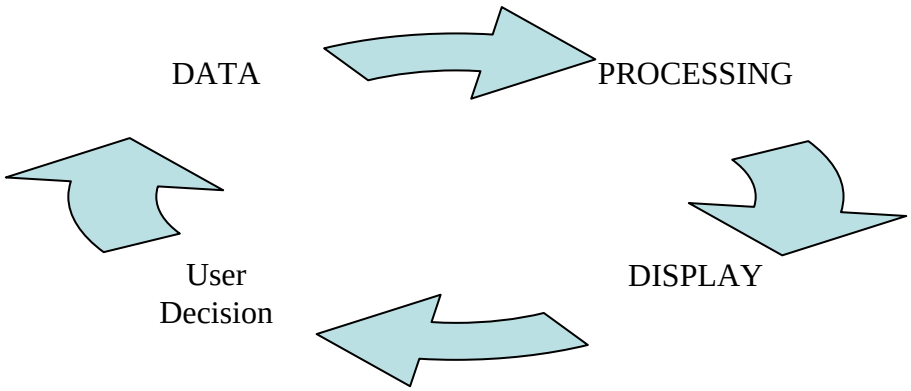

Figure 82. A general depiction of the data processing and interpretation work flow.

In order to meet the requirements of such a work flow, we enabled the ability to work with many disparate types of information, many views of the data, and to have the ability to quickly make changes to the data and re-run the seismic processing. This we have done by using and extending a communication library based upon the Qt signal and slot construct.

Task 13

Test the high-level communication library for robustness and speed using synthetic and field datasets. Test parallel actions and data streams going to and from clusters and workstations, onto a target display workstation.

We developed a tool as part of the VSP Work Bench application that is used to transfer data collected with a seismic recording system directly to the Work Bench. The recording system runs in a Windows environment; the transfer piece and the VSP Work Bench can of course run in either a Windows or Unix environment. The data files are not particularly large, but they can be generated over a long period of time, hence the need for a fast transfer operation that handles the book-keeping aspects of potentially hundreds of thousands of data files. The data transfer operation is typically performed in the field, running on equipment that is inside of the data acquisition truck at a job site. The transfer operation uses a unique feature of the Qt signal and slot functionality called a *timer*. The timer capability allowed us to build a data transfer mechanism whereby the slot function is called repeatedly at a specified time interval. The slot function then is responsible for such things as moving the data from one machine to another, and the data book-keeping functions including organizing the data into sub-folders, writing headers, formatting, and writing the files to tape. The analyst is then able to view and monitor the data for QC purposes essentially in real time as the data are being recorded in the field. Figure 83 shows the launching of the data transfer operation from the VSP Work Bench. Figure 84 shows a display of some raw recorded data that have been transferred into the VSP Work Bench.

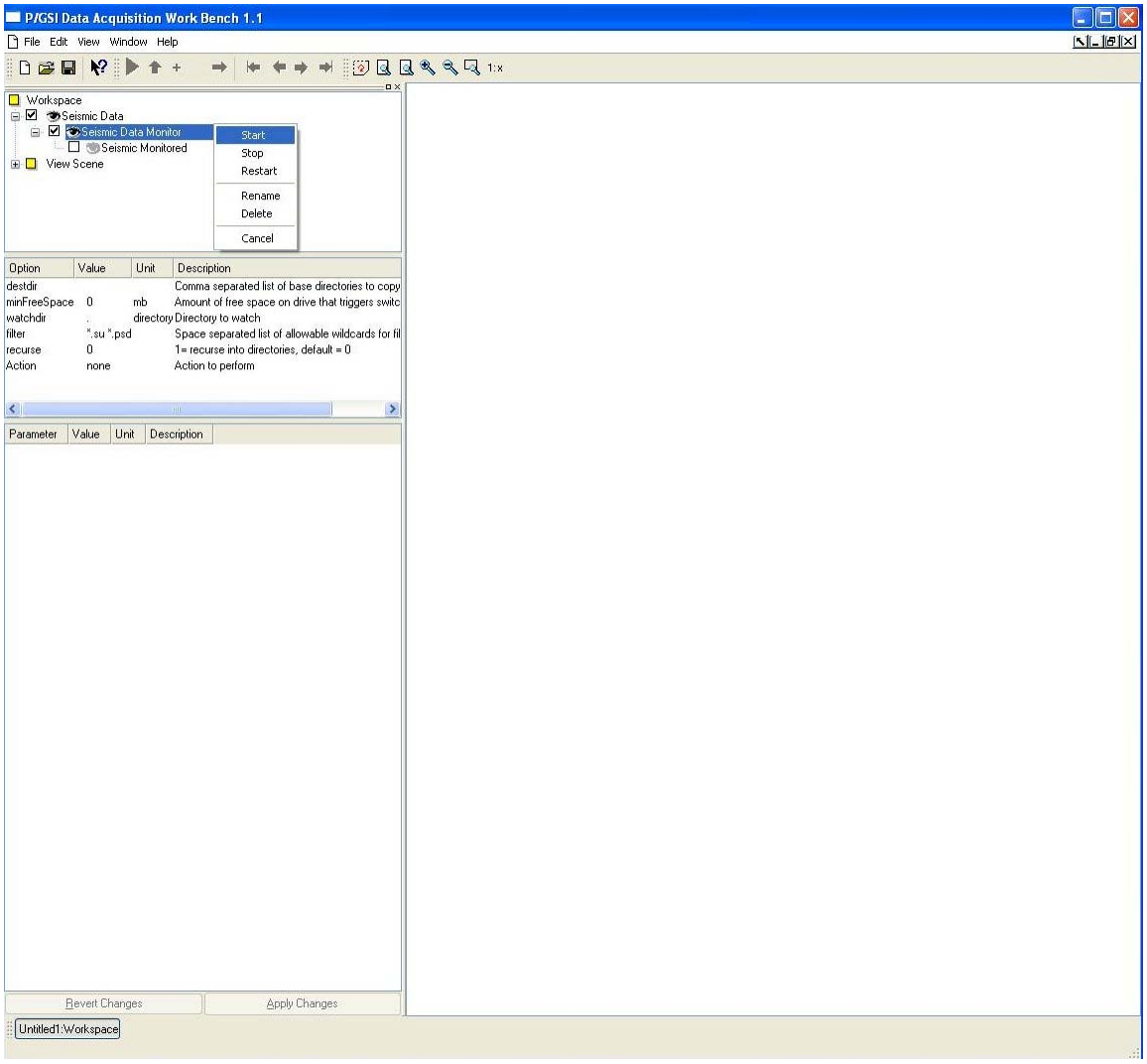

Figure 83. Launching the Data Transfer operation from the VSP Work Bench.

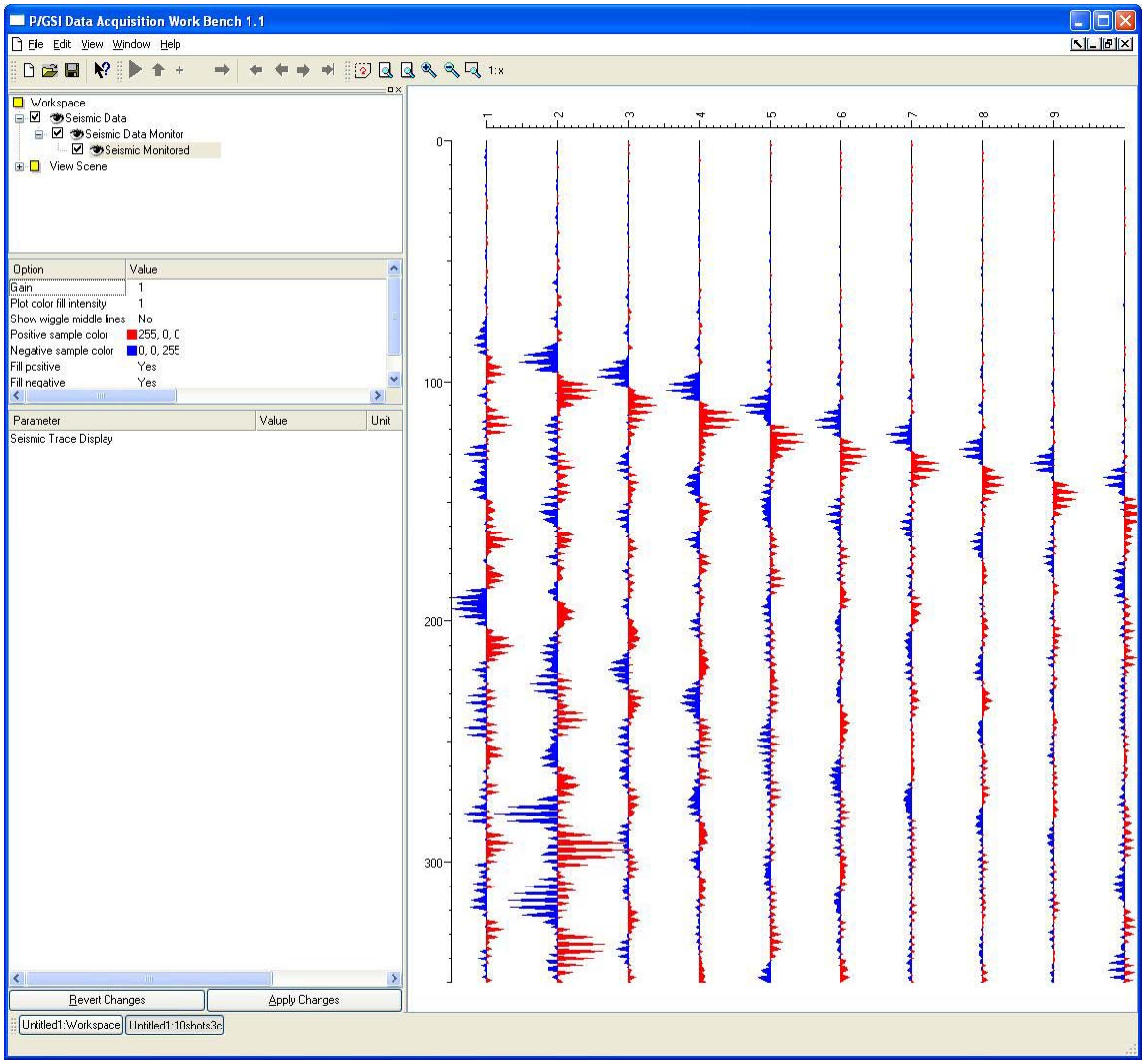

Figure 84. A display of the raw recorded data after being transfered from the field recording system into the VSP Work Bench.

Task 14

Design the interconnect of the communication libaray with the multi-component 3D display framework.

Many PG-UItems have a class associated with them for displaying purposes, derived from the low-level abstract class PG-DItem, as discussed in Task 6. The PG-DItem, or PGDisplayItem provides a connection between data attached to PG-UItem and the display framework based on the OpenInventor toolkit. A collection of PG-UItems, a PG-UItem Tree, provides a number of functions:

- Displaying properties of the data in a user-friendly and editable way
- Displaying the data attached in a graphical form using an OpenInventor window in the form a particular data can be displayed.
- If the user modifies the parameters of PG-UItems, some data may need to be calculated or updated. Updates to the data are synchronized on the OpneInventor display window.

This process is controlled by the use of a Task Manager class, as shown in Figure 85.

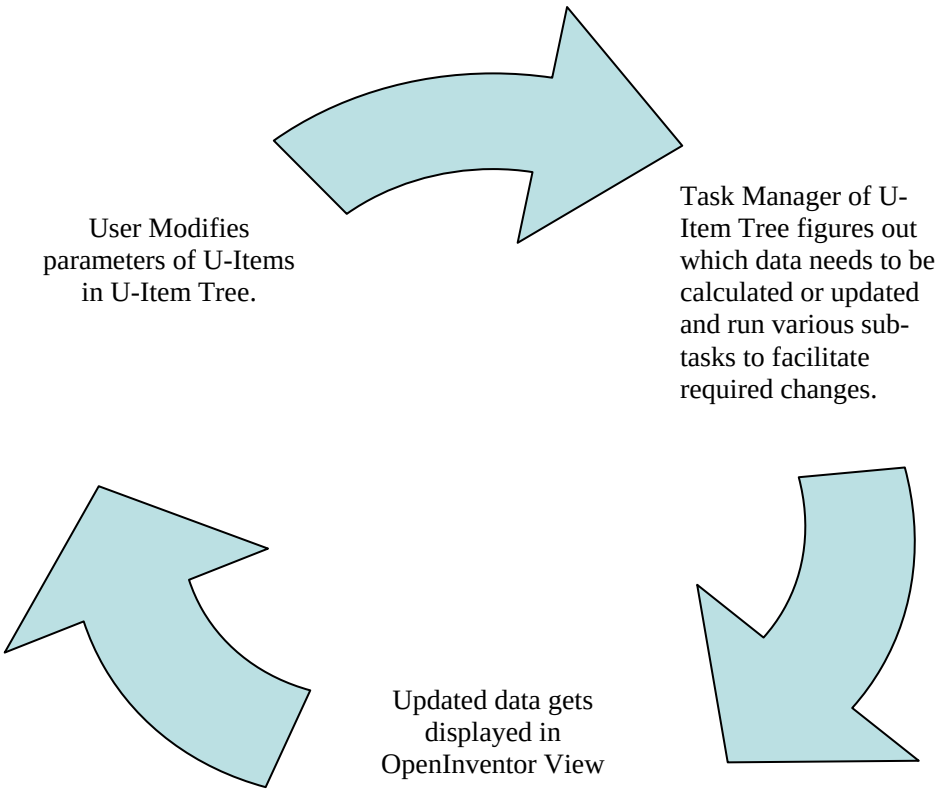

Figure 85 Overview of the Task Manager.

Task 15

Implement and integrate the multi-component and accessory data objects with the interactive display framework and the parallel computational framework.

The VSP Work Bench provides a powerful day-to-day toolkit for our earth science professionals, enabling them to perform the tasks of data processing, analysis and interpretation more quickly and more accurately. In addition, the tool runs on both Linux and Windows platforms, and can be run from a typical office workstation, a simple Windows laptop, a cluster computer, and even from a workstation in the field recording truck. The Work Bench is intuitive and easy to use, so the learning curve is short. Professionals on our staff are able to quickly learn the tool and use it as an integral part their daily work flows. Following are a set of figures that demonstrate the complexity and flexibility of the Work Bench.

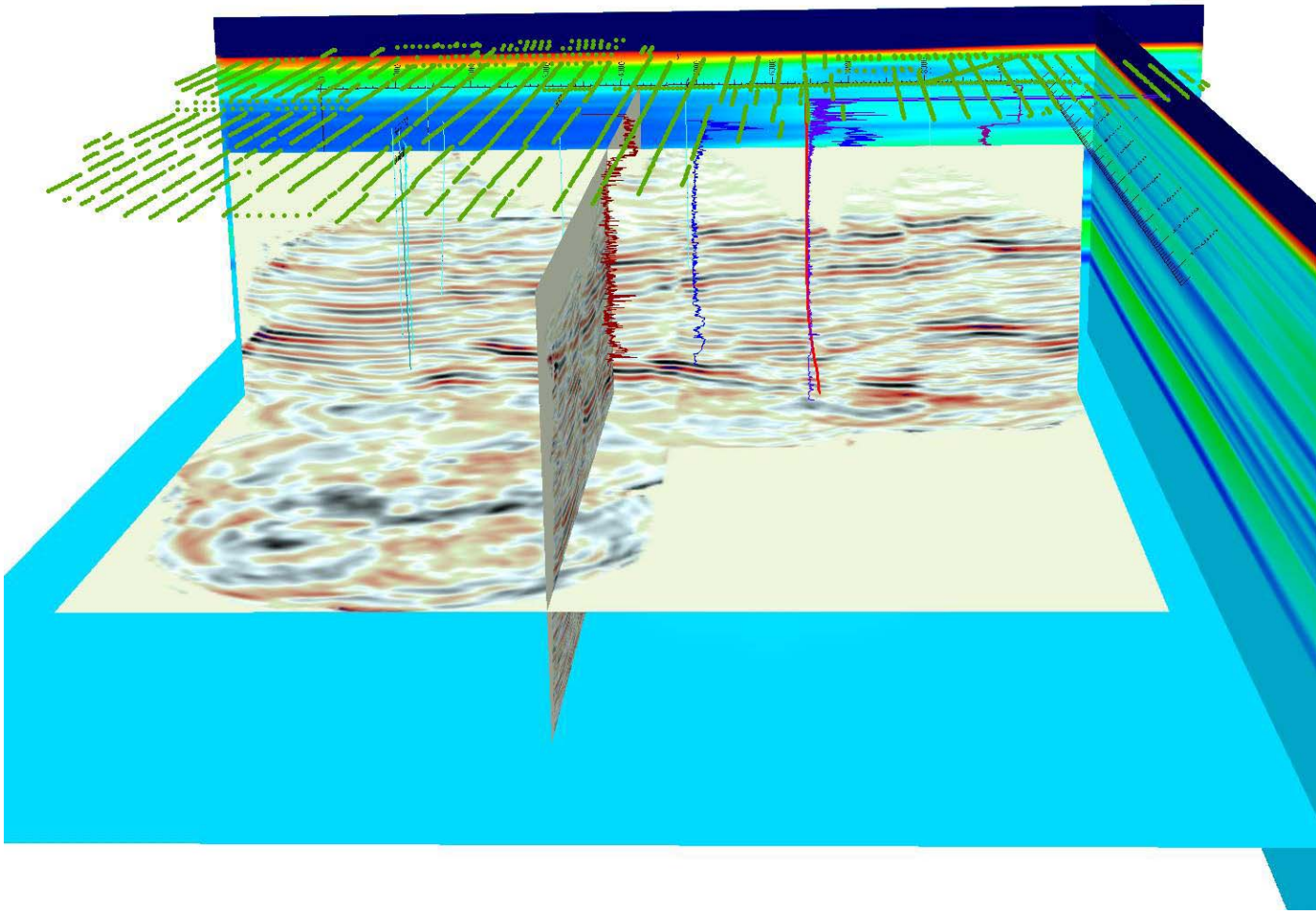

Figure 86 Multi-well test dataset withwells, shot maps, velocity model and seismic image volume.

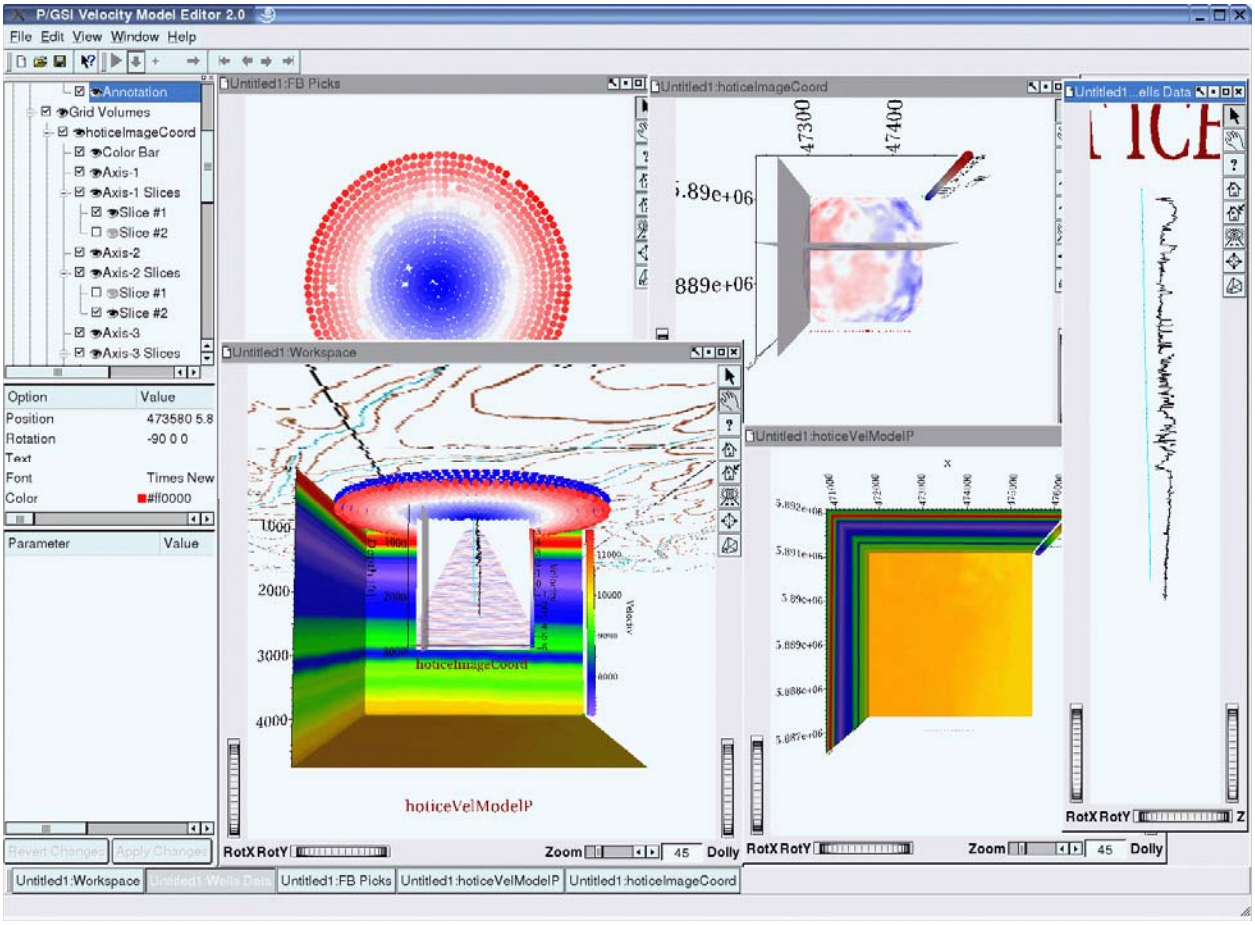

Figure 87 VSP Work Bench showing the many types of data that can be loaded and used during the processing and interpretation work flow.

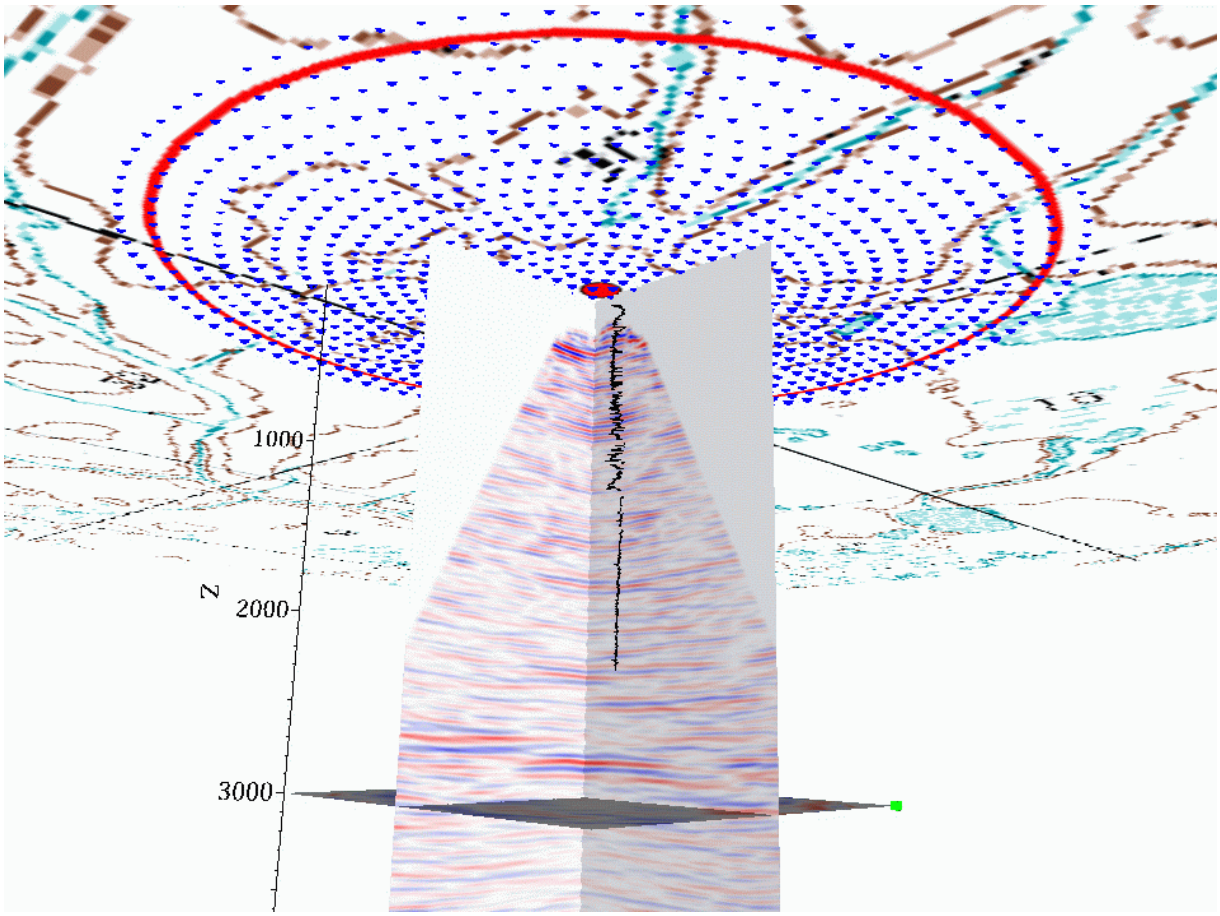

Figure 88 Example of a complex display that the user is able to create in the VSP Work Bench, and then save future use.

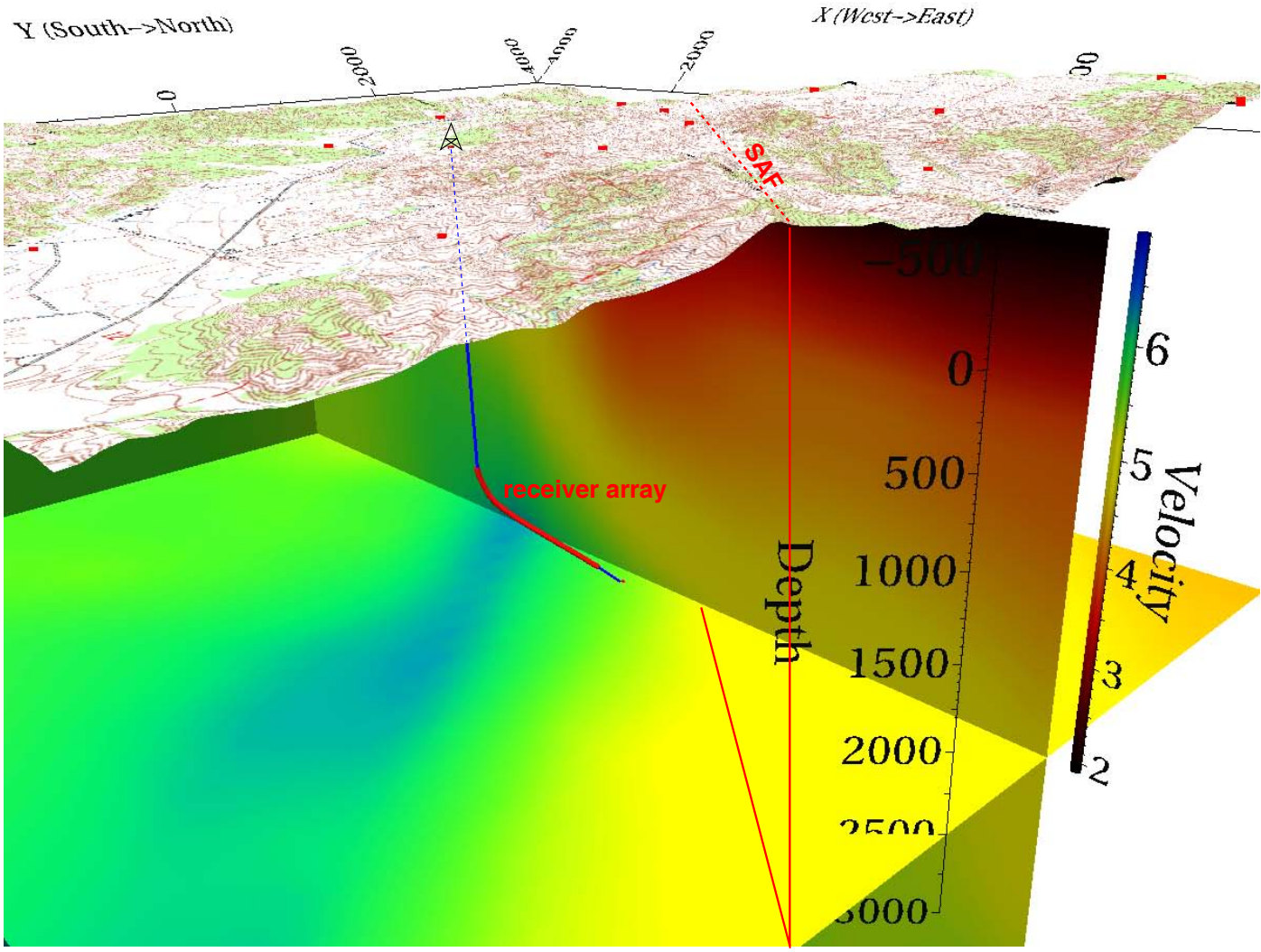

Figure 89 Example of many types of data displayed within a single viewing window. Here we see a topographic map, the wellbore and receiver array, and a velocity model.

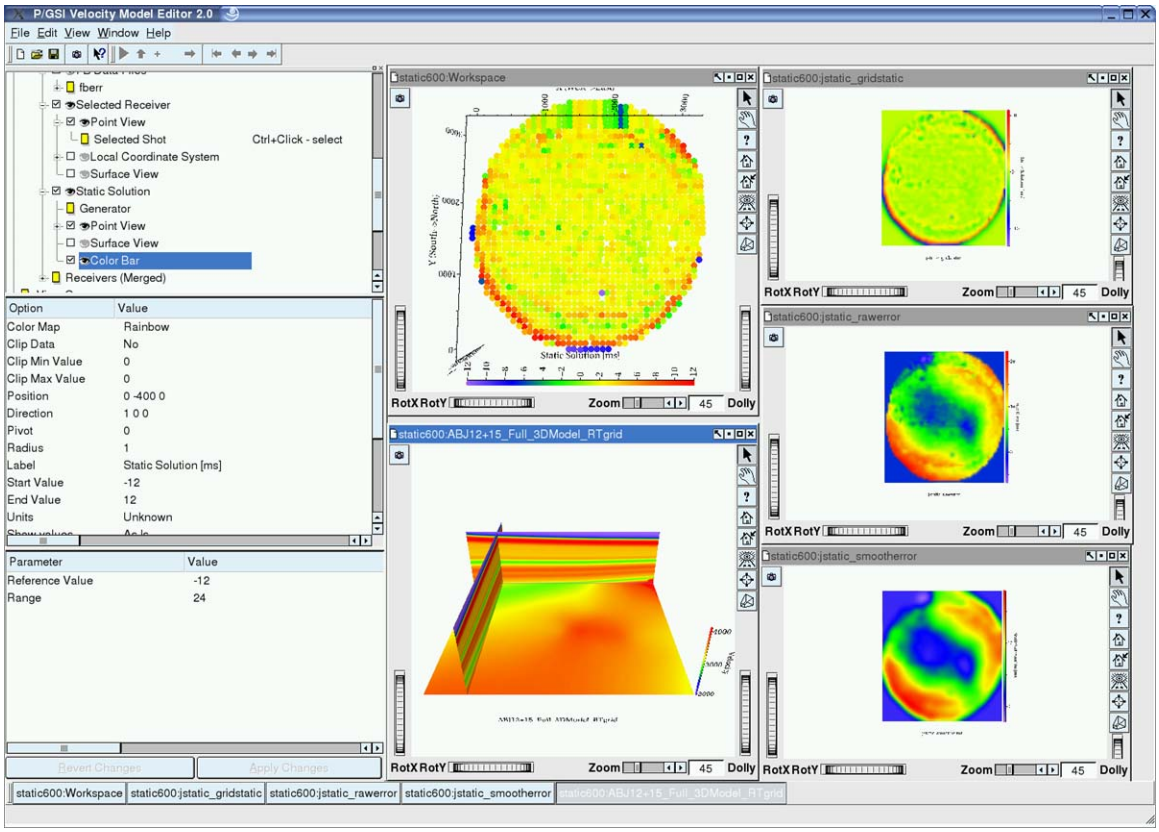

Figure 90 Custom view for the analysis of 3D VSP statics. A static solution is computed in a given velocity model. Comparison windows are shown for actual travel time error, smoothed error and static values at the source locations.

Task 16

Test the system by performing reliability, speed and usability tests on selected synthetic and recorded 3D VSP data. Tune the software to user needs by actually using the software as part of the multi-component processing and interpretation workflow.

Testing and tuning has been an ongoing process, done in conjunction with development, and using the Work Bench for processing and interpretation of real and synthetic datasets. The system is designed from the ground up to run under both Unix (Linux) and Windows operating systems. We have found it advantageous to have users and developers working in both environments, so problems are uncovered early on and modifications to the software can be made in a timely fashion. The primary key to performance of the VSP Work Bench is the speed and configuration of the hardware, not the operating system itself.

One of the issues we faced within the last year was that of porting the software to 64-bit Linux machines. Due to compiler differences, many of the underlying C++ templates had to be modified to compile in both 32 and 64-bit mode. In the end, strict adherence to the latest C++ standard guarantees portability.

Task 17

Complete the documentation and prepare the final report and deliverables.

Preparation of this report and the final deliverables is the essence of this task.

CONCLUSIONS

Throughout the course of this project, we have worked on several tasks simultaneously. In general, there was a mix of design, prototyping, development and testing tasks taking place at any given time, with much overlap. This is to be expected in a project of this magnitude, and in fact helped to speed the development along. We have accomplished what we set out to do, which is to provide our geoscience professionals with a toolkit with a rich set of features and capabilities that can be used for interactive 3D VSP processing and interpretation.

ACKNOWLEDGEMENTS

EarthScope, USGS and NSF – for facilitating the collection of VSP and Micro-seismic data at the SAFOD site.

Department of Energy, National Energy Technology Laboratory for supporting the development of large borehole seismic arrays that were used to collect most of the real 3D VSP data used in this project.

NORSAR software was used for synthetic data generation and model building of ray tracer synthetics.

REFERENCES

Bale, R., Dumitru, G. and Probert, T., 2000, Analysis and stacking of 3-D converted-wave data in the presence of azimuthal anisotropy, 70th Ann. Mtg: Soc.of Expl.Geophys.,1189-1192.

Gaiser, J. and Van Dok, R., 2001, Green River basin 3-D/3-C case study for fracture characterization: Analysis of PS-wave birefringence, 71st Ann. Internat. Mtg: Soc. of Expl. Geophys., 764-767.

Van Dok, R., Gaiser, J. and Markert, J., 2001, Green River basin 3-D/3-C case study for fracture characterization: Common-azimuth processing of PS-wave data, 71st Ann. Mtg: Soc. of Expl. Geophys., 768-771.

Garotta, R. and Granger, P. Y., 1988, Acquisition and processing of 3C x 3-D data using converted waves, 58th Ann. Internat. Mtg: Soc. of Expl. Geophys., Session:S13.2.

Garotta, R. and Granger, P., 2001, Some requirements of PS mode acquisition, 71st Ann. Internat. Mtg: Soc. of Expl. Geophys., 809-812.

Hokstad, K. and Sollie, R., 1998, Multi-component elastic anisotropic Kirchhoff migration, 68th Ann. Internat. Mtg: Soc. of Expl. Geophys., 2044-2047.

Hokstad, K. and Sollie, R., 1999, Multicomponent elastic Kirchhoff migration in TIV media, 61st Mtg.: Eur. Assn. Geosci. Eng., Session:P006.

Lynn, H., Stewart, R. R., Garotta, R. and Thomsen, L., 2001, 4C-ing the future--a word from the "gurus": The Leading Edge, **20,** no. 9, 978-982.

Meadows, M. A. and Winterstein, D. F., 1994, Seismic detection of a hydraulic fracture from shear-wave VSP data at Lost Hills field, California: Geophysics,Soc.of Expl.Geophys., **59,**11-26.

Majer, E.L., et al., Fracture detection using cross well and single well surveys, Geophysics, 62, 495 – 504, 1998.

Mueller, M. C., Barkved, O. I. and Thomsen, L., 1999, A strategy for vector interpretation of multicomponent ocean bottom seismic data, 61st Mtg.: Eur. Assn. Geosci. Eng., Session:P067.

Barkved, O. I., Mueller, M. C. and Thomsen, L., 1999, Vector interpretation of the Valhall 3D/4C OBS dataset, 61st Mtg.: Eur. Assn. Geosci. Eng., Session:6042.

Thomsen, L., 1998, Converted-wave reflection seismology over anisotropic, inhomogenous media, 68th Ann. Internat. Mtg: Soc. of Expl. Geophys., 2048-2051.

Nelson, Ronald A., 2001, Geologic analysis of naturally fractured reservoirs: Gulf Prof. Pub, Boston.

Ohanian, V. and Beckham, W. E., 1992, Depth variant fracture orientation from multicomponent VSP, 62nd Ann. Internat. Mtg: Soc. of Expl. Geophys., 177-180.

Paulsson, B.N.P. and Fairborn, J.W., Site Investigation and Characterization Using Reverse VSP combined with Cross Well Seismic Imaging, Proc., Intern. Soc. of Rock Mechanics Annual Meeting, New York, June 1997a

Paulsson, B.N.P., Fairborn, J.W., Fuller, B.N., Advanced Borehole Seismology, *Proc.*, Offshore Technology Conference, Houston, May 5-7, 1998

Paulsson, B.N.P., Fairborn, J.W., Fuller, B.N., Imaging of thin beds using advanced borehole seismology, Geophysics: The Leading Edge of Exploration, July 1998b

Simmons, J., Jr. and Backus, M., 1999, Shear-wave splitting: Tutorial, issues, and implications for 9-C 3-D seismic reflection data, 69th Ann. Internat. Mtg: Soc. of Expl. Geophys., 788-791.

Thomsen, L., 1998, Converted-wave reflection seismology over anisotropic, inhomogenous media, 68th Ann. Internat. Mtg: Soc. of Expl. Geophys., 2048-2051.

Wills, P.B., DeMartini, D.C., Vinegar, H.J., Shlyapobersky, J., Deeg, W.F., Woerpel, J.C., Fix, J.E., Sorrells, G.G., and Adair, R.G., Active and passive imaging of hydraulic features, The Leading Edge, Vol. 11, No. 7, 15-22, 1992

Winterstein, D.F. and Paulsson, B.N.P., Velocity Anisotropy in Shale Determined from Cross-Hole Seismic and VSP Data, Geophysics, Vol. 55, NO. 4, April 1990, P. 470-479.

Winterstein, D.F., De, G.S. and Meadows, M.A., 2001, Twelve years of vertical birefringence in nine-component VSP data: Geophysics, Soc. of Expl. Geophys., **66,** 582-597.

RELEVANT PUBLICATIONS

There are the following relevant publications for which some of the software tools have been used either for display, processing or interpretation.

Paulsson, B., Karrenbach, M., Milligan, P., Goertz, A., and Hardin, A., 2004, High resolution 3D seismic imaging using 3C data from large downhole seismic arrays, First Break volume 23, October 2004

McGuire, D., Runyon, S., Williams,T., Paulsson, B., Goertz, A. and Karrenbach, M., 2004, Gas Hydrate Exploration with 3D VSP Technology, North Slope, Alaska, 74th Ann. Internat. Mtg: Soc. of Expl. Geophys.

Karrenbach, et al., 2004, High-resolution 3D VSP Imaging, Seismic Reflection Workshop, Seeheim.

Paulsson, B, Karrenbach, M., Goertz, A. , Milligan, P., 2004 , High-resolution Fault Zone Monitoring and Imaging Using Long Borehole Arrays, AGU meeting.

Goertz, A., Milligan, P., Karrenbach, M., Paulsson, B. ,2005, Optimized 3D VSP Survey Geometry Based on Fresnel Zone Estimates, 75th Ann. Internat. Mtg; Soc. of Expl. Geophys.

Chavarria, J.A, Goertz, A, Karrenbach, M., Milligan, P., Paulsson, B., 2005, Characterization of the San Andreas Fault at Parkfield Using a Massive 3D VSP, EOS Transactions, AGU Meeting

APPENDICES

Appendix A. Deliverables

Technical Progress Reports
15418R01.pdf
15418R02.pdf
15418R03.pdf
15418R03A.pdf
15418R04.pdf

Final Report
15418R05.pdf

Synthetic Data
The data are delivered on an LTO2 tape. All of the data directories include an Inputs and a Synthetics sub-directory. Input files are ASCII grids with a header and Synthetics files are in SEGY format.

Synthetic Model 1
Synthetic Model 2
Synthetic Model 3
Synthetic Model 4
Synthetic Model 5
Synthetic Model 6

Source Code
Source code is delivered on a CD, and in addition, the documentation is delivered in hard copy form. The source code directories contain configuration files, Makefiles, C++ source files, and header files.

docs -- documentation for the source code
libpgoi -- library of Dipslay items and their communication with OpenInventor objects
lipgoiutils – utility library for communication with OpenInventor objects
libpgoiwidgets -- higher level display widgets
pgsi3CWorkBench -- main application level 3C Work Bench tool
pgsiDAWorkBench -- main application level DA Work Bench tool
pgsiVelModEdit -- main application level Velocity Model Editor tool